

IN VIVO MODELS TO INVESTIGATE MECHANISMS OF RARE BONE PATHOLOGIES  
AND THERAPEUTIC TREATMENT

A Dissertation

by

DIARRA KEVIN WILLIAMS

Submitted to the Office of Graduate and Professional Studies of  
Texas A&M University  
in partial fulfillment of the requirements for the degree of

DOCTOR OF PHILOSOPHY

Chair of Committee,	Larry J. Suva
Co-Chair of Committee,	Dana Gaddy
Committee Members,	Robert Burghardt Ken Muneoka
Head of Department,	Larry J. Suva

August 2018

Major Subject: Biomedical Sciences

Copyright 2018 Diarra K. Williams

## ABSTRACT

Genetic disorders associated with skeletal disease are extremely complex and vary greatly in their clinical phenotypes. Thus, *in vivo* models that accurately recapitulate these rare bone pathologies are essential for understanding the mechanisms of disease and can serve as tools for evaluating therapeutic treatments while providing insight into normal bone physiology. However, by their nature these rare diseases combined with a deficiency in animal models can significantly delay mechanistic understanding and even therapeutic development. Therefore, the goal of this work was to evaluate murine models of Down syndrome (DS) and develop an appropriate model of human Hypophosphatasia (HPP).

The low bone mass phenotype in DS is defined by low bone turnover due to decreased osteoclast and osteoblast activity, decreasing the utility of anti-resorptive agents in people with DS. Thus, we examined the effects of a known bone anabolic agent – sclerostin antibody (SclAb). Male Ts65Dn and age-matched WT littermate mice (8 weeks old) were treated with 4 weekly *i.v.* injections of 100 mg/kg SclAb. Analysis by DXA, microCT, and *ex vivo* bone marrow cultures revealed that SclAb had a significant anabolic effect on both controls and Ts65Dn DS mice that was osteoblast mediated, without significant changes in osteoclast numbers. Additionally, comparative gene profiling by RNAseq of whole femurs from 7 month old male Ts65Dn mice and WT provided insight into the molecular mechanisms underlying this unusual and rare bone phenotype.

Moreover, we successfully generated the first large animal model of a rare human bone disease using CRISPR/Cas9 to introduce a single point mutation in the tissue nonspecific alkaline phosphatase (TNSALP) gene (*ALPL*) (1077C>G) in sheep, thereby creating HPP. Compared to wild-type (WT) controls, HPP sheep have reduced serum alkaline phosphatase

activity, decreased tail vertebral bone size, and metaphyseal flaring, consistent with mineralization deficits observed in human HPP. Oral radiographs and computed tomography revealed thin dentin and wide pulp chambers in incisors, and radiolucency of jaws in HPP vs. WT sheep. Skeletal muscle biopsies reveal aberrant fiber size and mitochondrial cristae structure in HPP vs. WT sheep. These genetically engineered sheep phenocopy HPP and provide a novel large animal platform for the longitudinal study of HPP progression, as well as other rare bone diseases.

## DEDICATION

To the people living with rare disease and their families;

To the boys and girls whom were ever made to feel as if you were not good enough or told you were anything, but amazing;

And lastly but certainly not least, to my big brother Chester Adisa Guster and all the young black men and women taken from this earth too soon; the individuals we lost to the struggle; To our brothers and sisters who will never have the opportunity to achieve milestones such as this one.

I dedicate this dissertation to you!

Let this body of work serve as proof that all things are possible with determination and belief. Keep pushing forward, keep fighting, and never listen to the “nay-sayers”!

With Love, D!

## ACKNOWLEDGEMENTS

First and foremost, I have to acknowledge and thank my family who have supported through not only this degree, but every endeavor I have pursued. I am especially thankful for my mom (Eunice Guster-Bray) and my sister (Baraka Williams) for their tireless support and everlasting love during the good times and the trying ones. To my aunt (Bigsis), thank you for patience, your love, and your support through all these years.

Life as a graduate student can be very demanding and it sometimes take a team of individuals and mentors to help one through this process. With that, I am thankful my advisors and mentors Dr. Larry Suva and Dr. Dana Gaddy. They have been instrumental to my matriculation through this degree program. I thank you both for your guidance, patience, and all of your efforts towards my academic, professional, and personal development these past 5 years. Their teachings have extended well beyond the laboratory and they were shy about provided helping me whenever I needed it. I thank my committee members, Dr. Robert Burghart and Dr. Ken Muneoka, for their guidance and advisement throughout this journey. To all the faculty and staff from UAMS and TAMU that have encouraged me along the way, I thank you.

Lastly, to all my friends that have I met along the way, I cannot say thank you enough for the great times and amazing memories.

## CONTRIBUTORS AND FUNDING SOURCES

This work was supervised by a dissertation committee consisting of Professors Larry J. Suva and Ken Muneoka from the Department of Veterinary Physiology and Pharmacology, Professor Dana Gaddy from the Department of Veterinary Integrative Biosciences, and Professor Robert Burghardt, Dean of the Office of Graduate Studies and Research – from the College of Veterinary Medicine and Biomedical Science.

Tissue sectioning and staining for paraffin and plastic slides in Chapter III and V was performed by Alyssa Falck (AF) and in Chapter IV by Frances L. Swain. Ex vivo bone marrow cultures were achieved by Diarra K. Williams (DKW) and Nisreen S. Akel (NSA) in Chapter IV and by DKW, AF, and Shannon Huggins (SH) in Chapter III. Enumeration of ex vivo cultures was done by Jamie Schmidt in Chapter IV under the supervision of DKW and by DKW alone in Chapter III. Chapter V experimental design was achieved by DKW, SH, Larry J. Suva (LJS), and Dana Gaddy (DG) in collaboration with the Reproductive Science Laboratory (RSL) under the supervision of Charles R. Long (CRL). MicroCT for Chapters II-V were performed by AF or LJS. RNA sequencing in Chapter IV was performed by the Genomics Core at the University of Arkansas for Medical Science (UAMS) under the supervision of Stewart MacLeod and Kartik Shankar, and RNA extraction, GO analysis, Signal Pathway mapping and analysis, and other analysis of RNA seq data was performed by DKW. Muscle samples in Chapter V were prepared by Ross Payne at the CVM Imaging Center and imaged by DG and AF. The primary sheep fibroblasts were a gift from RSL. All other work conducted for the dissertation was completed by the student.

The research for Chapter V was partially supported by the Center for Cell and Organ Biotechnology (CCOB) Innovation Kitchen Grant (awarded to DKW) and Texas A&M

University (LJS/DG). Graduate study was supported by the Initiative to Maximize Student Diversity Training Grant from University of Arkansas for Medical Science and the Porter Physiology Development Fellowship from the American Physiological Society.

## NOMENCLATURE

ALPL	Alkaline Phosphatase
ACTRIIA	Activin Receptor Type-IIA
BMD	Bone Mineral Density
BMU	Basic Multicellular Unit
BV/TV	Bone Volume / Total Volume
Cas	CRISPR-associated Genes
CRISPR	Clustered Regularly Interspaced Short Palindromic Repeats
DNA	Deoxyribonucleic Acid
DXA	Dual Energy X-ray Absorptiometry
DMP1	Dentin Matrix Protein 1
DS	Down syndrome
FSH	Follicle Stimulating Hormone
GFP	Green Fluorescent Protein
HDR	Homology Directed Repair
HPP	Hypophosphatasia
Inh	Inhibin
mCSF	Macrophage Colony Stimulating Factor
MSC	Mesenchymal Stem Cell
mTOR	Mammalian Target of Rapamycin
OPG	Osteoprotegerin
OPN	Osteopontin



PAM	Protospacer Adjacent Motif
PEA	Phosphoethanolamine
PCR	Polymerase Chain Reaction
PLP	Pyridoxal 5' Phosphate
PPi	Inorganic Pyrophosphate
PTH	Parathyroid Hormone
RANK	Receptor Activator of Nuclear Factor kappa B
RANKL	Receptor Activator of Nuclear Factor kappa B Ligand
RNA	Ribonucleic Acid
RUNX1	Runt-related Transcription Factor 1
RUNX2	Runt-related Transcription Factor 2
RTSK	Serine/Threonine Receptor Kinase
SOST	Sclerostin
sFRP`	Secreted Frizzled-Related Protein
TGFβ	Transforming Growth Factor Beta
TNF	Tumor Necrosis Factor
TNSALP	Tissue Nonspecific Alkaline Phosphatase
TbTh	Trabecular Thickness
TbN	Trabecular Number
TbSp	Trabecular Spacing
TRAF6	Tumor Necrosis Factor Receptor Associated Factor 6
WT	Wild Type

## TABLE OF CONTENTS

	Page
ABSTRACT .....	ii
DEDICATION.....	iv
ACKNOWLEDGEMENTS.....	v
CONTRIBUTORS AND FUNDING SOURCES .....	vi
NOMENCLATURE.....	viii
TABLE OF CONTENTS .....	x
LIST OF FIGURES .....	xiii
LIST OF TABLES .....	xv
CHAPTER I INTRODUCTION AND LITERATURE REVIEW.....	1
Introduction.....	1
Literature Review.....	5
Bone Remodeling and the Basic Multicellular Unit (BMU) .....	5
Osteocyte .....	9
Osteoblast.....	10
Osteoclast.....	13
Down Syndrome.....	14
Hypophosphatasia .....	20
Specific Aims .....	24
References .....	26
CHAPTER II MATERIALS AND DETAILED METHODS.....	40
Animals.....	40
Skeletal Phenotyping Analyses.....	41
Dual-Energy X-ray Absorptiometry: Bone Mineral Density (BMD) .....	41
Micro Computed Tomography (microCT): Ex vivo determination of Trabecular architecture and Cortical Geometry .....	42
Histology and Bone Histomorphometry .....	43
Ex Vivo Bone Marrow Cultures.....	44
Development of a Large Animal Model of HPP in Ovis Aries (Sheep).....	45
Identification and Confirmation of ALPL Mutation Locus.....	45

sgRNA <i>In Silico</i> Design and Preparation for Microinjection .....	46
sgRNA Cloning into Cas9 Plasmid and Preparation for Microinjection.....	47
Design of Single Stranded Oligonucleotide (ssODN) Repair Template .....	48
Primary Sheep Fibroblast Establishment and Culture.....	49
Detection of sgRNA Targeting Efficiency .....	49
Collection of <i>In Vivo</i> Matured Oocytes and Zygotes .....	50
Microinjection of Zygotes, <i>In Vitro</i> Culture, and Transfer into Recipient Ewes.....	51
Polymerase Chain Reaction (PCR) and Genomic Sequencing .....	52
Phenotyping of ALPL Exon 10 c.1077C>G Sheep.....	53
References .....	54
CHAPTER III RELEVANT MURINE MODELS OF LOW BONE MASS PHENOTYPE IN DOWN SYNDROME: UNDERSTANDING THE CONTRIBUTIONS OF GENOTYPE AND SEX .....	57
Introduction.....	57
Study Design.....	60
Results .....	60
Bone mineral density (BMD) is decreased in male, but not female Dp(16)1Yey DS mice ..	60
Skeletal phenotype of trabecular and cortical bone in male and female Dp(16)1Yey.....	61
Altered bone cell recruitment and differentiation could explain sex-specific low bone mass phenotype in Dp(16)1Yey mice .....	64
Discussion.....	66
Future Directions.....	68
Gonadal effects on bone loss in Down syndrome .....	68
References .....	73
CHAPTER IV MECHANISMS OF LOW BONE MASS PHENOTYPE AND THERAPEUTIC TREATMENT IN TS65DN MALE MICE.....	78
Introduction.....	78
Sclerostin Antibody Treatment Stimulate Bone Formation and Normalize Bone Mass in Male Down Syndrome.....	80
Study Design.....	80
Results.....	82
Discussion .....	91
Effects of Trisomy 21 on Gene Expression in the Bone and Bone Marrow Microenvironment.....	94
Hypothesis and Study Design .....	94
Results.....	95
Conclusions and Future Directions .....	110
References.....	117
CHAPTER V GENETICALLY ENGINEERED SHEEP WITH A MISSENSE MUTATION IN ALKALINE PHOSPHATASE GENE RECAPITULATE HUMAN HYPOPHOSPHATASIA .....	130

Introduction.....	130
Results .....	132
Confirmation of ALPL exon 10 mutation-specific locus .....	132
Design of sgRNA and ssODN Repair Template Targeting Sheep <i>ALPL</i> .....	133
Efficient targeting of the selected locus in sheep fibroblasts by CRISPR/Cas9 .....	134
Generation of <i>ALPL</i> Genetically Modified Lambs .....	137
Confirmation of <i>ALPL</i> Mutation Incorporation in Newborn Lambs .....	138
<i>ALPL</i> Genetically-Modified Lambs Recapitulate Human HPP .....	139
Discussion .....	146
Future Directions .....	149
References .....	149
 CHAPTER VI SUMMARY .....	 155
 APPENDIX AWARDS AND HONORS .....	 157
Awards and Honors.....	157
Poster/Oral Presentations.....	158

## LIST OF FIGURES

	Page
Figure 1. Schematic of the BMU and bone remodeling.....	8
Figure 2. Histological section of the BMU and the major bone cells involved in bone remodeling.....	11
Figure 3. Schematic representation of Hsa21 orthologous regions in mice and murine models of trisomy 21.....	19
Figure 4. Three-dimensional model of TNSALP with Ile359Met mutation.....	24
Figure 5. Representative image of microinjection in sheep zygotes.....	52
Figure 6. BMD is significantly decreased in male Dp16 mice, but not female mice. ....	61
Figure 7. Trisomy effects on trabecular microarchitecture in Dp16 mice. ....	62
Figure 8. Trisomy effects on cortical parameters at the tibial midshaft in Dp16 mice. ....	63
Figure 9. Alterations in bone cell parameters of Dp16 male and female mice .....	65
Figure 10. Hypothalamic-Pituitary-Gonadal-Skeletal Axis. ....	69
Figure 11. BMD is similar between male and female Dp16 DS mice.....	70
Figure 12. Schematic of study design for the treatment of male Ts65Dn mice with SclAB. ....	82
Figure 13. Sclerostin Antibody increased BMD in Ts65Dn and WT mice .....	84
Figure 14. Sclerostin antibody treatment significantly improved bone microarchitecture assessed by microCT.....	86
Figure 15. Representative images of dual fluorochrome labeling of trabecular bone surfaces ....	90
Figure 16. Sclerostin antibody increases osteoblast recruitment but not osteoclastogenesis.....	91
Figure 17. Differential gene expression profile of the WNT signaling pathway. ....	104
Figure 18. MTOR signaling effect on bone and the BM microenvironment. ....	105
Figure 19. Differential gene expression profile of TGF $\beta$ signaling pathway .....	108
Figure 20. Differential gene expression profile of the Osteoclast differentiation pathway .....	110

Figure 21. Schematic of the mechanisms and molecular factors associated with the low bone mass phenotype in Ts65Dn male mice. ....	116
Figure 22. Amino Acid sequence alignment of human, sheep and mouse alkaline phosphatase to reference sequence via NCBI BLAST. ....	133
Figure 23. Loci of CRISPR constructs relative to <i>ALPL</i> target mutation site.....	134
Figure 24. Efficient targeting of <i>ALPL</i> gene by CRISPR Cas9 in primary sheep fibroblasts.....	136
Figure 25. PCR and T7E1 genotype screening for genetically modified lambs .....	139
Figure 26. Representative chromatographs and photos of genetically modified lambs .....	140
Figure 27. Reduced serum Alkaline Phosphatase levels in 2 month old mutant lambs.....	141
Figure 28. Skeletal phenotype is not due to a “failure to thrive” phenotype.....	143
Figure 29. Tail radiographs reveal skeletal phenotype in <i>ALPL</i> mutant lambs.....	144
Figure 30. Dental phenotype in <i>ALPL</i> c.1077C>G targeted sheep. ....	145
Figure 31. Skeletal muscle histological phenotype in <i>ALPL</i> c.1077C>G targeted sheep .....	146

## LIST OF TABLES

	Page
Table 1. Clinical forms of HPP and their clinical presentations [28, 125, 129, 132]. .....	22
Table 2. Primer sequences for amplification of sheep ALPL exon 10 target site. ....	46
Table 3. SgRNAs designed to target the sheep ALPL exon 10 c.1077C>G HPP mutation. ....	47
Table 4. <i>ALPL</i> exon 10 repair template with c.1077C>G HPP mutation and PAM mutation .....	48
Table 5. Effect of sclerostin antibody treatment on cortical bone geometry of the tibia assessed by microCT (mean $\pm$ S.D.) .....	87
Table 6. Expected Outcomes for Differential Gene Expression Profile of Ts65Dn mice .....	95
Table 7. GO analysis of upregulated genes associated with osteoblast differentiation .....	98
Table 8. GO analysis of upregulated genes associated with ossification.....	99
Table 9. Differentially expressed genes on mouse chromosome 16 in Ts65Dn mice. ....	112
Table 10. Generation of <i>ALPL</i> gene-modified lambs with CRISPR/Cas9.....	138

# CHAPTER I

## INTRODUCTION AND LITERATURE REVIEW

### **Introduction**

There are approximately 30 million people in the United States living with a rare disease and 350 million estimated worldwide [1]. A rare disease in the U.S. is defined as one that affects less than 200,000 individuals with approximately 7000 such diseases reported to date [2]. More than 80% of these diseases are genetic in origin [2, 3]. Although the individual diseases are rare, the impact on patients and families affected by these potentially debilitating or even lethal diseases is tremendous. Collectively, rare disease place an enormous financial burden on societies and health care ecosystems [2].

Currently, there are nearly 500 known bone-related dysplasia's comprising approximately 5 percent of the total number of birth defects and affecting ~1 in 5000 live births [4]. Similar to other genetic disorders, the skeletal- and other related complications associated with the defective gene and/or genes in rare bone pathologies are present throughout the individual's life, often vary in severity, and have no cure [5-8]. In addition to disease rarity and the phenotypic heterogeneity of rare bone pathologies, a complete understanding of disease pathophysiology is paramount, yet sorely lacking [5-8].

Animal models of human disorders (largely murine) have provided enormous insight into the pathophysiology of rare bone dysplasias. These preclinical models have proven to be invaluable for the development and testing of novel therapeutics. However, it is important to recognize that all animal models of human disease have important limitations. The scientific knowledge and understanding gained from each individual disease model – most specifically



from rodent models are unlikely to recapitulate all features of the human disease. In the context of the development of novel bone disease models and their validation this is an extremely important point. Indeed, existing and well-studied murine models have provided considerable insight into the control of bone mass and architecture. Such knowledge is vital for the development of effective bone-active therapeutics and to expand and clarify our overall understanding of bone disease. Thus, the objective of my research was two fold: **1)** to identify and validate relevant *in vivo* models for Down syndrome (DS) and, in the case of Hypophosphatasia (HPP), develop an appropriate model and **2)** to determine the efficacy of current bone anabolic therapies to improve bone mass and strength in the setting of DS.

DS is a common human genetic disorder that is not solely characterized as a bone disease. In fact, this birth defect, arising from trisomy of human chromosome 21 (Hsa21) alters human development and presents with a wide variety of clinical issues such as learning disability, heart defects, sleep apnea, profound hypogonadism, and infertility as well as a plethora of endocrine and metabolic abnormalities [9-13]. The past several decades have seen significant increases in the average life expectancy of individuals with DS due in part to improved health care and the establishment of specialized health care guidelines [9, 14, 15]. Amidst this increase in longevity, skeletal complications such as osteopenia and bone fragility that were not previously recognized in the DS community have begun to appear in a growing number of people with DS [10, 16]. Consequently, the current available health care guidelines lack pertinent information regarding bone health in DS.

Previous studies by us and others revealed that the osteopenic bone phenotype is associated with low BMD and is the result of low bone turnover - decreased osteoblast and osteoclast numbers [17, 18]. This suggests that the current use of anti-resorptive agents to treat

the low bone mass in people with DS is likely contraindicated. Even so, the mechanistic basis and appropriate bone-related treatments for this bone phenotype in DS remains unknown and underexplored. Therefore, we determined the bone phenotype of the two of the most commonly used murine models of DS at the time – Tc1 and Ts65Dn [19, 20].

The literature suggested that these murine models recapitulated many of the characteristics of human DS such as the mental and behavioral deficits as well cardiovascular and hypogonadism [21-25]. However, to our knowledge no data existed regarding any prevailing bone phenotype. Our studies demonstrated that the Ts65Dn mice had a low bone mass phenotype that was identical to that seen in human DS [17, 18], whereas Tc1 mice completely lacked any discernible bone phenotype. In order to obtain unbiased and accurate assessment of the mechanisms underlying bone deficits, identification of the most relevant disease model is of the utmost importance. Thus, the difference in bone phenotype between two of the most-cited *in vivo* models gave good cause for concern. Additionally, the limited availability of characterized skeletal phenotypes of other DS murine models could be problematic in securing the most appropriate disease model for performing mechanistic studies and assessing relevant pharmaceutical therapies for this underserved population.

Chapter III and IV efforts focus on my analysis of relevant *in vivo* models of DS to assess the mechanisms driving the low bone mass bone phenotype and assess the utility of potential bone anabolic agents for the treatment of low bone mass and strength in people with DS. More specifically, the aim of Chapter III is to characterize the skeletal phenotype of Dp(16)1Yey (Dp16) mice – a novel murine model of DS [26]. We hypothesized that Dp16 mice would phenocopy the low bone mass phenotype exhibited in human and Ts65Dn DS populations. The aim of Chapter IV is to evaluate the efficacy of sclerostin antibody treatment to increase bone

mass in a relevant murine model of DS. Given the low BMD and low bone turnover state in DS humans and Ts65Dn DS mice [17, 18], we hypothesized that sclerostin antibody treatment would be an efficacious therapeutic for improving bone mass and strength in DS.

Contrary to DS, Hypophosphatasia (HPP) is a rare inherited disorder of metabolism that is characterized by both musculoskeletal and tooth abnormalities [27, 28], and biochemically by low serum activity levels of the tissue-nonspecific isoenzyme of alkaline phosphatase (TNSALP) [29]. The disease is the result of loss-of-function mutations in the TNSALP coding *ALPL* gene and like DS and other genetic disorders, is accompanied by a highly variable clinical presentation and variable severity [8, 30]. The rarity of the disease combined with the lack of an appropriate disease model (until 1999) significantly delayed therapeutic advancement. However, Asfotase Alfa (bone targeted delivery of human recombinant alkaline phosphatase) was approved by the FDA in 2015 [8, 31]. Similar to most other human disease models, the current models of HPP have been engineered exclusively in rodents – specifically mice harboring nonspecific knock-out loss of function mutations in *ALPL*. Although they have proven useful for modeling some aspects of HPP, murine models harboring *ALPL* mutations do not faithfully represent the broad spectrum of human HPP clinical phenotypes. Chapter V will address this important issue and describe the development of the first genetically engineered large animal model of HPP using sheep. Sheep bone remodeling, bone size, and tooth development are all analogous to humans and the sheep TNSALP amino acid sequence shares around 90% identity with the human protein[32]. Therefore, we hypothesized that the incorporation of a missense mutation in the sheep *ALPL* gene would produce an animal model that more accurately represented the bone and tooth pathophysiology observed in human HPP and would provide a novel approach in which to study the disease progression and development with age.

## **Literature Review**

### Bone Remodeling and the Basic Multicellular Unit (BMU)

The mammalian skeleton is a very dynamic and metabolically active organ [33]. This durable structure provides support to an organism and protects against damage to the organisms soft tissues. The mature skeleton of vertebrates is composed of 2 tissues: a hard outer layer called cortical bone that makes up ~80% of the skeleton and the other 20% of bone is comprised of spongy inner layer referred to as trabecular (or cancellous) bone [34]. The development and maintenance of the mammalian skeleton involves pivotal processes called bone modeling and bone remodeling, respectively, and it is these processes that ultimately determine bone health and strength [34]. Bone modeling is the process of shaping or reshaping the skeleton through the independent actions of 2 bone cells – osteoclasts and osteoblasts [35, 36]. Bone modeling is defined by the development and growth of the vertebrate skeleton, but can also continue throughout life [37].

Bone remodeling, on the other hand, occurs throughout our lifetime for the purpose of maintaining bone mass, bone microarchitecture and strength. Bone remodeling occurs through the coupled activity of osteoclast and osteoblast. The manner by which these cells exert their actions on the skeleton is considered “coupled”, because bone is resorbed or broken down by osteoclast and rebuilt/formed by osteoblast in a sequential manner [38]. This process takes place throughout the skeleton in distinct units called the basic multicellular unit (BMU) [33] and largely regulated by the actions of another resident bone cell – the osteocyte. The osteocyte, a matrix embedded osteoblast, is the most abundant cell in bone. The osteocyte has been demonstrated to be critical for bone homeostasis and its function is subject to endocrine and paracrine regulation as well as mechanical stimuli such as loading [39, 40]. The cellular

recycling of osteoclasts and osteoblasts or bone remodeling rate in the BMU – mediated by the molecular actions of osteocytes or other mechanisms – is responsible for the control of bone turnover [41].

As mentioned above, the normal bone remodeling cycle maintains bone integrity through the balanced activity of bone resorption (osteoclast) and bone formation (osteoblast) in the BMU [35, 36] (**Figure 1**). The bone remodeling cycle begins in the quiescent state (**Figure 1A**). Micro-damage, mechanical loading, or some other local or endocrine stimuli is sensed by osteocytes, which in turn, lead to the recruitment of osteoclast progenitor cells from either the bone marrow or from the capillaries [35]. The osteoclast progenitor cells (monocyte/macrophage lineage) arrive and interact with the bone surface to proliferate and eventually differentiate and fuse into mature polarized multinucleated osteoclasts. This process occurs under the control of monocyte/macrophage colony stimulating factor (mCSF) and receptor activator of nuclear factor  $\kappa$ B (NF $\kappa$ B) ligand (RANKL) [42]. These cells are then uniquely capable of the resorption (removal) of the damaged bone [34] (**Figure 1B**). While resorption pits are continually being formed, osteoclasts release cytokines and other factors that lead to the recruitment and proliferation of mesenchymal derived osteoblast progenitors, from the marrow or adjacent blood vessels [34, 35]. The subsequent differentiation of osteoprogenitors into mature bone forming cells leads to apoptosis of the osteoclast (**Figure 1C**). Mature osteoblasts in a coordinated fashion begin laying down new osteoid (unmineralized bone matrix) in the recently evacuated resorption pits (**Figure 1D**). The newly formed osteoid is eventually mineralized forming new bone (**Figure 1E**) [33, 34]. When the bone remodeling process is complete, the remaining osteoblasts either undergo apoptosis, form lining cells or become embedded in new bone. Osteoblast cells that become embedded in the newly formed bone further differentiate into

osteocytes that contain long dendritic cell processes and the cycle repeats [36, 43] (**Figure 1A**), thus completing the entire process and repopulating the new bone with osteocytes.

Both the modeling and remodeling of the skeleton can be affected by endogenous factors such as the endocrine system [44, 45]. Additionally, the cellular components of bone remodeling are controlled by paracrine, autocrine, or endocrine signals in the bone and bone marrow environment [46]. Any altered bone turnover and bone homeostasis due to imbalances in the number and/or activity of these cells can be detrimental to (or improve) bone health. For instance, increases in bone formation with no change in osteoclast function causes osteosclerosis, whereas, decreases in bone resorption (osteoclast defects) lead to osteopetrosis [47]. In both scenarios, the result is – too much bone [47]. Alternatively, increases in osteoclast and osteoblast numbers, activity, or both to the point where bone resorption surpasses bone formation leads to brittle and fragile bones termed osteoporosis [37, 48, 49]. Therefore, understanding the basic biology of bone remodeling is critical to appreciate the effects of altering the cellular and molecular mechanisms of bone turnover seen in human bone disease. For this reason, I will describe in greater detail the dynamic processes and factors underlying the development and regulation of osteocytes, osteoblasts, and osteoclasts – the 3 major cells of the BMU – in the following sections.

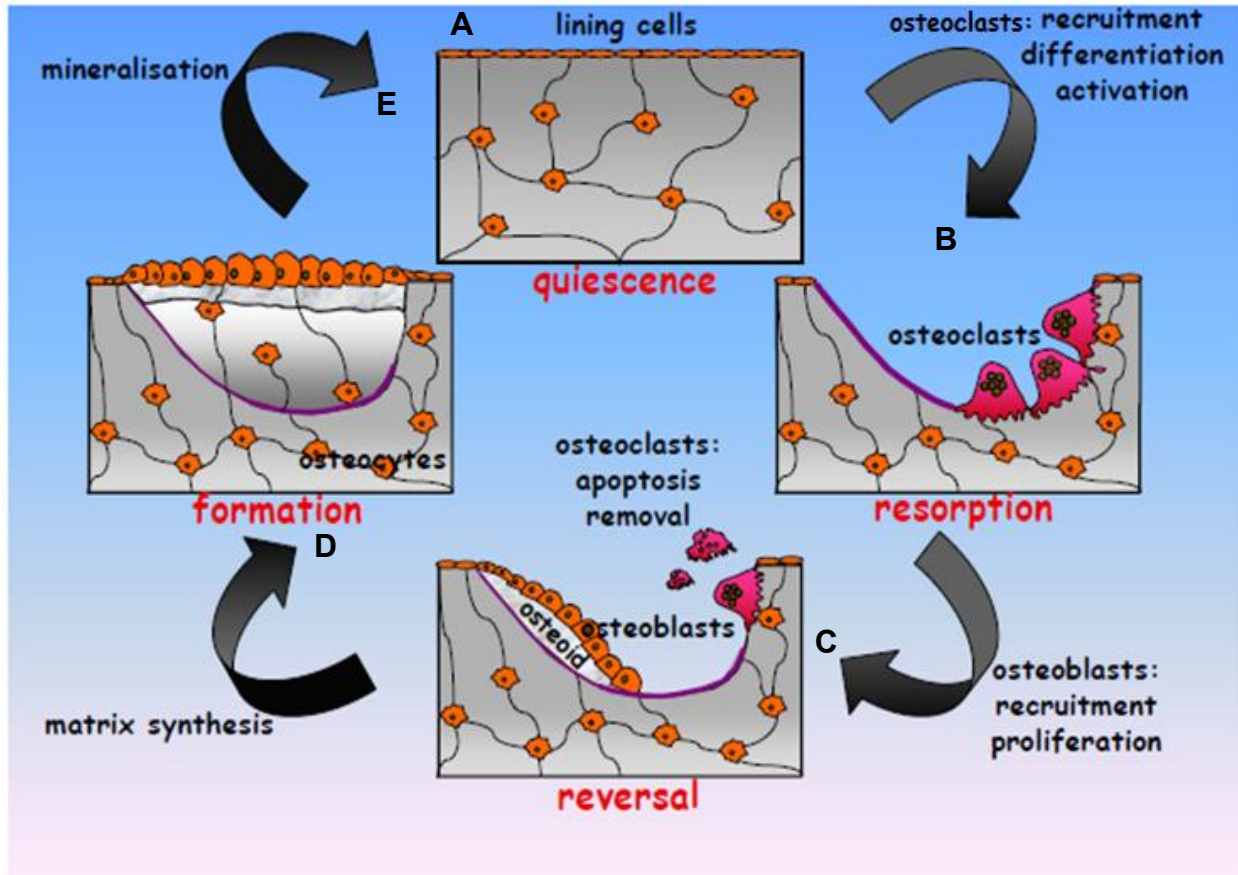


**Figure 1. Schematic of the BMU and bone remodeling.** Bone remodeling is essential for the maintenance of bone mass and skeletal microarchitecture. It occurs in the basic multicellular unit that consists of osteoclasts, osteoblasts, and osteocytes. **(A)** Bone remodeling generally begins from a quiescent state. **(B)** Then, sensing of mechanical stressors by osteocytes lead to signals that recruit osteoclast progenitor cells to the BMU environment. The osteoclast progenitor cells are then activated by RANKL stimulation, and subsequently proliferate, differentiate and fuse into mature multinucleated osteoclasts. These multinucleated osteoclasts are then capable of bone resorption. **(C)** During bone resorption, osteoclasts themselves release cytokines and other factors that lead to the recruitment of osteoblasts progenitors to the BMU and subsequently their proliferation. This recruitment is also supported by the release of bone-trapped cytokines by the process of bone resorption. Once osteoblasts are recruited and the process of bone formation begins, osteoclasts undergo apoptosis stimulated by secreted factors from osteoblasts and osteocytes. The cuboidal osteoblasts begin to lay osteoid in the resorption pits, **(D)** which begin to form new matrix. **(E)** This matrix is subsequently mineralized to form new bone. Following completion of the cycle, osteoblasts may undergo apoptosis, form new lining cells at the surface of the newly formed bone or become entrapped in the new bone, where they differentiate in new osteocytes. The process is then complete and this particular BMU returns back to the quiescent state

## Osteocyte

Osteocytes are the most abundant and long-lived cells in the skeleton, comprising 90-95% of all bone cells with a lifespan up to 25 years [50, 51], although some osteocytes may reside in the skeleton throughout life [52] (**Figure 2**). Osteocytes are located within lacunae in the bone matrix; they are of mesenchymal origin and are the terminally differentiated state of osteoblasts [53]. During the process of bone formation, some osteoblasts become embedded into the newly formed matrix where they differentiate; inducing a profound morphologic change whereby they acquire long dendritic processes that allow constant contact with neighboring osteocytes and other cells at bone surface, such as osteoclasts and osteoblasts [34, 54] and the bone marrow. For the longest time, the function of these matrix-embedded osteoblasts was undefined and the cells were merely considered trapped cells responsive to mechanical loading [34, 50]. However, advancements in the understanding of bone biology and improved biochemistry and cell biology techniques has demonstrated that these cells are indeed critical for maintaining bone homeostasis and microarchitecture [34].

Through the osteocyte network of cellular processes, these cells sense mechanical influences such as loading and unloading leading to signal transmissions to either osteoblasts to form bone or osteoclasts to resorb bone, respectively [54, 55]. In addition to mechanical stimuli, it has also been shown that osteocytes are capable of sensing metabolic signals, as increased osteocyte death occurs during loss of ovarian function, nutrient deficiency, and unloading of bone during aging [53]. In sum, these once-forgotten cells are now receiving the majority of investigative attention and are currently positioned as the primary skeleton-regulation in bone.

In order to regulate bone homeostasis and strength, osteocytes secrete many factors associated with bone metabolism [56]. In the case of bone unloading via hind limb suspension,



osteocytes secrete factors that increase bone resorption and osteoclastogenesis such as RANKL [56]. The stimulation of osteoclast progenitors by RANKL is essential for osteoclast differentiation, and osteocytes are thought to be the major source of RANKL controlling bone homeostasis [56-59]. In addition to upregulating osteoclast differentiation during unloading (or loading), osteocytes secrete factors that negatively regulate bone mass via suppression of osteoblast differentiation such as Dickkopf-1 (DKK) and sclerostin, potent WNT signaling pathway inhibitors [60]. These osteocyte-secreted proteins inhibit bone formation by binding lipoprotein receptor-related protein (LRP) 5, LRP6, or via inhibition of the WNT signaling pathway [60-63]. Both of these WNT antagonists are highly secreted by osteocytes [37, 62]. Interestingly, the secretion of sclerostin is largely osteocyte-specific, whereas DKK1 expression is not [60, 64]. In contrast, mechanical sensing by osteocytes leads to increases in bone formation, and the suppression of osteoclastogenesis via the secretion of osteoprotegerin (OPG) the soluble decoy receptor for RANKL [56, 60]. All of these osteocyte-derived factors exert effects on either osteoclasts or osteoblasts and are necessary for maintaining bone homeostasis, and thus healthy bone mass and strength.

### Osteoblast

Osteoblasts are derived from the mesenchymal cell lineage and comprise 4-6% of bone cells [53, 65] (**Figure 2**). The primary function of osteoblasts in the BMU and the skeleton is to form bone. Derived from the mesenchymal lineage, mature osteoblasts (observed as cuboidal shaped cells on the bone surface) arise from multipotent progenitor cells (often misnamed as mesenchymal stem cells (MSC) that have the capacity to differentiate into adipocytes, chondrocytes, myoblasts, fibroblasts, and of course osteoblasts [50, 66]. However, the commitment of these multipotent progenitor cells towards the osteoblast lineage requires the

temporal expression of specific transcriptional regulators, such as runt-related transcription factors 2 (RUNX2), osterix, and  $\beta$ -catenin [67].

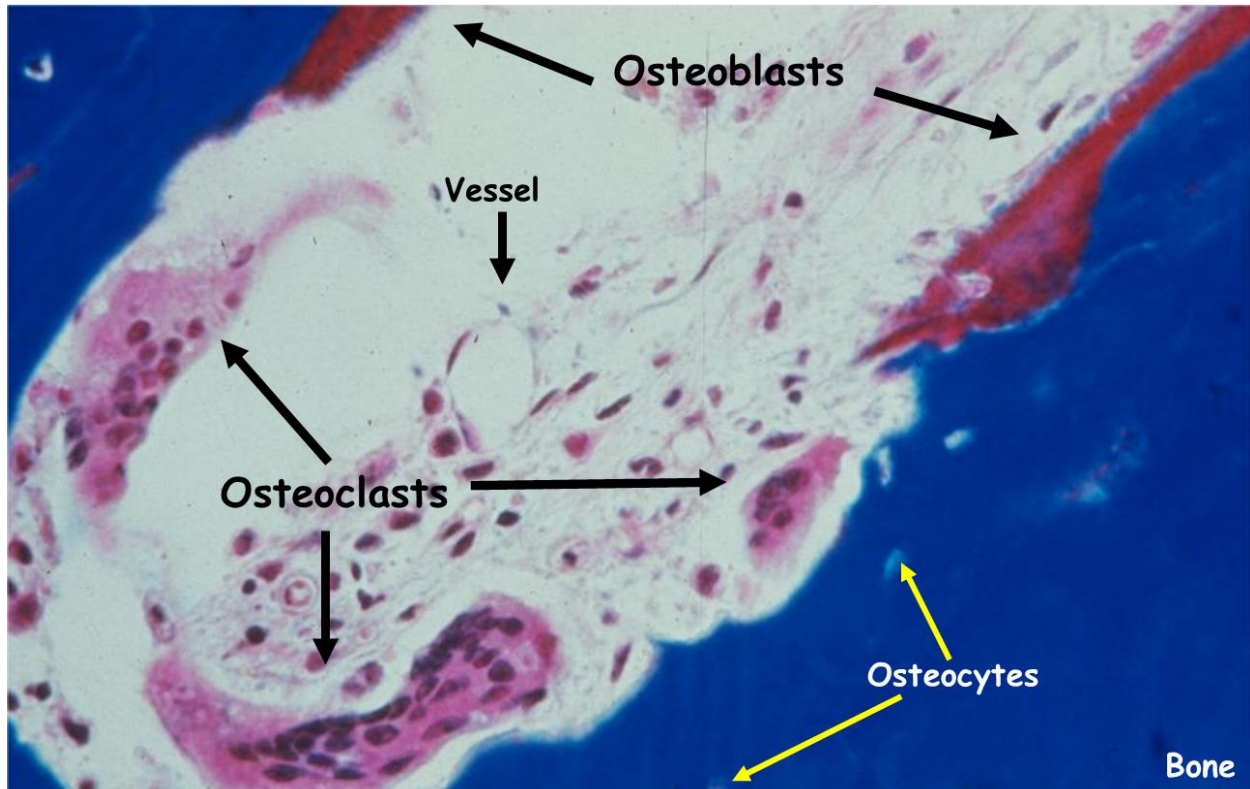


**Figure 2. Histological section of the BMU and the major bone cells involved in bone remodeling.** The osteoblasts are derived from the mesenchymal cell lineage and constitute up 4-6% of bone cells. The osteocytes (matrix-embedded osteoblasts) are located within lacunae of the bone matrix and make up 95% of the total numbers of bone cells. The osteoclasts are large multinucleated cells attached to the bone surface and are derived from the hematopoietic cell lineage.

RUNX2 is considered the master regulator of osteoblast differentiation, since its expression at different stages of the differentiation can positively or negatively regulate downstream osteoblast-specific genes including alkaline phosphatase (*ALPL*), collagen type I (*COL1A1*), osteopontin (*OPN* or *SPP1*), or osteonectin (*ON*) [68, 69]. The temporal activation of  $\beta$ -catenin, the major transcriptional regulator of the canonical WNT signaling pathway, and downstream

expression of its gene transcripts can lead to either inhibition or activation of osteoprogenitor cells towards the osteoblast lineage [70-72]. The presence of  $\beta$ -catenin during the early stages of mesenchymal lineage selection inhibits MSC selection down the osteo-chondrocyte lineage [73-75]. However,  $\beta$ -catenin is an important factor in driving osteoblast differentiation during later stages of maturation [71, 72]. The canonical WNT pathway, which includes  $\beta$ -catenin activation, is the predominant WNT pathway affecting bone formation and bone cells, more specifically osteoblast differentiation [61, 71, 72, 76].

In addition to the WNT pathway, the transforming growth factor- $\beta$  (TGF $\beta$ ) and members of TGF $\beta$  superfamily play a major role in bone remodeling [77-80]. TGF $\beta$  dimerizes and activates serine/threonine receptor kinases (RTSK), which subsequently phosphorylate and activate SMAD proteins – SMAD2 and SMAD3. These activated SMAD proteins then associate with other SMAD proteins that facilitate their translocation to the nucleus where they and other factors bind promoter regions of DNA that control gene expression [77, 81, 82].

TGF- $\beta$ , one of the most abundant cytokines in bone matrix, can have both negative and positive effects on bone formation [82-84]. TGF $\beta$  inhibits the osteoclastogenesis by inhibiting the formation of osteoclast precursors, thus suppressing bone resorption [82]. However, TGF $\beta$  signaling can have the opposite effect on osteoblastogenesis, and actually induce osteoblast differentiation and proliferation depending on the context or stage of differentiation [82].

Bone morphogenetic proteins (BMPs) are members of the TGF $\beta$  superfamily, and are important factors necessary for skeletal development and bone homeostasis [85-87]. In a similar mechanism to TGF $\beta$ , these proteins dimerize RTsKs and activate their respective downstream SMAD signaling proteins (SMAD1, SMAD5, and SMAD8). SMADs translocate to the nucleus and associate with other transcriptional factors to control osteoblastic gene expression [88].

During the initiation of osteogenesis, SMAD1 and SMAD5 interact with RUNX2 in the nucleus where the complex controls subsequent osteoblast-specific gene expression [77, 80, 82, 83]. The dysregulation of the BMP pathway or any of its components is implicated in many bone-related disorders including leukemia [87], and fibrodysplasia ossificans progressiva (FOP), where gain-of-function mutations in BMP signaling leads to extensive ectopic ossification [89-92]. BMPs can both stimulate and inhibit osteoblast differentiation [88]. Given the significant role played by osteoblasts in maintaining bone homeostasis and hematopoiesis, the dysregulation of any of the signals or processes associated with osteogenesis could have a significant impact on bone and the local cells of the bone marrow microenvironment.

### Osteoclast

Bone homeostasis is tightly regulated by the bone forming actions of the osteoblast, as discussed above, and the osteoclast. Derived from the monocyte/macrophage arm of the hematopoietic lineage, osteoclasts are terminally-differentiated large multinucleated cells formed by the fusion of mononuclear progenitor cells [33, 34]. During bone metabolism, these highly specialized cells primary function is to resorb mineralized bone [93]. Alterations in bone resorption due to changes in osteoclastogenesis negatively impacts bone health, eventually leading to bone disease [37, 46, 94, 95]. Therefore, osteoclast differentiation and activity is under tight control by factors secreted locally as well as endocrine signals [45, 61, 96].

In the presence of macrophage colony stimulating factor (mCSF), monocyte/macrophage precursor cells are recruited into the osteoclast lineage. mCSF functions as a survival factor for osteoclast precursor cells and upregulates the expression RANK, the receptor for receptor activator of nuclear factor kappa-B (NFκB) ligand (RANKL) [93]. In turn, RANKL is indispensable for normal physiologic osteoclastogenesis and is secreted by osteocytes, mature

osteoblasts, and mesenchymal stromal cells [35, 42, 65]. In the combined presence of sufficient mCSF and RANKL, osteoclastogenesis proceeds [97]. Recent studies, however, have shown that osteocytes are likely major source of RANKL during bone remodeling, especially in young growing animals [56, 58]. During normal bone remodeling, the regulation of osteoclastogenesis is also under the control of cells of the osteoblast lineage, as both osteocytes and mature osteoblast secrete osteoprotegerin (OPG), a soluble decoy receptor that binds and antagonizes RANKL signaling to inhibit osteoclast formation and activity [47, 69]. To begin the process of bone resorption, multinucleated osteoclast cells are activated and become polarized mature osteoclasts capable of bone resorption [98]

### Down Syndrome

“Those who have given any attention to congenital mental lesions, must have been frequently puzzled how to arrange, in any satisfactory way, the different classes of this defect which may have come under their observation”[99]. In his reports entitled “Observations of an Ethnic Classification of Idiots”, John Langdon Down, MD detailed for the first time the physical phenotype and intellectual properties of what is now known as Down syndrome (DS)[100]. However, it was not until 1959 that advancements in genetic science allowed for the identification of DS as a chromosomal abnormality, individuals with this particular disorder had 47 instead of 46 chromosomes [101]. Today, further advancements in both medicine and science has provided great insight into the cause of disease and the many deleterious phenotypes associated with the disease.

DS is a chromosomal aneuploidy specifically characterized by trisomy of chromosome 21 syndrome [102]. DS is the most common birth defect in the United States [100], comprising approximately 0.45% of all pregnancies [103]. The most common cause of trisomy 21 is

nondisjunction. Trisomy 21 due to nondisjunction occurs when the chromosome 21 pair in either the egg from mother or the sperm from the father fails to separate. Thus, leading to replication of 3 copies of the gene instead of 2 in the cells of the body during embryogenesis. Additionally, Mosaicism and partial trisomy due to translocations defects account the other 5% of DS cases.

Although DS was initially identified in 1866, it remains a major public health concern as it and other genetic abnormalities continue to be a leading cause of infant mortality and lifelong disabilities [14, 102, 104]. Trisomy 21 specifically alters human development and leads to a variety of clinical issues such as mental impairment, heart defects, sleep apnea, hypogonadism, infertility as well as deficiencies in bone health [102, 104-107]. DS is also associated with a 500-fold increase in the risk of acute megakaryoblastic leukemia [108] and the majority of people with DS suffer from learning disabilities, muscle hypotonia, and craniofacial manifestations, although the clinical penetrance of all the consequences of trisomy 21 vary [102].

Nevertheless, the past several decades have brought about significant increases in the average life expectancy of individuals with DS, due in part to social inclusion, improved access to health care and the establishment of specialized health care guidelines [14, 15, 109]. These easily accessible guidelines help define health care needs and potential risk factors associated with DS and allow for better communication amongst people with DS, their caretakers and their primary care physician. Amidst the increase in longevity, skeletal complications such as osteopenia and bone fragility that were not previously recognized in the DS community have begun to appear [10, 16, 110-112]. Consequently, the increased rate of low or minimal trauma fractures are important causes for morbidity in DS [18]. Even so, little is known about the etiology or the mechanistic underpinnings associated with trisomy of human chromosome 21, thus making appropriate recommendations for treatment difficult.

There are currently two hypotheses that exist to explain the very complex and variable clinical phenotype in DS– the “gene dosage effect” or the “amplified developmental” effect [113, 114]. The gene-dosage effect hypothesis proposes that the clinical phenotypes of DS are direct consequences of the imbalance of individual genes found on chromosome 21; thus, suggesting that the different phenotypic consequences are due to overexpression of specific chromosome 21 genes [114, 115]. However, the amplified developmental instability hypothesis proposes that the expression of the different DS phenotypes is due to a non-specific disturbance of chromosome balance which results in a disruption of homeostasis; a theory derived by an effort to explain the similarities between the different aneuploidy states [114, 116]. In an attempt to dissect the pathophysiology of DS, many animal models, more specifically murine models, have been developed.

### **Murine Models of Down syndrome**

Murine models of DS have been instrumental in understanding the impact of trisomy 21 on development and homeostasis in mammalian species [13, 19, 104, 116]. To dissect the mechanistic underpinnings of DS clinical phenotypes and answer the question of how trisomy of chromosome 21 lead to this variable set of phenotypes (gene-dosage vs. amplified development instability), animal models targeting single genes of chromosome 21 and the entire segments of genes have been developed (**Figure 3**). However, deciphering causality between the 2 hypotheses in murine models has been very complex given the distribution and genetic make-up of mouse Hsa21 orthologous genes.

Today, it is estimated that Hsa21 contains between 200 and 300 protein coding genes [117, 118] and just as many non-coding RNA genes [9, 119]. However, there are only 166 orthologous Hs21 genes found in mice across 3 mouse chromosomes (Mmu) – Mmu10, Mmu16,

and Mmu17 [25]. Mmu16 has the largest total number of conserved Hsa21 genes with an estimated 110 orthologous genes [25]. Mmu10 is thought to have next largest number syntenic Hsa21 genes with 37 orthologous genes and finally Mmu 17 with 19 orthologous genes (**Figure 3**). Thus, there have been several mouse models generated with sets of orthologous mouse genes of Hsa21 [120] and more recently the entire set (166 Hsa21 mouse orthologous genes) [121].

The most commonly used murine model of DS is Ts65Dn, developed in 1993 [20]. The Ts65Dn mouse has a partial trisomy of Hsa21 syntenic genes found on Mmu16 and contains approximately 92 of these orthologues [20]. Although this mouse model also contains an additional 60 genes from Mmu17 that are not syntenic to Hsa21 [20], the DS phenotypes have been well-characterized in Ts65Dn and many of its phenotypes mimic the molecular, cellular, physiological, and behavioral aspects of human DS [25], particularly the low bone mass phenotype [17]. Ts65Dn mice also recapitulate the cardiac, behavioral, craniofacial, myeloproliferative, and hypotonia phenotypes seen in DS [109, 122].

However, in an effort to generate a more complete trisomic 21 mouse model, Li and colleagues [26] duplicated the entire Hsa21 syntenic region of Mmu16 in a murine model for DS – Dp(16)1Yey (**Figure 3**). This murine model was also shown to have similar cardiovascular, gastrointestinal, and craniofacial phenotypes as Ts65Dn and human DS [26, 121]. However, the bone defects as in Ts65Dn is not well-characterized. Additionally, the same research team went on to establish other segmental trisomic murine models containing the entire Hsa21 syntenic region for Mmu 10 and Mmu17 [25]. More importantly, Yu and associates finally created a mouse model trisomic for all the Hsa21 syntenic regions of Mmu10, Mmu16, and Mmu17 by using cross-breeding techniques of the 3 models [123].



In contrast to segmental murine models of DS, the Tc1 murine model of DS contains a triplicate of human chromosome 21 generating a trans-species model of DS [19]. This “transchromosomal” model of DS contains ~83% of the genes found on Hsa21 (**Figure 3**) and presents with variable levels of mosaicism of the extra-chromosome in different tissues [25]. Even so, this model presents with similar, yet variable phenotypic alterations including cardiac, neuronal, and, behavioral abnormalities as seen in DS [19, 25, 124]. These models of DS and others provide opportunities to systematically study and understand the contributions of genotype to DS phenotypes. However, for us to pursue our goal of testing a potential bone anabolic agent that can be developed as a therapeutic agent in DS people, we need to utilize the best mouse model that recapitulates the mechanism and phenotypic bone loss observed in humans. Thus, Aim 1 in this dissertation in Chapter III will test whether the bone phenotype of the Dp16(1Yey) mouse model is superior to the Ts65Dn model we have already characterized.

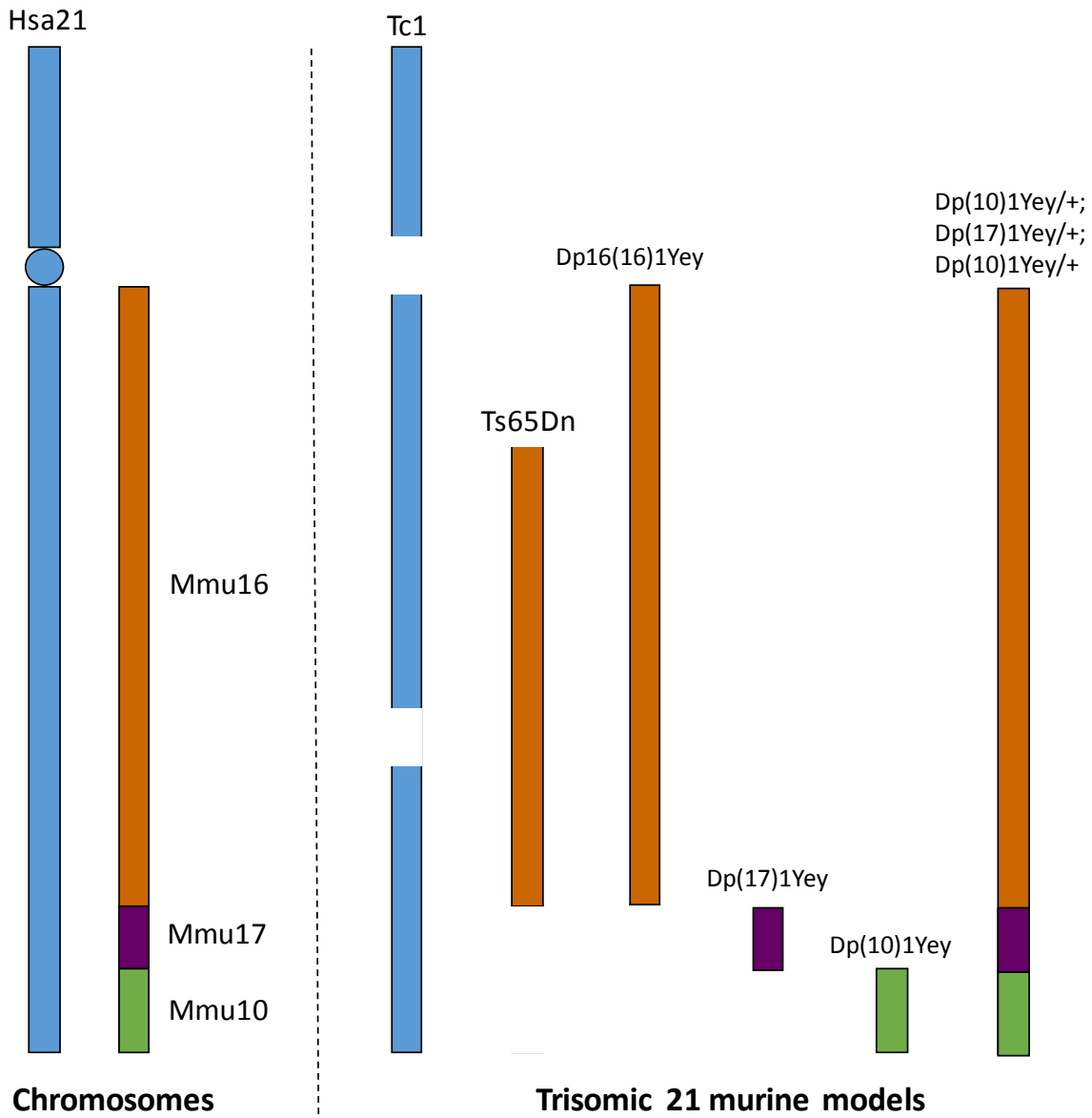


**Figure 3. Schematic representation of Hsa21 orthologous regions in mice and murine models of trisomy 21.** There are ~200-300 protein coding genes found on human chromosome 21. There are 166 orthologous Hsa21 genes found in mice, which are found on Mmu10 (37 genes), Mmu16 (110 genes), and Mmu17 (19 genes).

## Hypophosphatasia

Hypophosphatasia (HPP) was first identified by John C. Rathbun (a Canadian pediatrician) in 1948 after reporting the death of his infant patient who died with severe rickets and seizures [28, 125]. Rathbun discovered later at autopsy that the infant patient presented with paradoxically low serum alkaline phosphatase [126]. Given that high phosphatase levels are typically found in patients with rickets, Rathburn coined the disease hypophosphatasia due to the developmental anomaly that led to his patient's demise [127]. Shortly after, it became seemingly clear that HPP was a heritable disease. In 1953, premature loss of deciduous/primary teeth emerged as a hallmark of the disease clinical presentations [128]. Characterized by decreased activity of serum alkaline phosphatase [129], it was found that patients with HPP presented with increased concentrations of phosphoethanolamine (PEA) in 1955, high levels of urinary inorganic pyrophosphate (PPi) in 1965, and elevated plasma pyridoxal 5' phosphate (PLP) in 1985 – all of which were later determined to be substrates of tissue nonspecific alkaline phosphatase (TNSALP). And in 1988, the disease manifestations were determined to be due to a loss of function mutations in TNSALP gene (*ALPL*) [28, 125, 126].

### **Incidence, Prevalence, and Nosology**

Hypophosphatasia is rare disease that has a presence worldwide and affect many different races of people [125, 130]. However, HPP is most common in Canada with an estimated prevalence rate of 1 per 100,000 live births for the severe form of the disease [131]. Certain communities in Canada, such as the Mennonites in Manitoba, have been shown to have much higher rates, estimating to be about 1 in 2500 individuals affected [130]. In the United States, it is predicted that HPP affects 1 in every 300,000 for the severe and moderately severe forms [130]. According to the reported cases of HPP, it also appears that HPP is more prevalent in

Caucasian than African American populations with the incidence of disease rising in black population [130]. Additionally, cases of HPP have been reported in Japanese, Hispanic, and Chinese people [8, 130].

One of the most thought-provoking challenges of HPP is its extraordinary range of severity and broad expressivity of clinical phenotypes [8]. Case reports of patients with HPP have been instrumental in defining the clinical, biochemical, and radiological features of the disease [125, 132]. Its variable clinical presentation is organized into a nosology that includes seven major clinical forms (odonto, adult, childhood, infantile, perinatal, pseudo, and benign prenatal) with the childhood form further divided into either mild or more severe subcategories [129, 132, 133].

The clinical expression of HPP includes less severe phenotypes such as dental complications with no skeletal defects to severe manifestations such as death *in utero* [129, 132]. Odonto-hypophosphatasia (odontoHPP) refers to dental complications with no noticeable radiographic changes to the skeleton, which is considered the least severe form of HPP [28, 134, 135]. In the middle of the disease spectrum is childhood HPP, which presents after 6 months of age, but usually before adulthood [125, 131, 136]. The severity of childhood form of HPP can be very variable, which is why it includes phenotypes observed in both mild and more severe forms of HPP such as premature loss of a few deciduous teeth with few skeletal abnormalities, to premature loss of the complete set of deciduous teeth and rachitic deformities [128, 137]. Furthermore, on the more severe end the disease spectrum lies perinatal HPP which can manifest *in utero* and can be seen at birth as completely unmineralized skeletons and is almost always fatal without treatment [132]. Seizures, sometimes fatal, are also observed in this most severe form of HPP.

**Table 1.** Clinical forms of HPP and their clinical presentations [28, 125, 129, 132].

<b>Clinical Form</b>	<b>Typical age of presentation</b>	<b>Clinical phenotype</b>
Odonto HPP	Any	Premature loss of deciduous teeth; no radiological or histopathologic evidence of rickets or osteomalacia
Adult HPP	Middle age	Loss of adult dentition; recurrent metatarsal stress fracture (hip and thigh discomfort); osteomalacia; pseudogout; ossification of ligaments
Childhood HPP (mild)	After 6 months; before adulthood	Premature loss of 1 or more primary teeth; skeletal disease manifesting as osteomalacia
Childhood HPP (severe)	After 6 months; before adulthood	Premature loss of most or all primary teeth; rachitic deformities; bowed long bones and knock knees; enlarge joints due to metaphyseal flaring; osteomyelitis-like disease;
Infantile HPP	After perinatal period; before 6 months of age	Failure to thrive; delayed motor skills accompanied by signs of rickets; short skulls; hypercalciuria; progressive thoracic deformity and rib fractures that predispose to pneumonia; decreased skeletal mineralization accompanied by fractures and bone deformities; respiratory complications
Perinatal HPP	In utero and at birth	Hypomineralization; short and deformed limbs; pyridoxine-dependent seizures; bradycardia, myelophthisic anemia; hypoplastic lungs; extreme rickets
Pseudo HPP	Unclear	Similar clinical presentations as infantile with normal to high levels of serum ALP activity
Benign Prenatal	In utero, but with improvements at birth	Resembles perinatal HPP in utero, but improvements in skeletal defects and postnatally.

### **Alkaline Phosphatase and its substrates in HPP**

Today, HPP is known as an inborn error of metabolism that presents biochemically with low activity levels of the alkaline phosphatase isoenzyme tissue-nonspecific alkaline phosphatase (TNSALP). As previously noted, this biochemical hallmark reflects loss-of-function mutations within the *ALPL* gene that encodes TNSALP. The enzyme TNSALP is a cell-surface associated homodimeric phosphohydrolase, with significantly increased expression in the skeleton, liver, kidney and developing teeth. More than 300 known loss of function mutations in *ALPL* are

accompanied by a highly variable severity and clinical expression [28, 132]. In HPP, the accumulation of TNSALP substrates such as PPi, which is a potent inhibitor of mineralization. Specifically, TNSALP is the critical rate-limiting enzyme in the release of Pi from PPi to bind to calcium to form the hydroxyapatite crystals in mineralization [126]. The insufficient Pi causes mineralization defects, and is the basis for the dental and skeletal complications, including premature tooth loss and rickets in HPP. The accumulation of PLP is thought to contribute to the neurological consequences such as seizures observed in HPP [126]. However, the role of PEA in HPP pathology is well understood [126].

In humans, there are 4 isozymes of alkaline phosphatase including TNSALP. The 3 isozymes are tissue specific – placental, germ cells, and intestinal [138]. The 3 tissue specific alkaline phosphatase enzymes have 90-98% homology to one another [138] and these isozymes are not compromised in HPP [126]. However, TNSALP has only an approximate 50% identity to the other 3 isozymes [138]. Discovered in 1923 by Robert Robinson as a phosphatase abundant in bone, TNSALP functions as a homodimer with the monomer-monomer interface exhibiting strong hydrophobic character that is crucial for enzyme stability and function [126]. Additionally, the crown domain and the N-terminal  $\alpha$ -helix help to stabilize the dimer [126]. Therefore, any mutations in the monomer-monomer interface, the crown domain, or the N-terminal arm that alter amino residues can cause HPP [126, 139] (**Figure 4**).

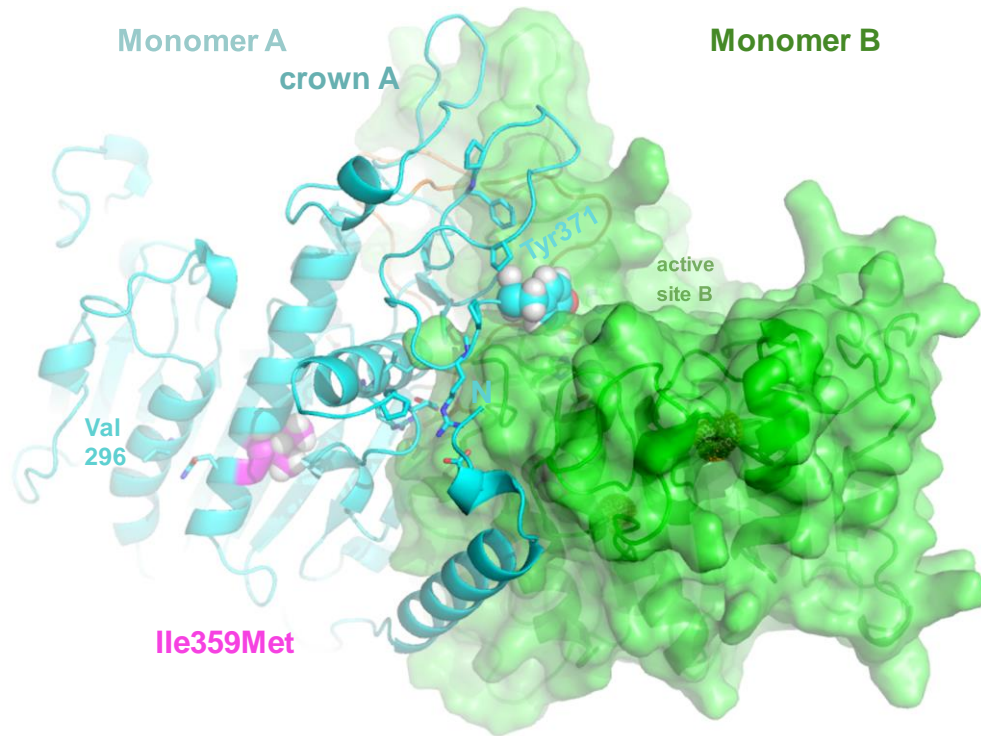


**Figure 4. Three-dimensional model of TNSALP with Ile359Met mutation.** The TNSALP dimer contains 2 monomers. The portion ribbon structure is shown for monomer A and it contains the Ile359Met mutation.

The current models of HPP have been engineered exclusively in mice harboring loss of function null mutations [139]. Although useful for modeling many of the metabolic and skeletal defects, murine models harboring *ALPL* mutations do not faithfully represent the broad spectrum of human HPP clinical presentations such as loss of deciduous teeth. This is partly due to the limiting physical and physiological differences such as size and gene expression and regulation. Due to the loss of deciduous teeth and presence of osteonal bone remodeling in the sheep, we hypothesize that a sheep model of HPP can be generated using CRISPR/Cas9 and will better phenocopy human HPP than mouse.

#### Specific Aims

**Specific Aim 1: Characterize the skeletal phenotype of Dp(16)1Yey DS mice.** Hypothesis: Dp(16)1Yey DS mice will phenocopy the low bone mass phenotype exhibited in human and Ts65Dn DS populations. The limited availability of DS murine models and the differences in phenotypic characteristics of current murine models that recapitulate many, but not all of those in human DS can be problematic in defining bone health guidelines for this population. Therefore, the identification of a low bone mass phenotype in another murine DS model will be advantageous. Like Ts65Dn, the Dp(16)1Yey mouse is trisomic for many of the same genes. Thus, we will employ our well-established model for skeletal phenotyping to characterize the bone phenotype of Dp(16)1Yey mice. These measures include *ex vivo* bone marrow cultures,  $\mu$ CT analyses, biochemical marker assays and bone histomorphometry.

**Specific Aim 2: Evaluate the efficacy of sclerostin antibody treatment to improve bone mass in Ts65Dn DS mice.** Hypothesis: Given the low BMD and low bone turnover states of both DS humans and Ts65Dn mice with no significant differences in sclerostin levels, sclerostin will be an efficacious therapeutic target for improving bone mass in DS. Our previous studies showed that intermittent PTH, the only approved bone anabolic treatment, significantly increased BMD in Ts65Dn mice. However, stopping PTH treatment causes dramatic reductions in bone mass; thus leading to our current hypothesis on the effects of sclerostin antibody (bone anabolic therapy) on BMD in Ts65Dn. Importantly, preliminary pilot studies showed that (SclAb) normalized whole body and spine BMD. To ascertain the duration of Scl-Ab action, male Ts(17<sup>16</sup>)65Dn (Ts65Dn) mice and wild-type (WT) mice were given 4 weekly injections of either sclerostin antibody (SclAb) or vehicle (VEH) (n=4-6/group each) for a total of four groups. Skeletal analysis by DXA,  $\mu$ CT, histology/histomorphometry, and *ex vivo* bone marrow cultures were performed.



**Specific Aim 3: Genetically engineer a large animal model of Hypophosphatasia in sheep using CRISPR/Cas9.** Hypothesis: TNSALP mutation-specific edits in sheep utilizing CRISPR/Cas9 would produce a model that accurately phenocopies the bone and tooth pathophysiology in the HPP. We have identified 4 different human variants of HPP we wish to model in sheep. Two are from an index patient with two distinct mutations in the *ALPL* gene [Alanine (GCC) → Threonine (ACC) in exon 5 (c.346 G>A) and Isoleucine (ATC) → Methionine (ATG) in exon 10 (c.1077 C>G)] that has a mild bone phenotype, with the primary defects being rhizomelia and early loss of deciduous teeth. Additional infantile lethal *ALPL* mutations Glutamine → Lysine at exon 6 (c.571G>A) and Aspartic Acid → Valine (c.1133A>T) at exon 10 were recurrent in patients with mild HPP. Thus, we will determine the efficiency of CRISPR Cas9 system to genetically edit TNSALP in sheep and characterize the novel genetically modified sheep bone phenotype.

## References

1. Griggs RC, Batshaw M, Dunkle M, Gopal-Srivastava R, Kaye E, Krischer J, et al. Clinical research for rare disease: opportunities, challenges, and solutions. *Mol Genet Metab.* 2009;96(1):20-6.
2. Boycott KM, Vanstone MR, Bulman DE, MacKenzie AE. Rare-disease genetics in the era of next-generation sequencing: discovery to translation. *Nat Rev Genet.* 2013;14(10):681-91.
3. Farber CR, Clemens TL. Contemporary Approaches for Identifying Rare Bone Disease Causing Genes. *Bone Res.* 2013;1:301-10.
4. Drake MT, Collins MT, Hsiao EC. The Rare Bone Disease Working Group: report from the 2016 American Society for Bone and Mineral Research Annual Meeting. *Bone.* 2017;102:80-4.

5. Amor IM, Rauch F, Gruenwald K, Weis M, Eyre DR, Roughley P, et al. Severe osteogenesis imperfecta caused by a small in-frame deletion in CRTAP. *Am J Med Genet A*. 2011;155A(11):2865-70.
6. Memin Y, Hiltenbrand C, Giudicelli C, Papillaud J. [A rare genotypic bone disease: "pseudohypoparathyroidism" (a new case in a 60-year-old man)]. *Rev Rhum Mal Osteoartic*. 1970;37(8):571-5.
7. Rai H, Pai SM, Dayakar A, Javagal V. A rare incident of Paget's disease of bone in early adult life. *J Oral Maxillofac Pathol*. 2014;18(Suppl 1):S147-50.
8. Whyte MP. Hypophosphatasia: Enzyme Replacement Therapy Brings New Opportunities and New Challenges. *J Bone Miner Res*. 32(4):667-75.
9. Keck-Wherley J, Grover D, Bhattacharyya S, Xu X, Holman D, Lombardini ED, et al. Abnormal microRNA expression in Ts65Dn hippocampus and whole blood: contributions to Down syndrome phenotypes. *Dev Neurosci*. 2011;33(5):451-67.
10. Costa R, De Miguel R, Garcia C, de Asua DR, Castaneda S, Moldenhauer F, et al. Bone Mass Assessment in a Cohort of Adults With Down Syndrome: A Cross-Sectional Study. *Intellect Dev Disabil*. 2017;55(5):315-24.
11. Sakadamis A, Angelopoulou N, Matziari C, Papameletiou V, Souftas V. Bone mass, gonadal function and biochemical assessment in young men with trisomy 21. *Eur J Obstet Gynecol Reprod Biol*. 2002;100(2):208-12.
12. Stefanidis K, Belitsos P, Fotinos A, Makris N, Loutradis D, Antsaklis A. Causes of infertility in men with Down syndrome. *Andrologia*. 2011;43(5):353-7.
13. Antonarakis SE, Lyle R, Dermitzakis ET, Reymond A, Deutsch S. Chromosome 21 and down syndrome: from genomics to pathophysiology. *Nat Rev Genet*. 2004;5(10):725-38.
14. Glasson EJ, Sullivan SG, Hussain R, Petterson BA, Montgomery PD, Bittles AH. The changing survival profile of people with Down's syndrome: implications for genetic counselling. *Clin Genet*. 2002;62(5):390-3.
15. Bittles AH, Glasson EJ. Clinical, social, and ethical implications of changing life expectancy in Down syndrome. *Dev Med Child Neurol*. 2004;46(4):282-6.

16. Guijarro M, Valero C, Paule B, Gonzalez-Macias J, Riancho JA. Bone mass in young adults with Down syndrome. *J Intellect Disabil Res.* 2008;52(Pt 3):182-9.
17. Fowler TW, McKelvey KD, Akel NS, Vander Schilden J, Bacon AW, Bracey JW, et al. Low bone turnover and low BMD in Down syndrome: effect of intermittent PTH treatment. *PLoS One.* 2012;7(8):e42967.
18. McKelvey KD, Fowler TW, Akel NS, Kelsay JA, Gaddy D, Wenger GR, et al. Low bone turnover and low bone density in a cohort of adults with Down syndrome. *Osteoporos Int.* 2013;24(4):1333-8.
19. O'Doherty A, Ruf S, Mulligan C, Hildreth V, Errington ML, Cooke S, et al. An aneuploid mouse strain carrying human chromosome 21 with Down syndrome phenotypes. *Science.* 2005;309(5743):2033-7.
20. Davisson MT, Schmidt C, Reeves RH, Irving NG, Akeson EC, Harris BS, et al. Segmental trisomy as a mouse model for Down syndrome. *Prog Clin Biol Res.* 1993;384:117-33.
21. Richtsmeier JT, Zumwalt A, Carlson EJ, Epstein CJ, Reeves RH. Craniofacial phenotypes in segmentally trisomic mouse models for Down syndrome. *Am J Med Genet.* 2002;107(4):317-24.
22. Sanders NC, Williams DK, Wenger GR. Does the learning deficit observed under an incremental repeated acquisition schedule of reinforcement in Ts65Dn mice, a model for Down syndrome, change as they age? *Behav Brain Res.* 2009;203(1):137-42.
23. Hill CA, Reeves RH, Richtsmeier JT. Effects of aneuploidy on skull growth in a mouse model of Down syndrome. *J Anat.* 2007;210(4):394-405.
24. Reeves RH, Irving NG, Moran TH, Wohn A, Kitt C, Sisodia SS, et al. A mouse model for Down syndrome exhibits learning and behaviour deficits. *Nat Genet.* 1995;11(2):177-84.
25. Rueda N, Florez J, Martinez-Cue C. Mouse models of Down syndrome as a tool to unravel the causes of mental disabilities. *Neural Plast.* 2012;2012:584071.

26. Li Z, Yu T, Morishima M, Pao A, LaDuca J, Conroy J, et al. Duplication of the entire 22.9 Mb human chromosome 21 syntenic region on mouse chromosome 16 causes cardiovascular and gastrointestinal abnormalities. *Hum Mol Genet.* 2007;16(11):1359-66.
27. Fedde KN, Michell MP, Henthorn PS, Whyte MP. Aberrant properties of alkaline phosphatase in patient fibroblasts correlate with clinical expressivity in severe forms of hypophosphatasia. *J Clin Endocrinol Metab.* 1996;81(7):2587-94.
28. Bianchi ML. Hypophosphatasia: an overview of the disease and its treatment. *Osteoporos Int.* 2015;26(12):2743-57.
29. Whyte MP. Hypophosphatasia - aetiology, nosology, pathogenesis, diagnosis and treatment. *Nat Rev Endocrinol.* 2016;12(4):233-46.
30. Whyte MP, Murphy WA, Fallon MD. Adult hypophosphatasia with chondrocalcinosis and arthropathy. Variable penetrance of hypophosphatasemia in a large Oklahoma kindred. *Am J Med.* 1982;72(4):631-41.
31. Whyte MP, Madson KL, Phillips D, Reeves AL, McAlister WH, Yakimoski A, et al. Asfotase alfa therapy for children with hypophosphatasia. *JCI Insight.*1(9):e85971.
32. Zarrinkalam MR, Beard H, Schultz CG, Moore RJ. Validation of the sheep as a large animal model for the study of vertebral osteoporosis. *Eur Spine J.* 2009;18(2):244-53.
33. Parfitt AM. The cellular basis of bone remodeling: the quantum concept reexamined in light of recent advances in the cell biology of bone. *Calcif Tissue Int.* 1984;36 Suppl 1:S37-45.
34. Hadjidakis DJ, Androulakis, II. Bone remodeling. *Ann N Y Acad Sci.* 2006;1092:385-96.
35. Seeman E. Bone modeling and remodeling. *Crit Rev Eukaryot Gene Expr.* 2009;19(3):219-33.
36. Migliaccio S, Falcone S, Spera G. Bone modeling and remodeling: from biology to clinical application. *Aging Clin Exp Res.* 2004;16 Suppl(3):20-2.

37. Langdahl B, Ferrari S, Dempster DW. Bone modeling and remodeling: potential as therapeutic targets for the treatment of osteoporosis. *Ther Adv Musculoskelet Dis.* 2016;8(6):225-35.
38. Rodan GA, Martin TJ. Role of osteoblasts in hormonal control of bone resorption - a hypothesis. *Calcif Tissue Int.* 1982;34(3):311.
39. Divieti Pajevic P, Krause DS. Osteocyte regulation of bone and blood. *Bone.* 2018.
40. Suva LJ, Gaddy D, Perrien DS, Thomas RL, Findlay DM. Regulation of bone mass by mechanical loading: microarchitecture and genetics. *Curr Osteoporos Rep.* 2005;3(2):46-51.
41. Sims NA, Martin TJ. Coupling the activities of bone formation and resorption: a multitude of signals within the basic multicellular unit. *Bonekey Rep.* 2014;3:481.
42. Takayanagi H. The role of NFAT in osteoclast formation. *Ann N Y Acad Sci.* 2007;1116:227-37.
43. Maggioli C, Stagi S. Bone modeling, remodeling, and skeletal health in children and adolescents: mineral accrual, assessment and treatment. *Ann Pediatr Endocrinol Metab.* 2017;22(1):1-5.
44. Hawli Y, Nasrallah M, El-Hajj Fuleihan G. Endocrine and musculoskeletal abnormalities in patients with Down syndrome. *Nat Rev Endocrinol.* 2009;5(6):327-34.
45. Perrien DS, Akel NS, Edwards PK, Carver AA, Bendre MS, Swain FL, et al. Inhibin A is an endocrine stimulator of bone mass and strength. *Endocrinology.* 2007;148(4):1654-65.
46. Komarova SV. Bone remodeling in health and disease: lessons from mathematical modeling. *Ann N Y Acad Sci.* 2006;1068:557-9.
47. Lazner F, Gowen M, Pavasovic D, Kola I. Osteopetrosis and osteoporosis: two sides of the same coin. *Hum Mol Genet.* 1999;8(10):1839-46.

48. Kreipke TC, Rivera NC, Garrison JG, Easley JT, Turner AS, Niebur GL. Alterations in trabecular bone microarchitecture in the ovine spine and distal femur following ovariectomy. *J Biomech.* 2014;47(8):1918-21.
49. Delmas PD, Vergnaud P, Arlot ME, Pastoureau P, Meunier PJ, Nilssen MH. The anabolic effect of human PTH (1-34) on bone formation is blunted when bone resorption is inhibited by the bisphosphonate tiludronate--is activated resorption a prerequisite for the in vivo effect of PTH on formation in a remodeling system? *Bone.* 1995;16(6):603-10.
50. Franz-Odenaal TA, Hall BK, Witten PE. Buried alive: how osteoblasts become osteocytes. *Dev Dyn.* 2006;235(1):176-90.
51. Buenzli PR. Osteocytes as a record of bone formation dynamics: a mathematical model of osteocyte generation in bone matrix. *J Theor Biol.* 2015;364:418-27.
52. Manolagas SC, Parfitt AM. For whom the bell tolls: distress signals from long-lived osteocytes and the pathogenesis of metabolic bone diseases. *Bone.* 2013;54(2):272-8.
53. Florencio-Silva R, Sasso GR, Sasso-Cerri E, Simoes MJ, Cerri PS. Biology of Bone Tissue: Structure, Function, and Factors That Influence Bone Cells. *Biomed Res Int.* 2015;2015:421746.
54. Main RP. Osteocytes and the bone lacunar-canalicular system: Insights into bone biology and skeletal function using bone tissue microstructure. *Int J Paleopathol.* 2017;18:44-6.
55. Joeng KS, Lee YC, Lim J, Chen Y, Jiang MM, Munivez E, et al. Osteocyte-specific WNT1 regulates osteoblast function during bone homeostasis. *J Clin Invest.* 2017;127(7):2678-88.
56. Nakashima T, Hayashi M, Fukunaga T, Kurata K, Oh-Hora M, Feng JQ, et al. Evidence for osteocyte regulation of bone homeostasis through RANKL expression. *Nat Med.* 2011;17(10):1231-4.
57. Xiong J, Piemontese M, Thostenson JD, Weinstein RS, Manolagas SC, O'Brien CA. Osteocyte-derived RANKL is a critical mediator of the increased bone resorption caused by dietary calcium deficiency. *Bone.* 2014;66:146-54.

58. Xiong J, Piemontese M, Onal M, Campbell J, Goellner JJ, Dusevich V, et al. Osteocytes, not Osteoblasts or Lining Cells, are the Main Source of the RANKL Required for Osteoclast Formation in Remodeling Bone. *PLoS One*. 2015;10(9):e0138189.
59. Fujiwara Y, Piemontese M, Liu Y, Thostenson JD, Xiong J, O'Brien CA. RANKL (Receptor Activator of NFkappaB Ligand) Produced by Osteocytes Is Required for the Increase in B Cells and Bone Loss Caused by Estrogen Deficiency in Mice. *J Biol Chem*. 2016;291(48):24838-50.
60. Baron R, Kneissel M. WNT signaling in bone homeostasis and disease: from human mutations to treatments. *Nat Med*. 2013;19(2):179-92.
61. Song W, Qian L, Jing G, Jie F, Xiaosong S, Chunhui L, et al. Aberrant expression of the sFRP and WIF1 genes in invasive non-functioning pituitary adenomas. *Mol Cell Endocrinol*. 2018.
62. Clines GA, Mohammad KS, Bao Y, Stephens OW, Suva LJ, Shaughnessy JD, Jr., et al. Dickkopf homolog 1 mediates endothelin-1-stimulated new bone formation. *Mol Endocrinol*. 2007;21(2):486-98.
63. McDonald MM, Reagan MR, Youlten SE, Mohanty ST, Seckinger A, Terry RL, et al. Inhibiting the osteocyte-specific protein sclerostin increases bone mass and fracture resistance in multiple myeloma. *Blood*. 2017;129(26):3452-64.
64. Sinnberg T, Levesque MP, Krochmann J, Cheng PF, Ikenberg K, Meraz-Torres F, et al. Wnt-signaling enhances neural crest migration of melanoma cells and induces an invasive phenotype. *Mol Cancer*. 2018;17(1):59.
65. Capulli M, Paone R, Rucci N. Osteoblast and osteocyte: games without frontiers. *Arch Biochem Biophys*. 2014;561:3-12.
66. Spector JA, Greenwald JA, Warren SM, Bouletreau PJ, Crisera FE, Mehrara BJ, et al. Co-culture of osteoblasts with immature dural cells causes an increased rate and degree of osteoblast differentiation. *Plast Reconstr Surg*. 2002;109(2):631-42; discussion 43-4.
67. Nakashima K, de Crombrughe B. Transcriptional mechanisms in osteoblast differentiation and bone formation. *Trends Genet*. 2003;19(8):458-66.

68. Komori T. [Cbfa1/Runx2, an essential transcription factor for the regulation of osteoblast differentiation]. *Nihon Rinsho*. 2002;60 Suppl 3:91-7.
69. Teitelbaum SL, Ross FP. Genetic regulation of osteoclast development and function. *Nat Rev Genet*. 2003;4(8):638-49.
70. Zhang J, Zhang X, Zhang L, Zhou F, van Dinther M, Ten Dijke P. LRP8 mediates Wnt/beta-catenin signaling and controls osteoblast differentiation. *J Bone Miner Res*. 2012;27(10):2065-74.
71. Day TF, Guo X, Garrett-Beal L, Yang Y. Wnt/beta-catenin signaling in mesenchymal progenitors controls osteoblast and chondrocyte differentiation during vertebrate skeletogenesis. *Dev Cell*. 2005;8(5):739-50.
72. Saidak Z, Le Henaff C, Azzi S, Marty C, Da Nascimento S, Sonnet P, et al. Wnt/beta-catenin signaling mediates osteoblast differentiation triggered by peptide-induced alpha5beta1 integrin priming in mesenchymal skeletal cells. *J Biol Chem*. 2015;290(11):6903-12.
73. Lavrentieva A, Hatlapatka T, Neumann A, Weyand B, Kasper C. Potential for osteogenic and chondrogenic differentiation of MSC. *Adv Biochem Eng Biotechnol*. 2013;129:73-88.
74. Posa F, Di Benedetto A, Cavalcanti-Adam EA, Colaianni G, Porro C, Trotta T, et al. Vitamin D Promotes MSC Osteogenic Differentiation Stimulating Cell Adhesion and alphaVbeta3 Expression. *Stem Cells Int*. 2018;2018:6958713.
75. Jing Y, Zhang JC, Li ST, Zhao JH, Wang J, Han XF, et al. Wnt/beta-catenin pathway might underlie the MET in trans- differentiation from MSC to MSC-derived neuron. *Zhongguo Ying Yong Sheng Li Xue Za Zhi*. 2015;31(6):572-6.
76. Du Y, Ling J, Wei X, Ning Y, Xie N, Gu H, et al. Wnt/beta-catenin signaling participates in cementoblast/osteoblast differentiation of dental follicle cells. *Connect Tissue Res*. 2012;53(5):390-7.
77. Staudacher JJ, Bauer J, Jana A, Tian J, Carroll T, Mancinelli G, et al. Activin signaling is an essential component of the TGF-beta induced pro-metastatic phenotype in colorectal cancer. *Sci Rep*. 2017;7(1):5569.



78. Massague J, Chen YG. Controlling TGF-beta signaling. *Genes Dev.* 2000;14(6):627-44.
79. Grafe I, Yang T, Alexander S, Homan EP, Lietman C, Jiang MM, et al. Excessive transforming growth factor-beta signaling is a common mechanism in osteogenesis imperfecta. *Nat Med.* 2014;20(6):670-5.
80. Fagenholz PJ, Warren SM, Greenwald JA, Bouletreau PJ, Spector JA, Crisera FE, et al. Osteoblast gene expression is differentially regulated by TGF-beta isoforms. *J Craniofac Surg.* 2001;12(2):183-90.
81. Mohammad KS, Chen CG, Balooch G, Stebbins E, McKenna CR, Davis H, et al. Pharmacologic inhibition of the TGF-beta type I receptor kinase has anabolic and anti-catabolic effects on bone. *PLoS One.* 2009;4(4):e5275.
82. Bonewald LF, Mundy GR. Role of transforming growth factor-beta in bone remodeling. *Clin Orthop Relat Res.* 1990(250):261-76.
83. Mundy GR, Bonewald LF. Role of TGF beta in bone remodeling. *Ann N Y Acad Sci.* 1990;593:91-7.
84. Bonewald LF, Schwartz Z, Swain LD, Ramirez V, Poser J, Boyan BD. Stimulation of plasma membrane and matrix vesicle enzyme activity by transforming growth factor-beta in osteosarcoma cell cultures. *J Cell Physiol.* 1990;145(2):200-6.
85. Aslan H, Ravid-Amir O, Clancy BM, Rezvankhah S, Pittman D, Pelled G, et al. Advanced molecular profiling in vivo detects novel function of dickkopf-3 in the regulation of bone formation. *J Bone Miner Res.* 2006;21(12):1935-45.
86. Hassan MQ, Tare RS, Lee SH, Mandeville M, Morasso MI, Javed A, et al. BMP2 commitment to the osteogenic lineage involves activation of Runx2 by DLX3 and a homeodomain transcriptional network. *J Biol Chem.* 2006;281(52):40515-26.
87. Zylbersztejn F, Flores-Violante M, Voeltzel T, Nicolini FE, Lefort S, Maguer-Satta V. The BMP pathway: A unique tool to decode the origin and progression of leukemia. *Exp Hematol.* 2018;61:36-44.
88. Salazar VS, Gamer LW, Rosen V. BMP signalling in skeletal development, disease and repair. *Nat Rev Endocrinol.* 2016;12(4):203-21.

89. Onal M, Bajin MD, Yilmaz T. Fibrodysplasia ossificans progressiva: a case report. *Turk J Pediatr.* 2014;56(5):561-4.
90. Maftai C, Rypens F, Thiffault I, Dube J, Laberge AM, Lemyre E. Fibrodysplasia ossificans progressiva: bilateral hallux valgus on ultrasound a clue for the first prenatal diagnosis for this condition-clinical report and review of the literature. *Prenat Diagn.* 2015;35(3):305-7.
91. Morales-Piga A, Bachiller-Corral J, Gonzalez-Herranz P, Medrano-SanIldelfonso M, Olmedo-Garzon J, Sanchez-Duffhues G. Osteochondromas in fibrodysplasia ossificans progressiva: a widespread trait with a streaking but overlooked appearance when arising at femoral bone end. *Rheumatol Int.* 2015;35(10):1759-67.
92. Lu G, Tandang-Silvas MR, Dawson AC, Dawson TJ, Groppe JC. Hypoxia-selective allosteric destabilization of activin receptor-like kinases: A potential therapeutic avenue for prophylaxis of heterotopic ossification. *Bone.* 2018;112:71-89.
93. Crockett JC, Rogers MJ, Coxon FP, Hocking LJ, Helfrich MH. Bone remodelling at a glance. *J Cell Sci.* 2011;124(Pt 7):991-8.
94. Bellon M, Ko NL, Lee MJ, Yao Y, Waldmann TA, Trepel JB, et al. Adult T-cell leukemia cells overexpress Wnt5a and promote osteoclast differentiation. *Blood.* 2013;121(25):5045-54.
95. Bendre M, Gaddy D, Nicholas RW, Suva LJ. Breast cancer metastasis to bone: it is not all about PTHrP. *Clin Orthop Relat Res.* 2003(415 Suppl):S39-45.
96. Gaddy-Kurten D, Coker JK, Abe E, Jilka RL, Manolagas SC. Inhibin suppresses and activin stimulates osteoblastogenesis and osteoclastogenesis in murine bone marrow cultures. *Endocrinology.* 2002;143(1):74-83.
97. Kamalakar A, Washam CL, Akel NS, Allen BJ, Williams DK, Swain FL, et al. PTHrP(12-48) Modulates the Bone Marrow Microenvironment and Suppresses Human Osteoclast Differentiation and Lifespan. *J Bone Miner Res.* 2017;32(7):1421-31.
98. Boyle WJ, Simonet WS, Lacey DL. Osteoclast differentiation and activation. *Nature.* 2003;423(6937):337-42.

99. Down JL. Observations on an ethnic classification of idiots. 1866. *Ment Retard.* 1995;33(1):54-6.
100. Hickey F, Hickey E, Summar KL. Medical update for children with Down syndrome for the pediatrician and family practitioner. *Adv Pediatr.* 2012;59(1):137-57.
101. Karamanou M, Kanavakis E, Mavrou A, Petridou E, Androutsos G. Jerome Lejeune (1926-1994): father of modern genetics. *Acta Med Hist Adriat.* 2012;10(2):311-6.
102. Kamalakar A, Harris JR, McKelvey KD, Suva LJ. Aneuploidy and skeletal health. *Curr Osteoporos Rep.* 2014;12(3):376-82.
103. Wiseman FK, Alford KA, Tybulewicz VL, Fisher EM. Down syndrome--recent progress and future prospects. *Hum Mol Genet.* 2009;18(R1):R75-83.
104. Hernandez-Gonzalez S, Ballestin R, Lopez-Hidalgo R, Gilabert-Juan J, Blasco-Ibanez JM, Crespo C, et al. Altered distribution of hippocampal interneurons in the murine Down Syndrome model Ts65Dn. *Neurochem Res.* 2015;40(1):151-64.
105. Carfi A, Antocicco M, Brandi V, Cipriani C, Fiore F, Mascia D, et al. Characteristics of adults with down syndrome: prevalence of age-related conditions. *Front Med (Lausanne).* 2014;1:51.
106. Hill CA, Sussan TE, Reeves RH, Richtsmeier JT. Complex contributions of *Ets2* to craniofacial and thymus phenotypes of trisomic "Down syndrome" mice. *Am J Med Genet A.* 2009;149A(10):2158-65.
107. Devenny DA, Wegiel J, Schupf N, Jenkins E, Zigman W, Krinsky-McHale SJ, et al. Dementia of the Alzheimer's type and accelerated aging in Down syndrome. *Sci Aging Knowledge Environ.* 2005;2005(14):dn1.
108. Roy A, Roberts I, Norton A, Vyas P. Acute megakaryoblastic leukaemia (AMKL) and transient myeloproliferative disorder (TMD) in Down syndrome: a multi-step model of myeloid leukaemogenesis. *Br J Haematol.* 2009;147(1):3-12.
109. Blazek JD, Malik AM, Tischbein M, Arbones ML, Moore CS, Roper RJ. Abnormal mineralization of the Ts65Dn Down syndrome mouse appendicular skeleton begins

- during embryonic development in a Dyrk1a-independent manner. *Mech Dev.* 2015;136:133-42.
110. Gonzalez-Aguero A, Vicente-Rodriguez G, Moreno LA, Casajus JA. Bone mass in male and female children and adolescents with Down syndrome. *Osteoporos Int.* 2011;22(7):2151-7.
  111. Kao CH, Chen CC, Wang SJ, Yeh SH. Bone mineral density in children with Down's syndrome detected by dual photon absorptiometry. *Nucl Med Commun.* 1992;13(10):773-5.
  112. Baptista F, Varela A, Sardinha LB. Bone mineral mass in males and females with and without Down syndrome. *Osteoporos Int.* 2005;16(4):380-8.
  113. Roper RJ, Reeves RH. Understanding the basis for Down syndrome phenotypes. *PLoS Genet.* 2006;2(3):e50.
  114. Pritchard MA, Kola I. The "gene dosage effect" hypothesis versus the "amplified developmental instability" hypothesis in Down syndrome. *J Neural Transm Suppl.* 1999;57:293-303.
  115. Jiang J, Jing Y, Cost GJ, Chiang JC, Kolpa HJ, Cotton AM, et al. Translating dosage compensation to trisomy 21. *Nature.* 2013;500(7462):296-300.
  116. Olson LE, Richtsmeier JT, Leszl J, Reeves RH. A chromosome 21 critical region does not cause specific Down syndrome phenotypes. *Science.* 2004;306(5696):687-90.
  117. Lana-Elola E, Watson-Scales SD, Fisher EM, Tybulewicz VL. Down syndrome: searching for the genetic culprits. *Dis Model Mech.* 2011;4(5):586-95.
  118. Xing Z, Li Y, Pao A, Bennett AS, Tycko B, Mobley WC, et al. Mouse-based genetic modeling and analysis of Down syndrome. *Br Med Bull.* 2016;120(1):111-22.
  119. Karaca E, Aykut A, Erturk B, Durmaz B, Guler A, Buke B, et al. MicroRNA Expression Profile in the Prenatal Amniotic Fluid Samples of Pregnant Women with Down Syndrome. *Balkan Med J.* 2018;35(2):163-6.

120. Olson LE, Roper RJ, Baxter LL, Carlson EJ, Epstein CJ, Reeves RH. Down syndrome mouse models Ts65Dn, Ts1Cje, and Ms1Cje/Ts65Dn exhibit variable severity of cerebellar phenotypes. *Dev Dyn*. 2004;230(3):581-9.
121. Starbuck JM, Dutka T, Ratliff TS, Reeves RH, Richtsmeier JT. Overlapping trisomies for human chromosome 21 orthologs produce similar effects on skull and brain morphology of Dp(16)1Yey and Ts65Dn mice. *Am J Med Genet A*. 2014;164A(8):1981-90.
122. Delabar JM, Aflalo-Rattenbac R, Creau N. Developmental defects in trisomy 21 and mouse models. *ScientificWorldJournal*. 2006;6:1945-64.
123. Yu T, Li Z, Jia Z, Clapcote SJ, Liu C, Li S, et al. A mouse model of Down syndrome trisomic for all human chromosome 21 syntenic regions. *Hum Mol Genet*. 2010;19(14):2780-91.
124. Gardiner K, Fortna A, Bechtel L, Davisson MT. Mouse models of Down syndrome: how useful can they be? Comparison of the gene content of human chromosome 21 with orthologous mouse genomic regions. *Gene*. 2003;318:137-47.
125. Whyte MP. Hypophosphatasia - aetiology, nosology, pathogenesis, diagnosis and treatment. *Nat Rev Endocrinol*. 12(4):233-46.
126. Millan JL, Whyte MP. Alkaline Phosphatase and Hypophosphatasia. *Calcif Tissue Int*. 98(4):398-416.
127. Rathbun JC. Hypophosphatasia; a new developmental anomaly. *Am J Dis Child*. 1948;75(6):822-31.
128. Sobel EH, Clark LC, Jr., Fox RP, Robinow M. Rickets, deficiency of alkaline phosphatase activity and premature loss of teeth in childhood. *Pediatrics*. 1953;11(4):309-22.
129. Whyte MP, Coburn SP, Ryan LM, Ericson KL, Zhang F. Hypophosphatasia: Biochemical hallmarks validate the expanded pediatric clinical nosology. *Bone*. 2018;110:96-106.
130. Whyte MP. Hypophosphatasia: An overview For 2017. *Bone*. 2017;102:15-25.

131. Fraser D. Hypophosphatasia. *Am J Med.* 1957;22(5):730-46.
132. Siller AF, Whyte MP. Alkaline Phosphatase: Discovery and Naming of Our Favorite Enzyme. *J Bone Miner Res.* 2018;33(2):362-4.
133. Camacho PM, Mazhari AM, Wilczynski C, Kadanoff R, Mumm S, Whyte MP. Adult Hypophosphatasia Treated with Teriparatide: Report of 2 Patients and Review of the Literature. *Endocr Pract.* 2016;22(8):941-50.
134. Millan JL, Plotkin H. Hypophosphatasia - pathophysiology and treatment. *Actual osteol.*8(3):164-82.
135. Rodrigues TL, Foster BL, Silverio KG, Martins L, Casati MZ, Sallum EA, et al. Hypophosphatasia-associated deficiencies in mineralization and gene expression in cultured dental pulp cells obtained from human teeth. *J Endod.*38(7):907-12.
136. Ukarapong S, Ganapathy SS, Haidet J, Berkovitz G. Childhood hypophosphatasia with homozygous mutation of ALPL. *Endocr Pract.* 2014;20(10):e198-201.
137. Whyte MP, Wenkert D, Zhang F. Hypophosphatasia: Natural history study of 101 affected children investigated at one research center. *Bone.*93:125-38.
138. Mornet E. Molecular Genetics of Hypophosphatasia and Phenotype-Genotype Correlations. *Subcell Biochem.* 2015;76:25-43.
139. Fedde KN, Blair L, Silverstein J, Coburn SP, Ryan LM, Weinstein RS, et al. Alkaline phosphatase knock-out mice recapitulate the metabolic and skeletal defects of infantile hypophosphatasia. *J Bone Miner Res.* 1999;14(12):2015-26.

## CHAPTER II

### MATERIALS AND DETAILED METHODS

This chapter describes the detailed methods and materials used for experimental design and analysis throughout the work presented in this dissertation. However, the study design and specific procedures applicable to the experiment described in individual chapters will be described in the appropriate chapter.

#### **Animals**

All animal studies performed in this dissertation were approved by the Institutional Animal Care and Use Committee (IACUC) at either Texas A&M University or the University of Arkansas for Medical Science (UAMS). All animal handling and experimentation were conducted in compliance with the recommendations of the National Institutes of Health Guide for the Care and Use of Laboratory Animals.

*Mice:* Male B6EiC3Sn a/A-Ts (17<sup>16</sup>)65Dn/J (hereafter called Ts65Dn); male and female B6.129S7-Dp(16Lipi-Zbtb21)1Yey/J (hereafter called Dp16), and age-matched littermate wildtype (WT) mice were ordered from Jackson Laboratory (Bar Harbor, ME) at 6-10 weeks of age. Mice were singly or group housed in cages of no more than 5 mice and fed food and water *ad libitum*. As required male mice were housed individually due to behavioral issues.

*Sheep:* Donor and recipient ewes (female sheep) were utilized for embryo collection and embryo transfer – respectively. Semen was collected from rams (male sheep) by standard electro-ejaculation [1]. To collect semen, the ram was manually restrained at the front and back to prevent movement and a rectal exam was administered while cleaning away fecal matter. A 75mm rectal probe was then placed in the ram and gradual increasing pulses of stimulus (2-3

second with 1 second of rest) were delivered until penile protrusion and release of seminal fluid commenced. Semen was collected, diluted, and tested for viability by assessing semen motility. The semen sample was either used immediately or frozen for later use. All sheep were identified by unique numbers and received a specific ear tag for subsequent identification. In accordance with FDA requirements, all genetically modified animals received permanent ear tattoos as a second identifier and were housed in approved pens and appropriately labeled. All sheep were fed water and hay *ad libitum* and other feed was given per experimental protocols. In all experiments, all appropriate and required efforts to minimize pain and suffering were employed. All surgeries (survival and otherwise) were performed under aseptic conditions.

### **Skeletal Phenotyping Analyses**

#### Dual-Energy X-ray Absorptiometry: Bone Mineral Density (BMD)

Dual energy X-ray absorptiometry (DXA; GE Lunar PIXImus 2 and Faxitron Ultra Focus) was used to measure in-life mouse (Ts65Dn, Dp16) total body (excluding head region), hind limb and spine BMD ( $\text{g}/\text{cm}^2$ ), bone mineral content (BMC), and total body percent fat. The anesthetized mouse was laid flat on the Piximus specimen tray or in the Faxitron imaging chamber with the front and hind limbs extended away from the body and the tail positioned inside the imaging view. Measurements were acquired at baseline and post-experimentation for mouse studies. Sub-region analysis of the mid-shaft of the tibia of all mice was also performed. The precision of DXA measurements in our laboratory is 1.7%, based on repeated measures [2, 3].

To prevent fecal matter from accumulating on tail and improve overall lamb health and welfare [4, 5], lamb tails were docked at 10 days of age. Tails were cut, proximally, at or near the 1<sup>st</sup> caudal vertebra and cauterized, simultaneously. Three caudal vertebrae from the anterior-most



end of each docked tail were collected, separated into 3 microcentrifuge tubes, and flash frozen in liquid nitrogen for later analysis. Finally, *ex vivo* DXA scans of lamb tails bones were obtained using the Faxitron Ultra Focus (Tucson, AZ).

#### Micro Computed Tomography (microCT): Ex vivo determination of Trabecular architecture and Cortical Geometry

Formalin-fixed tibiae of Down syndrome mice were imaged using high-resolution microcomputed tomography ( $\mu$ CT40, Scanco Medical, Brüttisellen, Switzerland) (1). Briefly, the proximal tibia (or femur) and tibial (or femoral) midshaft regions were scanned as 6  $\mu$ m isotropic voxel size using 55 kVp, 114 mA, and 200-ms. Bone volume fraction (BV/TV, %), trabecular thickness (Tb.Th, mm), trabecular separation (Tb.Sp, mm), trabecular number (Tb.N, 1/mm), connectivity density (ConnD 1/mm<sup>3</sup>), and structure model index (SMI) were calculated using previously published methods [6]. The cancellous bone region was obtained using a semi-automated contouring program that separated cancellous from cortical bone. At the midshaft, of the tibia (or femur), total cross sectional area (CSA, mm<sup>2</sup>), medullary area (MA, mm<sup>2</sup>) and cortical thickness (Ct.Th, mm) were assessed in a 1-mm-long region centered at the midshaft. Bone was segmented from soft tissue using the same threshold for all groups, 245 mg HA/cm<sup>3</sup> for trabecular and 682 mg HA/cm<sup>3</sup> for cortical bone. All microCT scanning and analyses were compliant with published American Society for Bone and Mineral Research (ASBMR) guidelines for rodents [7].

Formalin-fixed ovine tail vertebral bones were scanned at 5  $\mu$ m isotropic voxel size using 55 kVp, 145 mA, and 400-ms ( $\mu$ CT50, Scanco Medical, Brüttisellen, Switzerland). Bone volume fraction (BV/TV, %), trabecular thickness (Tb.Th, mm), trabecular separation (Tb.Sp, mm), trabecular number (Tb.N, 1/mm), connectivity density (ConnD 1/mm<sup>3</sup>), and structure model

index (SMI) were calculated. Bone was segmented from using the same threshold for all specimens manually determined to be 250 mg HA/cm<sup>3</sup> for trabecular bone.

### Histology and Bone Histomorphometry

Quantitative static and dynamic histomorphometry was performed on paraffin embedded decalcified mouse tibiae or methyl methacrylate-embedded non-decalcified mouse tibiae as previously described [2, 3, 8]. For static histomorphometric analyses, 4-5  $\mu\text{m}$ -thick central saggital sections were stained for TRAP and counterstained with hematoxylin to determine osteoclast numbers and eroded surface, or with Masson's Trichrome to measure osteoblast surface (Ob.S/BS, %), as defined by Parfitt using Osteomeasure software (Osteometrics, Atlanta, GA) [6, 8]. For dynamic histomorphometry, calcein (15 mg/kg) and alizarin red complexome (40 mg/kg) were injected intraperitoneally 8 and 2 days, respectively, in DS mice (both Ts65Dn and Dp16) and age-matched wildtype mice prior to euthanasia. Tibiae and femora were harvested at sacrifice and the muscle dissected away before fixation in Mallonig's [2]. The proportion of single and double labeled perimeters and the interlabel distance between the calcein and alizarin red fluorophores were measured in the cancellous bone of unstained sections adjacent to those used for static measurements. All cancellous bone measurements were made within the area defined by 700-1400  $\mu\text{m}$  distal to the growth plate and 150  $\mu\text{m}$  away from either endocortical surface.

Mineralizing surface per bone surface (MS/BS, %) and mineral apposition rate (MAR,  $\mu\text{m}/\text{d}$ ) were measured in unstained sections under ultraviolet light, and used to calculate bone formation rate with surface referent (BFR/BS,  $\mu\text{m}^3/\mu\text{m}^2/\text{d}$ ). Terminology and units adhere to the recommendations of the histomorphometry nomenclature committee of the ASBMR [9].

## Ex Vivo Bone Marrow Cultures

Bone marrow cells were isolated from mice femurs and tibias and primary *ex vivo* bone cultures were performed exactly as previously described [10]. The bones were flushed using alpha minimum essential medium ( $\alpha$ -MEM) (Gibco) containing 15% FBS (Hyclone Laboratories, Logan, UT) with 1x antibiotics (basal media). Bone marrow from the same treatment group was then pooled, triturated with several passes through a 22-gauge syringe, and filtered (40  $\mu$ m cell filters) to obtain a single cell suspension. The cellular suspension was pelleted (500G, 10 min) and resuspended in basal medium supplemented with ascorbic acid (50 $\mu$ g/mL) and  $\beta$ -glycerophosphate (10mM), collectively comprising osteogenic (OB) medium.

For osteoclastogenic cultures, OB medium was supplemented with 10nM 1,25 (OH)<sub>2</sub>-vitamin D3 (Sigma Aldrich, St. Louis, MO). Cells were plated in 24 well (2 x 10<sup>6</sup> cells/well) or 48 well (1 x 10<sup>6</sup> cells/well) plates (Becton Dickinson Labware) with 3-6 replicate wells and maintained in culture for 10 days (differentiated osteoclast). Half of the culture medium was replaced with fresh supplemented medium on day 5 and aspirated media collected on feed/harvest days. At time of harvest, cells were fixed in 4% neutral buffered formaldehyde, the cell plate was rinsed 3X with filtered water to remove fixative. Plates were kept wet with PBS until stained for tartrate resistant acid phosphatase (TRAP) activity as previously described [11]. The number of TRAP+ multinucleated cells (cells containing 3 or more nuclei) enumerated. Cells were half-fed on day 5 with supplemented medium and aspirated media collected on feed/harvest days.

For osteogenic cultures, bone marrow cells harvested from tibias or femurs were seeded in triplicates in 12 well plates (Becton Dickinson Labware) at a density of 1 x 10<sup>6</sup> cells per well to determine recruitment of cells into the osteoblast lineage or 2 x 10<sup>6</sup> cells per well (CFU-OB)

to determine osteoblast maturation (differentiation), and maintained to day 10 or 28 days, respectively. Medium (1 mL) from each well was replaced every 5 days. The capacity to recruit mesenchymal progenitors into the osteoblastic lineage was determined by alkaline phosphatase-positive (AP+) staining for colony forming unit-fibroblast (CFU-F) (Sigma Alkaline Phosphatase Kit, St. Louis, MO) on day 10 of culture. The number of AP+ colonies per well was enumerated in each of 3 wells per treatment. Plates were then counterstained with 5% fast green and the number of total colonies were enumerated in each well as an indicator of mesenchymal progenitor proliferation.

To determine mature osteoblast (OB) differentiation (mineralization), cells were cultured for 28 days, fixed with 50% ethanol, and stained using a 1% solution of Alizarin Red S (Sigma, St. Louis, MO) for 30 minutes or until red-stained cells were evident. OB culture were then washed gently with filtered water to remove excess stain. The number of mineralized bone nodules representing colony forming units-osteoblasts (CFU-OB) was then enumerated in each well.

## **Development of a Large Animal Model of HPP in Ovis Aries (Sheep)**

### Identification and Confirmation of ALPL Mutation Locus

To identify the specific region in the sheep genome for targeting, the only available NCBI *Ovis aries* V4.0 tissue non-specific alkaline phosphatase (*ALPL*) gene sequence, which is from the Texel breed of sheep, was imported into Benchling (Benchling, San Francisco, CA) and aligned to the human genome using nucleotide BLAST suite (<https://blast.ncbi.nlm.nih.gov/>). The protein sequence was confirmed using NCBI protein Blast (<https://blast.ncbi.nlm.nih.gov/>). Following identification of the human *ALPL* c1077 mutation locus in sheep *ALPL*, a primer pair flanking exon 10 (used to generate ~1kb PCR product) of the sheep *ALPL* gene was designed

using Primer3 software (v. 0.4.0) [12, 13] (**Table 2**). We then confirmed the NCBI reference sequence of the ~1kb gene region via Sanger sequencing of DNA extracted from Rambouillet primary sheep fibroblasts as well as from blood taken from the donor Rambouillet ram and ewes.

**Table 2.** Primer sequences for amplification of sheep ALPL exon 10 target site.

<b>Target</b>	<b>Primer Direction</b>	<b>Primer Sequence</b>	<b>Annealing Temp (T<sub>m</sub>)</b>	<b>Amplicon size (bp)</b>
<b>Sheep ALPL gene exon 10 (c.1077)</b>	Forward	ATGTTGGGCCCTTTCCTAA	65°C	916
	Reverse	CAACATGACCCCTGGACCAA		

#### sgRNA *In Silico* Design and Preparation for Microinjection

sgRNAs targeting exon 10 were designed using the Benchling web based CRISPR sgRNA design tool (Benchling, San Francisco, CA). In Benchling, SNPs discovered in the Rambouillet sheep *ALPL* gene via Sanger sequencing of locus-specific DNA from the sire were incorporated into the Benchling reference sequence and this sequence was used to design more selective sgRNAs. A 100bp region flanking the target site was selected with the computer cursor on the Benchling DNA sequence map. After selecting the target site nucleotides, the CRISPR tool icon was highlighted, the CRISPR tool icon was selected from the tool bar on the Benchling dashboard and then “Design and Analyze Guides” was clicked. The guide parameters included single guides for Wild-type Cas9, guide length is 20bp, genome is OAR\_V3.1 (Ovis Aries) and the PAM selected was NGG. Next, the target region was confirmed and available guides for the selected region were annotated on the reference DNA sequence map. The two sgRNAs (**Table 3**) closest to the target mutation site at c.1077 were selected and off-target effects were assessed.

**Table 3.** sgRNAs designed to target the sheep ALPL exon 10 c.1077C>G HPP mutation.

sgRNA	Sequence	PAM	Strand Direction	Distance from Target Cut Site (bp)
1	GGACCAGGCCATCGGGCAGG	CGG	Sense	5
2	GGCGGGCGCTATGACCTCCG	TGG	Sense	23

#### sgRNA Cloning into Cas9 Plasmid and Preparation for Microinjection

Custom sgRNAs (purchased from IDT technologies) were then cloned into the All-in-One CRISPR/Cas9 vector (pCas-Guide-EF1a-GFP) by Origene Technologies (Rockville, MD). For manual cloning of the designed sgRNAs into the PX458 [pSpCas9(BB)-2A-GFP] plasmid backbone, guide oligonucleotides with sticky ends were annealed by combining 0.5 $\mu$ M of each oligo and heating to 95°C in thermocycler for 5 min. Oligo mix was then allowed to cool for to room temperature guides. Next, the PX458 plasmid was digested using the digestive enzyme BbsI (Thermo Fisher Scientific, Waltham, MA) for 30 min- 1 h at 37°C. The annealed guide RNA oligos were then ligated to the digested PX458 backbone. 50ng of the linear vector and 0.5 $\mu$ M of annealed oligos was added to the mixture of ligation buffer and T4 DNA ligase (Roche) and incubated at room temperature for 1 h. Lastly, the sgRNA/Cas9 construct was transformed into *E. coli* using One Shot Top10 competent cells (Thermo Fisher Scientific, Waltham, MA) per manufacturer's instructions. These CRISPR Cas9 constructs/plasmids were used for functional validation experiments of sgRNA/Cas9 targeting efficiency in primary sheep fibroblasts.

For the production of the mRNA of the sgRNA used for microinjection into embryos, mRNA by reverse transcription of the plasmid DNA described above was synthesized using the MEGAscript T7 transcription kit (Thermo Fisher Scientific, Waltham, MA) per manufacturer's instructions [14]. Briefly, the kit reagents (10X Reaction Buffer and the 4

ribonucleotide solutions: ATP, CTP, GTP, UTP) were thawed, then vortexed until completely mixed into solution. The RNA Polymerase Enzyme mix was kept on ice, while all other reagents were left at room temperature. Next, the transcription reaction was assembled in a 1.5mL microcentrifuge tube at room temperature by mixing 2µL of each ribonucleotide solution, 2µL of 10X reaction buffer, 0.5-1µg of linear DNA template, and 2µL of enzyme. Thorough mixing was accomplished by flicking the microcentrifuge tube. The *in vitro* transcription reaction mixture was then incubated for 4 h. Finally, the newly synthesized mRNA from the DNA template was recovered using the Phenol-chloroform extraction method followed by isopropanol precipitation of the RNA. The supernatant was removed, the RNA was allowed to dry in a sterile area, and resuspended in 10 µl of sterile Tris -EDTA (TE) buffer.

#### Design of Single Stranded Oligonucleotide (ssODN) Repair Template

A 91 base pair single stranded oligonucleotide (ssODN) repair template was designed to stimulate homology directed repair (HDR) for the insertion of the c.1077C>G missense mutation in the sheep *ALPL* gene. Benchling sequencing map was used to design the ssODN and manipulate the sheep reference DNA sequence. The repair template contained 45 bp homology arms flanking the target point mutation. The DNA sequence was manipulated to contain a guanine in place of the cytosine at the target site (c.1077C>G) and adenine in place of a guanine was incorporated into the PAM sequence to prevent excessive cleavage by Cas9 after mutation incorporation (**Table 4**). The repair template was purchased as a 4 nmole Ultramer DNA Oligo from Integrated DNA Technologies (IDT; San Diego, CA).

**Table 4.** *ALPL* exon 10 repair template with c.1077C>G HPP mutation and PAM mutation

<b>ssODN repair template sequence</b>
AGCCAAGCAGGCACTGCACGAGGCGGTGGAGATGGACCAGGCCATGGGGCAGGCG AGCGCTATGACCTCCGTGGAAGACACACTGACCGTT

### Primary Sheep Fibroblast Establishment and Culture

Primary sheep fibroblast cultures were established from sheep dermal biopsies as described [15]. Briefly, skin samples were harvested from Rambouillet sheep under anesthesia, cut into 0.5mm sections and placed in Ca and Mg free Dulbecco's Phosphate-Buffered Serum (DPBS) (Life Technologies, Gaithersburg, MD) on ice. The samples were quickly washed in a 0.2% (v/v) chlorhexidine gluconate in DPBS and then again in two sterile DPBS washes. The washed sample was then placed into a 10 cm petri dish and cut into small pieces (<5 mm). The tissue was then washed through 5 series of 1x DPBS washes in a 12 ml conical tube. Washed tissue was resuspended in Dulbecco's Modified Eagle Medium (DMEM) with nutrient mixture F-12 (DMEM/F12) (Life Technologies, Gaithersburg, MD) supplemented with 10% FBS (Atlanta Biologicals, Atlanta, GA), 1x Antibiotics/Mycotic and 1x Gentamycin (Life Technologies). The prepared tissue was then placed in a T25 tissue culture flasks and cultured at 37°C in a 95% O<sub>2</sub>, 5% CO<sub>2</sub> humidified incubator. Cells were passaged at 80% confluence.

### Detection of sgRNA Targeting Efficiency

The T7E1 assay was used to determine sgRNA/Cas9 targeting in primary sheep fibroblasts and to confirm Cas9 activity in DNA from newborn lambs [16]. In brief, 3x10<sup>5</sup> sheep fibroblasts were seeded in 1% gelatin coated 6-well plates and grown until the confluency reached 80%. Cells were transfected with 2.5 µg Cas9/sgRNA plasmid using Lipofectamine 3000 (Thermo Fisher Scientific) and maintained in culture at 37°C during 48-72 h according to the manufacturers' instructions. Transfected cells were harvested and genomic DNA was extracted using the DNA Blood and Tissue Kit (Qiagen, Germantown, MD). The targeted exon 10 region was PCR amplified (~1kb PCR product) and the amplicon purified using PCR



Purification Kit (Qiagen). Next, 200 ng of each purified PCR amplicon was denatured, re-annealed, and digested with T7 endonuclease I. Re-annealed heteroduplex fragments were electrophoresed on a 2% TAE agarose (90v for 3 h) and enzymatic cleavage visualized. In order to determine gene modifications in newborn lambs, DNA was extracted from umbilicus and blood samples and the same T7E1 protocol was used.

#### Collection of *In Vivo* Matured Oocytes and Zygotes

Ten (10) mature Ramboillet donor ewes were estrus synchronized by treating with controlled internal drug release (CIDR) devices containing 300mg progesterone (Zoetis) for 12 days. On the day of CIDR insertion (Day 0), all ewes received 0.25mg cloprostenol sodium (Merck) i.m. to induce luteolysis in any corpus luteum (CL) present. Superovulation was induced days 9-12 with 200mg of FSH (Bioniche) administered i.m. in eight decreasing doses (40mg x 2, 30mg x 2, 20mg x 2, 10mg x 2). CIDR devices were removed on day 12, and 0.05mg GnRH (Merial, City, state) was administered i.m. 36 h later. At 51 h post CIDR removal laparoscopic artificial insemination was performed using fresh collected ovine semen. Twenty (20) mature cross bred recipient ewes were also synchronized on the same schedule as the donor ewes using CIDR devices and 0.25mg cloprostenol sodium on day 0. CIDR devices were removed day 12 and 0.05mg GnRH was administered 36 h later. Heat was confirmed on the recipient ewes by exposure to epididymectomized rams with marking harnesses.

Zygotes were recovered from donor ewes surgically 24 h post-GnRH treatment by mid-ventral laparotomy. For this, sheep were anesthetized with an intravenous injection of telazol, ketamine, xylazine mixture, with anesthesia maintained under 5% isoflurane inhalation. The reproductive tract was exposed and the oviducts were flushed with 25 ml of HEPES-buffered medium into a 50 ml conical tube. Recovered medium was examined under a dissecting

microscope and the embryos collected. All recovered *in vivo* zygotes were placed immediately into a drop of TL-HEPES medium for microinjection.

#### Microinjection of Zygotes, *In Vitro* Culture, and Transfer into Recipient Ewes

Presumptive zygotes, were vortexed and further cleaned with a stripper pipette (125  $\mu$ m diameter) to remove sperm and any remaining cumulus cells. Cleaned zygotes were placed in Hanks 199 (Gibco-BRL) supplemented with 10 % Hyclone FBS (GE) and gentamicin. Microinjection pipettes were treated using a 2:6 or 4:6 ratio of Hydrofluoric acid (Sigma, St. Louis, MO) (47%) to DNase free water under a Nikon TE300 inverted scope. Zygotes were injected with 10ng/ $\mu$ l Cas9 mRNA (Thermo), 30ng/  $\mu$ l of Cas9 protein (Thermo), 5 or 50 ng/ $\mu$ l of ssODN repair template, and 5ng/ $\mu$ l *in vitro* transcribed sgRNA produced as described above (**Figure 5A & 4B**). Injections were performed under positive pressure until a slight expansion of the cell membrane was observed. All injected zygotes were placed in 4-well multi-dish with each well containing 500ul of culture medium (IVF Bioscience, Falmouth, England) and cultured at 37°C in a 5% O<sub>2</sub>, 5% CO<sub>2</sub> humidified incubator (Nuair) prior to transfer into recipient ewes. Twenty microinjected presumptive zygotes and 1 control zygote were left in *in vitro* culture (IVC) for 6-7 days until the hatched blastocyst stage (**Figure 5C**). After 7 days, blastocysts were rinsed three times with TL-HEPES containing 0.3% BSA and Gentamicin. Hatched blastocysts were then washed twice in DNase-free PBS Ca/MG free medium (GIBCO) and transferred, individually, into separate 0.2 ml PCR tubes containing 5  $\mu$ l of DNase-free PBS. Labeled zygotes were then stored in -20°C until genetic analysis. All other zygotes were immediately transferred surgically to recipient ewes under general anesthesia. A Drummond pipette was used to transfer two or three blastocysts into the uterine horns ipsilateral to a corpus luteum [15].



**Figure 5. Representative image of microinjection in sheep zygotes.** Presumptive (A) 1 cell and (B) 2 cell zygotes were microinjected with Cas9 mRNA, Cas9 protein, sgRNA mRNA, and 5ng or 50ng of ssODN repair template. (C) Twenty zygotes were kept in IVC for 6-7 days until the hatched blastocyst stage.

### Polymerase Chain Reaction (PCR) and Genomic Sequencing

Genomic DNA was extracted from cells, skin, umbilicus, and blood samples using Qiagen DNeasy Blood and Tissue Kit. In brief, primary sheep fibroblasts (at a density up to  $5 \times 10^6$ ) were centrifuged 5 min at 300xG in 50 mL conical tube to pellet cells. Cell pellet was then resuspended in 200 $\mu$ L of PBS and 20  $\mu$ L of proteinase K. For blood samples, 100 $\mu$ L of anticoagulated blood was placed in 20  $\mu$ L of proteinase K and the volume was adjusted to 220 $\mu$ L total by adding 100 $\mu$ L of PBS. Next, 200  $\mu$ L of lysis buffer was added to the resuspended cell mixture and blood mixture, vortexed, and incubated at 56°C for 10 min. For skin and umbilicus samples, the tissue was cut into small 0.5-1cm pieces and placed into a 1.5mL microcentrifuge tube. Tissue lysis buffer (180  $\mu$ L) was added to the sample. Next, 20  $\mu$ L of proteinase K was added to the sample, vortexed, and incubated until the tissue was completely lysed. Then, the cell lysis buffer (200 $\mu$ L) was added and the sample mixed thoroughly by vortexing. At this point in the protocol, all of the samples are handled the same. Next, 200  $\mu$ L of 96% ethanol was added to each sample and vortexed again. The sample mixture was then placed into a DNeasy Mini spin column in a 2 mL collection tube and centrifuged for 1 minute at 8000 rpm. The collection tube was then discarded, the mini spin column was placed into a new collection tube. 500  $\mu$ L of wash

buffer #1 was then added to each sample, centrifuged for 1 min at 8000 rpm, and collection tube was discarded and replaced. This step was repeated with wash buffer #2 and then centrifuged at 14,000 rpm. The DNeasy mini spin column was then eluted with DNase-free water into a clean 1.5 mL microcentrifuge tube and stored at -20°C.

The extracted and purified DNA was used for PCR amplification. PCR amplification was performed using 200 ng of DNA and the Cloneamp HiFi PCR premix (Clontech, Mountain View, CA) according to the following protocol: 95°C for 5 min followed by 95°C for 30 s, 66°C for 30s, 72°C for 45s, and 72°C for 10 min after 35 cycles. PCR products were gel purified by electrophoresing on a 1% TAE agarose gel (90v, ~2h) with a 1kb plus DNA molecular marker (Invitrogen) and gel extracted using QIAquick gel extraction kit (Qiagen). All isolated and purified PCR products were analyzed via Sanger sequencing [17].

#### Phenotyping of ALPL Exon 10 c.1077C>G Sheep

Blood was collected by jugular venipuncture at 2 months of age and serum was extracted from the blood. The blood was allowed to coagulate and centrifuged at 2000rpm for 10 min. The serum layer was then removed from the blood cells and placed into a clean 1.5mL microcentrifuge tube and stored at -20°C until analysis. The isolated serum was then analyzed for alkaline phosphatase activity at pH 10.4 using p-nitrophenol phosphate as the colorimetric substrate (Invitrogen, Carlsbad, CA).

Additionally, images of the docked formalin-fixed tail vertebrae at 10 days of age were taken by DXA using a Faxitron Ultrafocus DXA (Tucson, AZ) as described above. At 2 months of age, lambs were assessed for the presence of dental and muscle HPP phenotype at the Texas A&M Institute for Genomic Medicine (TIGM) by Dr. Alan Glowczwski. Head radiographs and

CT was performed, and muscle biopsies collected from mutant and WT lambs under ketamine sedation and isoflurane anesthesia.

Muscle biopsies were obtained from the gluteal muscle group by non-invasive ultrasound-guidance using a 14 gauge needle. Muscle samples were minced to 1mm cubes and fixed in 0.1M sodium cacodylate buffered 2% glutaraldehyde, 2.5% paraformaldehyde overnight. Samples were then washed in cacodylate buffer and post-fixed in 1% osmium tetroxide with 1% potassium ferrocyanate for 1h at RT and then washed 2X in cacodylate buffer. Samples were then processed through a graded ethanol series for 10 mins each of 30, 50, 70, 80, 90 and 95% cold ethanol, 95% warm ethanol, followed by 3X 100% and finally in 2 X 5 min propylene oxide. Subsequently, samples were infiltrated with epoxy in graded fashion with 1 h incubations at 35, 60, 85% and 100 % X 2 of epon araldite with 1.5% DMP-30, followed by 100% epoxy overnight on a rotator. Samples were then transferred to Beem capsules and heat cured at 65C for 2 days, and then sectioned on an LKB microtome. Light microscopy sections were stained with Richards stain, and thin sections were on grid stained with 1% uranyl acetate for imaging by transmission electron microscopy.

## References

1. Fischman ML, Suhevic J, Rivolta MA, Cisale HO. Collection of wild boar semen by electroejaculation. *Vet Rec.* 2003;153(12):365-6.
2. Rzonca SO, Suva LJ, Gaddy D, Montague DC, Lecka-Czernik B. Bone is a target for the antidiabetic compound rosiglitazone. *Endocrinology.* 2004;145(1):401-6.
3. Engle MR, Singh SP, Czernik PJ, Gaddy D, Montague DC, Ceci JD, et al. Physiological role of mGSTA4-4, a glutathione S-transferase metabolizing 4-hydroxynonenal: generation and analysis of mGsta4 null mouse. *Toxicol Appl Pharmacol.* 2004;194(3):296-308.

4. Small AH, Marini D, le Floch M, Paull D, Lee C. A pen study evaluation of buccal meloxicam and topical anaesthetic at improving welfare of lambs undergoing surgical mulesing and hot knife tail docking. *Res Vet Sci.* 2018;118:270-7.
5. Llonch P, King EM, Clarke KA, Downes JM, Green LE. A systematic review of animal based indicators of sheep welfare on farm, at market and during transport, and qualitative appraisal of their validity and feasibility for use in UK abattoirs. *Vet J.* 2015;206(3):289-97.
6. Suva LJ, Hartman E, Dilley JD, Russell S, Akel NS, Skinner RA, et al. Platelet dysfunction and a high bone mass phenotype in a murine model of platelet-type von Willebrand disease. *Am J Pathol.* 2008;172(2):430-9.
7. Bouxsein ML, Boyd SK, Christiansen BA, Guldberg RE, Jepsen KJ, Muller R. Guidelines for assessment of bone microstructure in rodents using micro-computed tomography. *J Bone Miner Res.* 2010;25(7):1468-86.
8. Perrien DS, Akel NS, Edwards PK, Carver AA, Bendre MS, Swain FL, et al. Inhibin A is an endocrine stimulator of bone mass and strength. *Endocrinology.* 2007;148(4):1654-65.
9. Parfitt AM, Drezner MK, Glorieux FH, Kanis JA, Malluche H, Meunier PJ, et al. Bone histomorphometry: standardization of nomenclature, symbols, and units. Report of the ASBMR Histomorphometry Nomenclature Committee. *J Bone Miner Res.* 1987;2(6):595-610.
10. Gaddy-Kurten D, Coker JK, Abe E, Jilka RL, Manolagas SC. Inhibin suppresses and activin stimulates osteoblastogenesis and osteoclastogenesis in murine bone marrow cultures. *Endocrinology.* 2002;143(1):74-83.
11. Fowler TW, McKelvey KD, Akel NS, Vander Schilden J, Bacon AW, Bracey JW, et al. Low bone turnover and low BMD in Down syndrome: effect of intermittent PTH treatment. *PLoS One.* 2012;7(8):e42967.
12. Koressaar T, Remm M. Enhancements and modifications of primer design program Primer3. *Bioinformatics.* 2007;23(10):1289-91.
13. Untergasser A, Cutcutache I, Koressaar T, Ye J, Faircloth BC, Remm M, et al. Primer3--new capabilities and interfaces. *Nucleic Acids Res.* 2012;40(15):e115.

14. Pfarr K, Heider U, Hoerauf A. RNAi mediated silencing of actin expression in adult *Litomosoides sigmodontis* is specific, persistent and results in a phenotype. *Int J Parasitol.* 2006;36(6):661-9.
15. Cornetta K, Tessanne K, Long C, Yao J, Satterfield C, Westhusin M. Transgenic sheep generated by lentiviral vectors: safety and integration analysis of surrogates and their offspring. *Transgenic Res.* 2013;22(4):737-45.
16. Crispo M, Mulet AP, Tesson L, Barrera N, Cuadro F, dos Santos-Neto PC, et al. Efficient Generation of Myostatin Knock-Out Sheep Using CRISPR/Cas9 Technology and Microinjection into Zygotes. *PLoS One.* 2015;10(8):e0136690.
17. No E, Zhou Y, Loopstra CA. Sequences upstream and downstream of two xylem-specific pine genes influence their expression. *Plant Sci.* 2000;160(1):77-86.

## CHAPTER III

### RELEVANT MURINE MODELS OF LOW BONE MASS PHENOTYPE IN DOWN SYNDROME: UNDERSTANDING THE CONTRIBUTIONS OF GENOTYPE AND SEX

#### **Introduction**

Trisomy of human chromosome 21, also referred to as Down syndrome (DS), is a common birth defect that affects 1 in every 700 live births worldwide. Although DS was initially identified in 1866, this genetic disorder remains a major public health concern as it and other genetic abnormalities continue to be a leading cause of infant mortality and lifelong disabilities [1]. Each year, approximately 6,000 DS babies are born in the United States alone [1]. Today, there are currently 400,000 people living with DS in the US [1-3]. This genetic birth defect alters human development and leads to a variety of clinical issues such as mental impairment, learning disabilities, congenital heart issues, sleep apnea, hypogonadism, infertility as well as significant deficits in bone health [4].

Similar to the prevalence of DS, the past several decades have brought about significant increases in the average life expectancy in people with DS as the average life expectancy went from 9 years to more than 50 years of age between 1960 and the 21<sup>st</sup> century [1, 5, 6]. As the life expectancy of DS approaches that of individuals without DS [7], the bone health of adolescent and adult DS patients has become an important medical issue [4, 8]. The DS population has been shown to have a low bone mineral density (BMD) which is associated with decreased skeletal maturation and bone mass accrual [9, 10] that predispose these patients to major risks of fracture – especially given their increased longevity. In addition to the increased life expectancy, the increase in active lifestyles (i.e. community engagement, recreational sports, etc.) further



complicate the issue of bone health in DS, as the increased risks of falls can compound fracture risk. Despite these observations and facts, the pathophysiology of the skeletal deficits in DS is still unclear.

Many factors such as low amounts of physical activity, poor calcium intake, thyroid dysfunction, as well as hypogonadism [11] have been proposed to contribute to the low BMD states identified in DS. However, a clinical study performed by our lab identified that low BMD was common in healthy, euthyroid, calcium-replete adults with DS and that is the result of low bone formation and decreased bone turnover [12]. Moreover, this study also revealed that the skeletal defects in DS were more pronounced in men than women. Indeed, the osteopenia appeared earlier in male DS populations than female DS patients, although skeletal deficits progressed with age in both men and women with DS [12]. So, to better understand bone health in DS and to evaluate the efficacy of novel and currently available therapeutics, the utilization of a DS model that mimics the genotype, in addition to the molecular, cellular, and physiological phenotypes observed in human DS is essential. Therefore, we determined the bone phenotype of 2 commonly used male DS murine models – Ts65Dn and Tc1 and, which differ in their genetic make-up as described in chapter I.

Although these murine models accurately recapitulate many of the characteristics of human DS such as the behavioral deficiencies [13], we identified that Tc1 mice lack a noticeable bone phenotype. Whereas the Ts65Dn mice have a low bone mass phenotype identical to that found in people with DS [14], Tc-1 do not. We demonstrated that the decreased bone accrual and low bone mass in Ts65Dn was the result of decreased bone formation and low bone turnover, which was the result of decreased function and numbers of osteoblasts and osteoclasts [14].

The analysis of the skeletal phenotype in a murine model of DS – specifically male Ts65Dn - were among the first to be reported and the data acquired from these studies provided insight into bone pathophysiology in DS [14, 15] and offered a relevant disease model to further investigate the trisomic effects of human chromosome 21 in skeletal development and maturation. Currently, a major deficit in the field is the lack of any skeletal evaluation of female DS animal models. In fact, to my knowledge, no studies have been performed that directly assess the skeletal phenotype of female Ts65Dn mice or any other DS murine model. In the case of female Ts65Dn, the lack of analysis is due to the inefficient development of female mouse litters [16]. The limited availability of DS murine models and the phenotypic variability amongst these models as well as the genetic differences between particular murine models as described in chapter 1 and the complexity of disease pathology complicates any mechanistic investigations of specific phenotypes such as the low bone mass phenotype in DS (**Figure 3**).

Unlike the Ts65Dn that contain only a segmental copy of Hsa21 syntenic genes of Mmu16 (Figure 3), Dp16 mice are trisomic for the entire mouse chromosome 16, which carry orthologous genes from human *Hsa21* chromosome without the addition of non-*Hsa21* genes [17] as discussed in chapter I. In this chapter, the skeletal phenotype of male Dp16 mice was determined, along with the first-ever data detailing the skeletal phenotype of a female murine model of DS. These studies provide novel insight into the potential mechanisms underlying the sex-specific low bone mass phenotype observed in adolescent and adult DS populations and establish another useful model in which to investigate the cellular and molecular factors responsible for the low bone mass common in DS.

## Study Design

To determine the skeletal phenotype of Dp(16)1Yey mice, 6 week old male and female Dp16 mice and littermate controls were purchased from Jackson Laboratories. Each mouse was housed in a room with 12 h light-dark cycles based on sex and genotype for a total of 4 groups: male Dp16 (n=6), female Dp16 (n=6), male WT (n=6), and female WT (n=6). Animals were allowed access to food and water, *ad libitum*. Intraperitoneal injections of calcein (-8 days) and alizarin red (-2 days) were performed before termination for histology/histomorphometry analysis. At the time of euthanasia (3 months of age), total body radiographs by DXA were acquired. Blood, long bones, and spines were harvested at this time for *ex vivo* bone marrow cultures and  $\mu$ CT analysis. For statistical analysis, sex-specific (male or female) comparisons between genotype (WT or Dp16) were performed using a t-test corrected for multiple comparisons using the Holm-Sidak method for each variable and computed using the Prism 7 software. All data are presented as mean  $\pm$  standard deviation and significance was determined at  $P < 0.05$ . Individual data points display the distribution of the data and significance is represented as  $p < 0.05$  (\*),  $p < 0.002$  (\*\*), or  $p < 0.001$  (\*\*\*)). Graphs were generated using Graphpad software.

## Results

### Bone mineral density (BMD) is decreased in male, but not female Dp(16)1Yey DS mice

Total body BMD (excluding the head) of male and female Dp(16)1Yey mice were analyzed by dual-energy X-ray absorptiometry (DXA). Similar to Ts65Dn mice [18], total body BMD was significantly reduced in male Dp16 compared to WT littermate controls ( $p = 0.007$ ) (**Figure 6A**). In contrast, female Dp16 total body BMD was not significantly different from female WT controls with no significant changes in BMD (**Figure 6A**). There were no differences in body weight or total percent fat in either male or female Dp16 mice (**Figure 6B**).

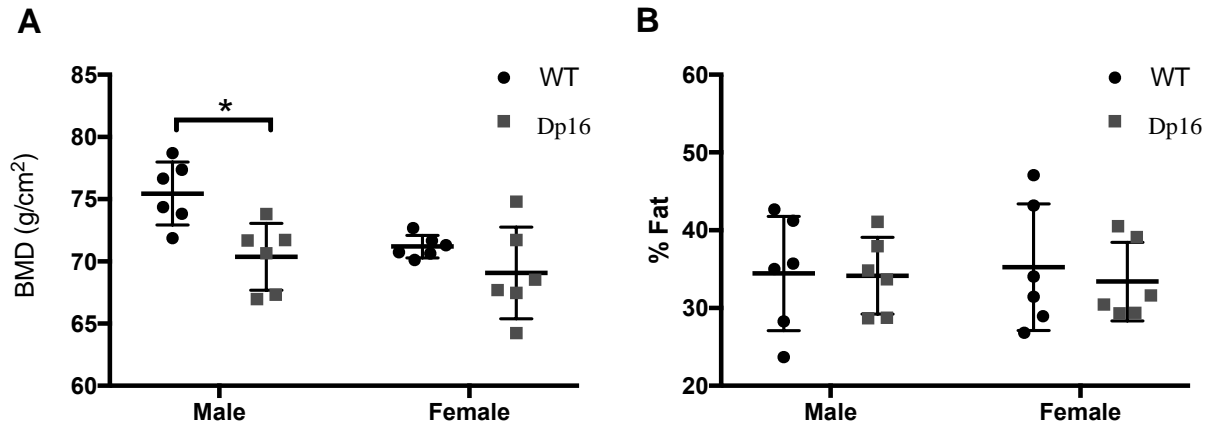


**Figure 6. BMD is significantly decreased in male Dp16 mice, but not female mice.** (A) BMD and (B) percent fat was measured by DXA at 3 months of age. BMD was significantly decreased in male Dp16 mice. However, there was no changes in BMD in female Dp16 mice. There were no changes in percent fat in either male or female Dp16 mice. Statistical significance is represented as  $p < 0.05$  (\*),  $p < 0.002$  (\*\*), or  $p < 0.001$  (\*\*\*) compared to WT gender-matched control.

#### Skeletal phenotype of trabecular and cortical bone in male and female Dp(16)1Yey

Three-dimensional analysis of trabecular microarchitecture by  $\mu$ CT revealed reduced bone volume in male, but not female Dp16 mice when compared to their respective WT controls. In male Dp16, bone volume/total volume (BV/TV) was significantly decreased by ~23% ( $p = 0.03$ ) (**Figure 7B**), which was likely due to a decrease in trabecular number (Tb.N.) ( $p = 0.008$ ) (**Figure 6C**) and a slight, but insignificant increase in trabecular spacing (Tb.Sp.) (**Figure 7D**). No significant changes in trabecular thickness (Tb.Th.) were observed (**Figure 7E**). These changes in trabecular microarchitecture were evident in the 3D reconstructions of the tibial metaphysis (**Figure 7A**). The trabecular parameters presented here are similar to those seen in male Ts65Dn mice, which were more pronounced at 35% decrease in BV/TV [14]. However, female Dp16 mice showed no changes in trabecular architecture, with no significant differences in BV/TV, Tb.N., or Tb.Th when compared to WT (**Figure 7A-E**).

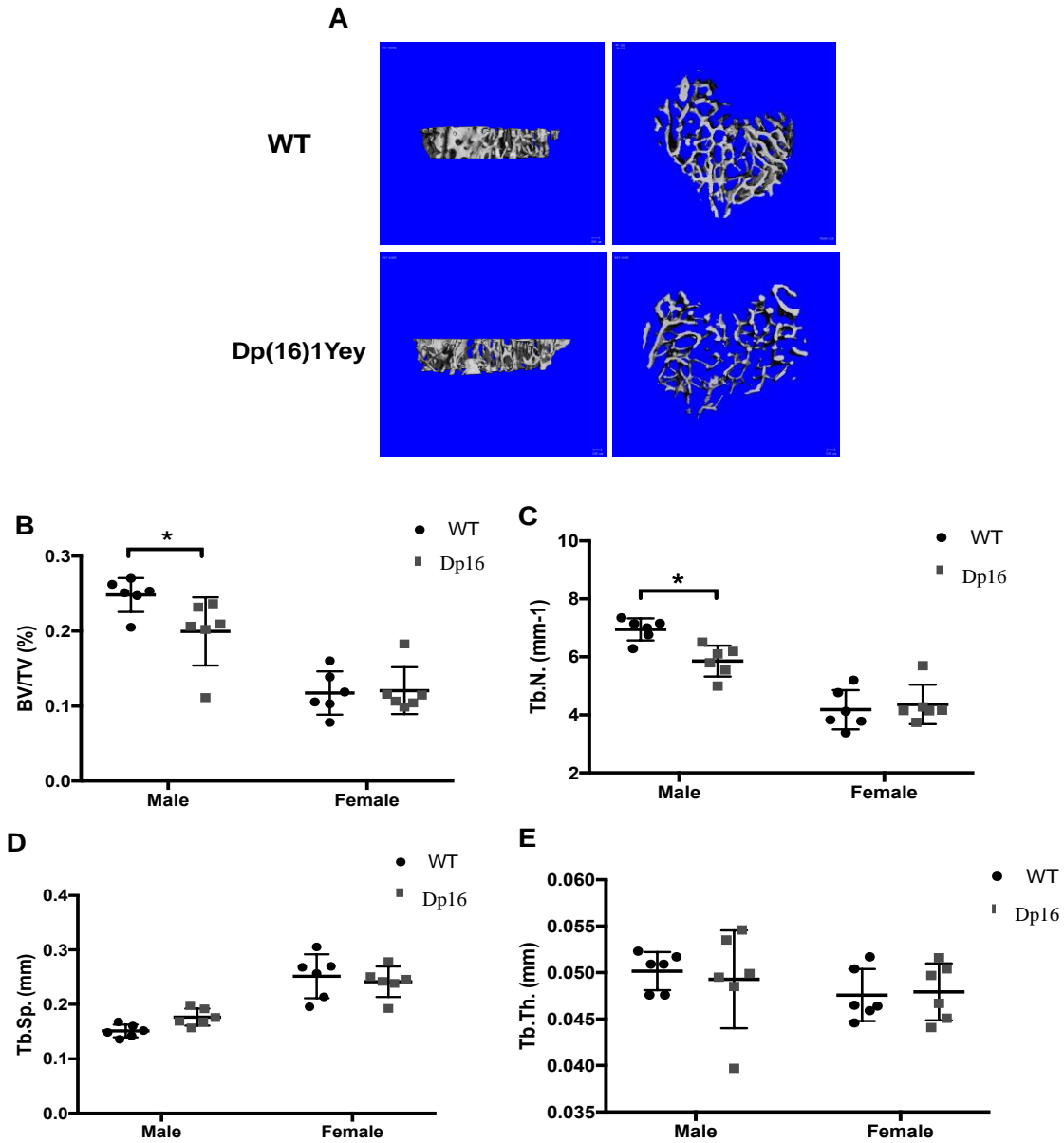


**Figure 7. Trisomy effects on trabecular microarchitecture in Dp16 mice.** Analysis of trabecular microarchitecture by  $\mu$ CT revealed reduced bone volume in male, but not female Dp16 mice when compared to their respective WT controls. **(A)** Representative image of  $\mu$ CT reconstructions. **(B)** When quantified, percent bone volume/total volume (BV/TV) was significantly reduced in male, but not female Dp16 mice. **(C)** The same decrease in male, but not female mice compared to WT was observed in the trabecular number (Tb.N.). No changes were observed in **(D)** trabecular spacing (Tb.Sp.) or **(E)** trabecular thickness (Tb.Th.) in either male or female mice. Statistical significance is represented as  $p < 0.05$  (\*) compared to WT gender-matched control.

Cortical analysis at the tibial midshaft of Dp16 mice by  $\mu$ CT also revealed a bone phenotype in males, but not females (**Figure 8**). Cortical cross-sectional area (CSA) (**Figure 8A**) and cortical thickness (Ct.Th.) (**Figure 8C**) were not significantly different. However, statistically significant decreases in total cross sectional area (Tt.CSA) (**Figure 8B**), periosteal perimeter (PP) (**Figure 8E**), and medullary area (MA) (**Figure 8D**) in male Dp16 compared to WT animals were observed. Again, no significant changes in any female Dp16 cortical bone parameters were observed. Given the lack of difference in body weight, the reduced cortical geometry and compromised trabecular architecture confirms the low bone mass phenotype in Dp16 male mice.

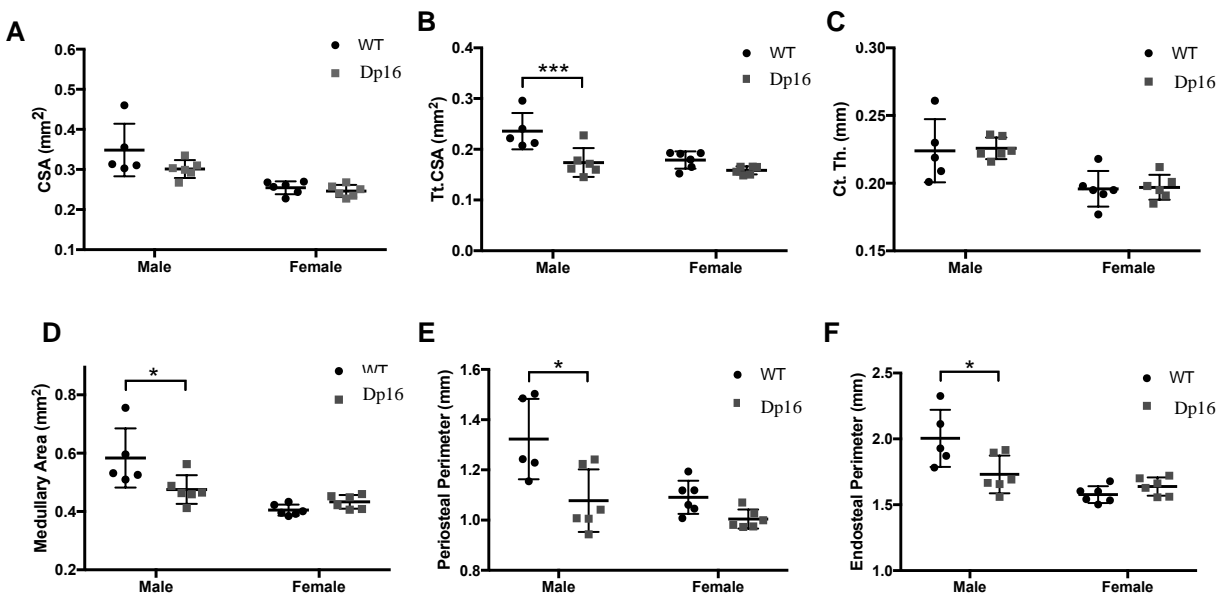


**Figure 8. Trisomy effects on cortical parameters at the tibial midshaft in Dp16 mice.**  $\mu$ CT analysis of cortical parameters revealed a bone phenotype in males, but not females Dp16 mice. (A) Cortical cross-sectional area (CSA) was not different in male or female mice. (B) Total Cross-sectional Area (Tt. CSA) was significantly decreased in male mice, with (C) no changes in cortical thickness (Ct.Th.). (D) Medullary Area (MA), (E) Periosteal Perimeter (PP), and (F) Endosteal Perimeter (EP) were all significantly decreased in male, but not female Dp16 mice. Statistical significance is represented as  $p < 0.05$  (\*),  $p < 0.002$  (\*\*), or  $p < 0.001$  (\*\*\*) compared to WT gender-matched control.

Altered bone cell recruitment and differentiation could explain sex-specific low bone mass phenotype in Dp(16)1Yey mice

To determine if the male-specific reductions in bone mass and microarchitecture in Dp16 mice were attributed to decreased osteoblast and osteoclasts numbers as reported in Ts65Dn male mice [14], *ex vivo* bone marrow cultures were initiated and stimulated towards both osteoblastogenesis and osteoclastogenesis (**Figure 9**). Interestingly, the capacity to recruit whole bone marrow derived from Dp16 mice into the osteoblast lineage was higher than WT controls in both male ( $p < 0.001$ ) and female ( $p = 0.01$ ) cultures, as measured by the percentage of alkaline phosphatase positive (AP+) colonies/total colonies (**Figure 9B**). Additionally, the number of total colonies was significantly higher in Dp16 male and female mice compared to WT controls, suggesting an increased pool of mesenchymal progenitors (**Figure 9A**). The measurement of alizarin red stained bone nodules/protein ratio bone marrow cultured to osteoblasts for 28 days revealed a marked increase in osteoblast maturation and differentiation capacity in female mice when compared to sex-specific WT controls ( $p < 0.001$ ) (**Figure 9C**), but there were no noticeable change in male mice cultures. Moreover, male Dp16 had higher numbers of osteoclasts than WT animals when multinucleated tartrate resistant acid phosphatase (TRAP+) cells were enumerated (**Figure 9D**). However, female mice osteoclast numbers were not altered (**Figure 9D**). These data suggest that the low bone mass observed in male, but not female Dp16 mice at 3 months of age maybe due to increased osteoclastogenesis. In addition, and as expected, Dp16 DS mice at 3 months of age, exactly as with Ts65Dn mice [14], have levels of bone turnover markers that are not different from controls (**Figure 9E,F**). We anticipate, as in Ts65Dn, that bone turnover will not increase with age in these mice as it does in WT mice. In our earlier studies, a significant difference in serum biochemical markers was only observed in aged Ts65 mice [14].

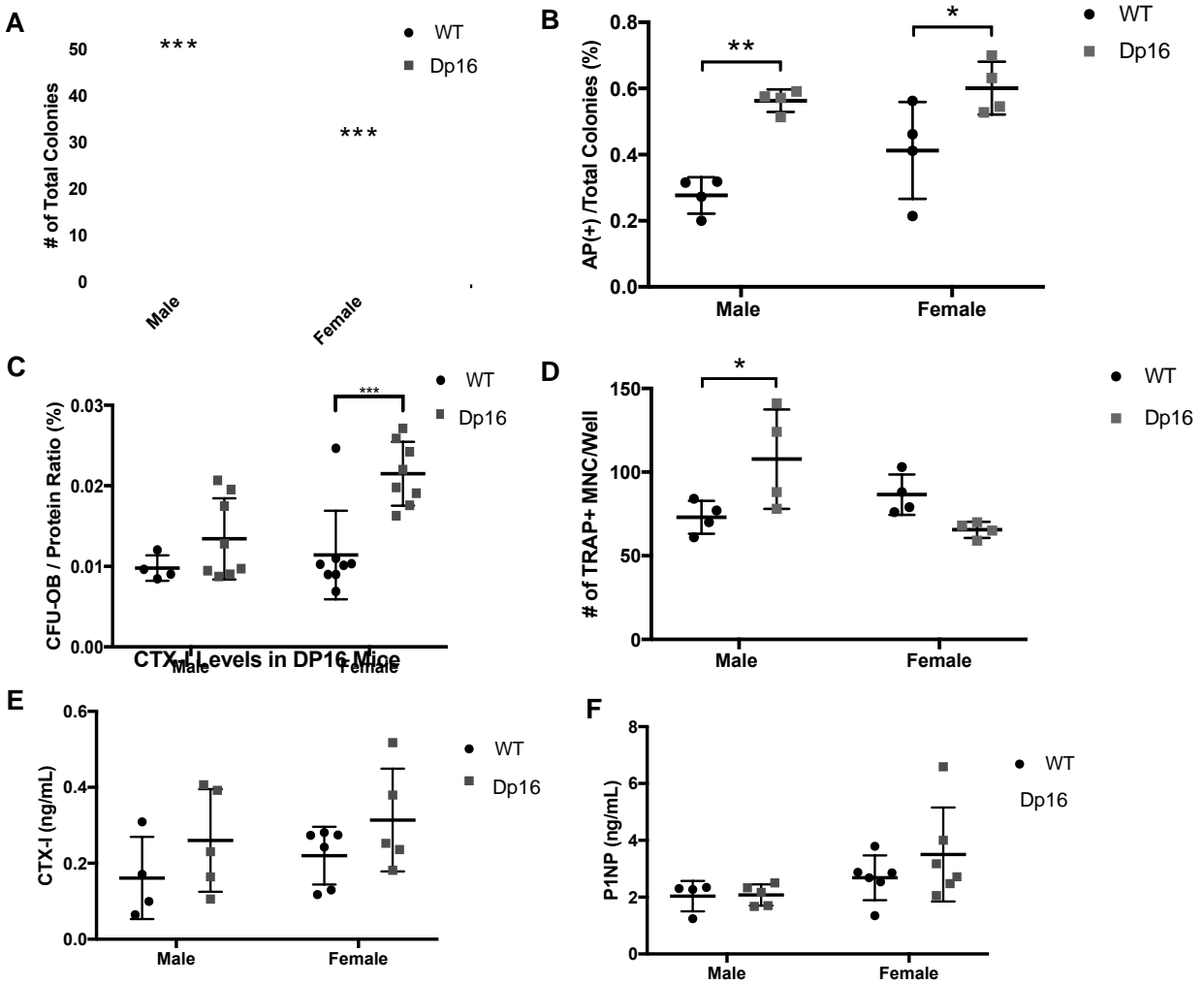


**Figure 9. Alterations in bone cell parameters of Dp16 male and female mice.** (A) The total number of mesenchymal progenitors and (B) recruitment into the osteoblast lineage as measured by the number of alkaline phosphatase positive (AP+) colonies/total colonies are both increased in both male and female Dp16 mice. (C) Enumeration of alizarin red stained bone nodules/protein ratio revealed a marked increase in osteoblast differentiation capacity in female mice, but not male Dp16 mice. (D) *Ex vivo* osteoclast differentiation was significantly increased in male, but not female Dp16 mice. There were no changes in bone turnover biomarkers for (E) resorption or (F) formation. Statistical significance is represented as  $p < 0.05$  (\*),  $p < 0.002$  (\*\*), or  $p < 0.001$  (\*\*\*) compared to WT gender-matched control.



## Discussion

Low bone mass associated with decreased bone mass accrual has become a well-recognized consequence in trisomy of human chromosome 21 within the past decade [12, 19]. As the prevalence and average life span of people with DS has increased, so does the prevalence of possible predisposing factors such as hypogonadism, vitamin D calcium insufficiency, age, and menopause that can contribute to increased risk for fragility fractures [12, 19, 20]. Given the complexity of DS pathogenesis as well as the highly variable expression of clinical phenotypes, the modality/context of bone disease progression, cause, and sex- and age-dependent differences of individuals with DS is not clear.

As mentioned previously, we and others have reported that decreased bone mass accrual and low bone turnover is the primary cause of the low bone mass in DS. Furthermore, we have demonstrated that this low BMD phenotype is more pronounced in male DS than female DS [4, 12]. Similarly, many clinical studies assessing bone mass in a cohort of both male and female Down syndrome adolescent or adults have reported the male gender as a major risk factor for low BMD [12, 19, 21]. Moreover, we have also demonstrated a low bone mass and low bone turnover phenotype in male Ts65Dn DS mice [14]. We have never had the opportunity to assess the skeletal phenotype of female Ts65Dn mice due to the unviability of breeding colonies for this gender. However, Dp16 mice provided us with not only another trisomic model to assess skeletal phenotype, but also a viable female model of DS. Thus, we characterized the phenotype of both male and females in a novel DS murine model – Dp16.

In this thesis chapter, we showed that the low bone mass common in human DS and male Ts65Dn is also evident in Dp16 male mice. Similar to human DS, the low bone mass phenotype is more pronounced in 3 month old male Dp16 mice than female mice of the same age. BMD in Dp16 males was significantly reduced as well as trabecular parameters (BV/TV, Tb.N) and

cortical parameters (TtCSA, PP, EnP, MA) compared to WT littermate controls. However, there were no significant changes in either the trabecular microarchitecture, cortical geometry or BMD in female Dp16 mice. More interestingly, analysis of *ex vivo* bone culture derived from femurs and tibias of Dp16 male and female mice suggested that the male-specific low bone mass phenotype is the result of increased osteoclastogenesis. These cellular findings differ from the consistently suppressed osteoblast and osteoclast differentiation in male Ts65Dn that provide the cellular basis for the low bone mass found in that mouse model of DS. We also suspect that the lack of bone phenotype in female Dp16 mice was due to an increased capacity of osteoblast recruitment and increased ratio of osteoblast maturation without altering osteoclastogenesis.

This unique and apparent bone phenotype could explain the sex-specific differences in bone mass of Dp16 mice. Infertility and hypogonadism in males with DS is very common, but there are numerous cases of successful pregnancies in females with DS [22, 23]. A study of the gonadal function in young women with DS by Angelopoulou and colleagues [24] reported normal uterine and ovarian size, but more importantly, they reported normal mean concentrations of FSH, DHEA-S and estrogen (E2). The important role of E2 in bone growth and maturation as well as its protective effect on bone by suppressing osteoclastogenesis is well-documented [25, 26]. However, in spite of gender differences, Costa and colleagues [19] revealed that the most relevant predisposing factors for osteopenia and osteoporosis are age and menopausal status. These data suggest that the protective effect of E2 on bone metabolism in women with DS will eventually be subjected to the age-related physiological and reproductive changes observed in women in the general population - although these changes may occur earlier in life.

## **Future Directions**

The clinical presentation of DS is very complex and highly variable [27-29]. As discussed in Chapter I, disturbances in the complex processes of skeletal homeostasis, growth and development further complicate our understanding of skeletal disease progression in DS and increase chances of variability in clinical phenotypes [15, 30-32]. Moreover, gonadal dysfunction and infertility are common in DS and any alterations to hormones in the hypothalamic-pituitary-gonadal-skeletal (HPGS) axis can dramatically impact bone health [26] (**Figure 10**). When all possible combinations of direct and secondary effects of trisomy 21 on bone are considered, defining a particular genotype-phenotype relationship seems almost impossible. Therefore, the separation of trisomic effects that disturb development from those that alter cellular function is key to defining the etiology of bone pathologies in DS [32]. More importantly, a better understanding of trisomic gene expression in DS, their context-dependent expression patterns in time and space, and their downstream effectors are absolutely necessary [32].

### Gonadal effects on bone loss in Down syndrome

Differences in bone mass, observed as low BMD, have been observed amongst adolescents, and adults with DS when compared to the general population [19, 21, 33, 34]. Additionally, sex-specific differences in bone mass between men and women with DS have been detected [19, 33, 35]. In a recent study assessing bone mass in a large cohort of Spanish adults with DS by Costa and colleagues [19], they noticed that Z-scores (comparison of BMD to age-matched controls) of male DS patients, compared with healthy individuals of same age and sex, were lower than DS females [19]. These clinical data are directly consistent with the low BMD reported in the male Dp16 DS mice, but not female mice in this chapter. Additionally, the BMD

of DS men and DS women, was similar in both sexes at all ages [19], whereas BMD is usually lower in women than men in the general population [36-38].

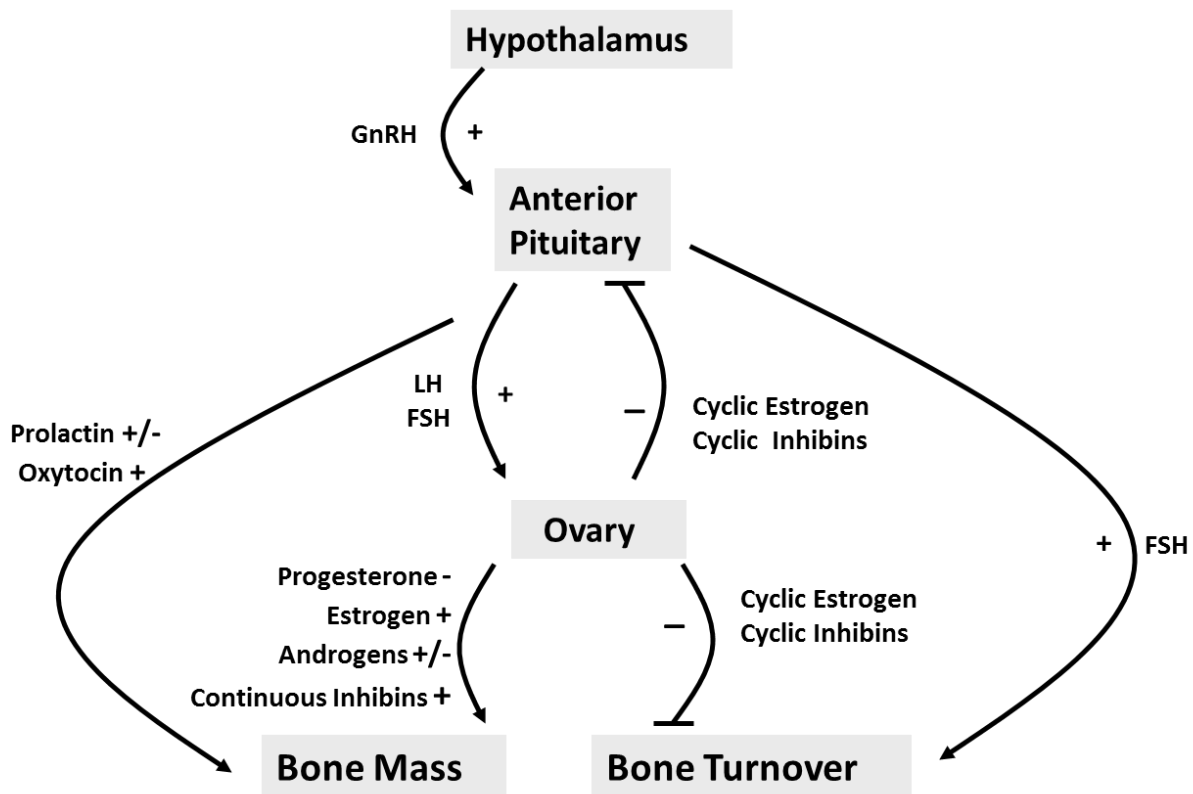


**Figure 10. Hypothalamic-Pituitary-Gonadal-Skeletal Axis.** Gonadotropin releasing hormone (GnRH) from the hypothalamus stimulates secretion of pituitary gonadotropins, luteinizing hormone (LH) and follicle stimulating hormone (FSH), which regulate ovarian function. FSH can stimulate osteoclastogenesis, thus increasing bone turnover; whereas LH does not appear to exert any direct effects on bone. Prolactin (PRL) exerts effects on bone cells in an age-dependent manner such that fetal/neonatal effects are stimulatory but adult effects are inhibitory. The pituitary hormones LH and FSH are negatively regulated by ovarian E2 and inhibins, respectively. Normal serum inhibin and E2 levels are altered as a function of the menstrual cycle. Cyclic exposure to inhibins and E2 suppress osteoclast differentiation (suppression of bone turnover), thus osteoblast differentiation; whereas continuous exposure is anabolic.

Given the pronounced lower BMD phenotype in DS males than females in both human and Dp16 DS when compared to healthy controls, we next reexamined the Dp16 BMD data using a two-way ANOVA to better understand any interactive effect of sex and genotype on the bone phenotype in Dp16 mice (**Figure 11**). Surprisingly, after this re-examination a similar effect of BMD in Dp16 mice as seen in the human DS populations studied by Costa [19] was observed. As shown (Figure 6) BMD in male Dp16 DS mice was significantly decreased from male WT mice ( $p=0.0162$ ), yet there were no significant differences in BMD between 3 month old adult male and female Dp16 DS mice ( $p=0.8351$ ). These data directly correlate with and support the sex-specific changes in bone mass observed in Dp16 mice and in human DS.

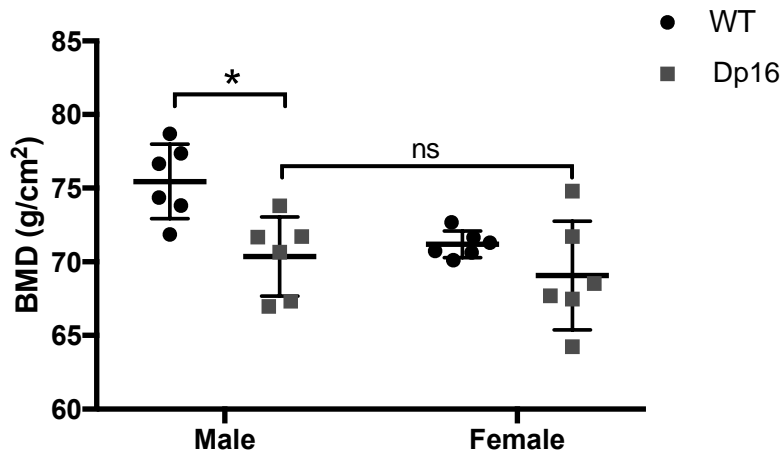


**Figure 11. BMD is similar between male and female Dp16 DS mice.** Statistical analysis by 2-way ANOVA was performed on the Dp16 BMD data to understand the effect of trisomy and sex on bone mass in DS. The results revealed decreased BMD within male Dp16 with no changes in female Dp16 mice, as we previously showed. However, there were no changes between male and female Dp16 DS mice. \* indicates  $p<0.05$ . (ns) indicates no significance.

### **Prolactin and inhibin control of bone cell differentiation and bone mass**

As mentioned earlier, Angelopoulou et al. [24] examined gonadal function in young women with DS by measuring pituitary and ovarian hormone levels [follicle stimulating hormone (FSH), luteinizing hormone (LH), E2, prolactin (PRL), testosterone, and 17-hydroxyprogesterone (17-OHP)] of 13 DS women aged 19-29. This study revealed normal gonadal function given the insignificant changes in menarche and the normal uterine and ovarian size as well as endometrial thickness in the women with DS [24]. However, higher levels of PRL compared to the control group, although within normal lab range, were reported. Prolactin is a pituitary hormone thought to have a direct effect on bone mass [26, 39] (**Figure 10**). These effects on bone cell maturation and differentiation are dependent on context and timing of hormone secretion [26]. In rats, PRL had a stimulatory effect on bone in young, but not adult animals [40], which could explain the significant increase in osteoblast maturation in young adult female Dp16 DS mice with little to no changes in osteoclast numbers when compared to WT and gender controls. Thus, the role of prolactin in regulating bone mass through bone cell differentiation and maturation – especially in female Dp16 mice – should be further explored. Additionally, LH, testosterone, and 17-OHP were reported as significantly elevated in this same cohort of young DS women [24].

Similarly, an earlier study [41] assessing gonadal function in people with DS showed that FSH levels in preputial boys and girls were 2 standard deviations above the mean of non-down syndrome children [41]. The same study reported mean serum levels of FSH and LH were significantly elevated in sexually mature men with DS when compared to non-down syndrome male individuals, but testosterone was normal [41], which suggests alterations in the HPGS axis due to some factor other than the sex steroid hormones. The increased FSH levels in all genders,

especially in young adolescence and young adults, without changes in sex steroids point to the FSH-regulatory hormones, inhibins, and activins as potential targets for our investigation into the sex-specific differences of bone mass in DS [42-44].

As mentioned above, infertility and hypogonadism are very common in both men and women with DS [41]. However, the literature suggests that the deficits in gonadal function and infertility are more pronounced in adolescent boys and young men, than adolescent girls and young women [24, 45]. The increases in FSH and LH levels, especially in adolescents and young adults suggest dysregulation of the HPGS at a much earlier age in DS, potentially as early as prenatally. For instance, the fact that prolactin effects on bone cells occur in an age dependent manner where effects are stimulatory during in utero development, but inhibitory in adults (**Figure 10**). Alterations in HPGS axis such as this one can dramatically impact bone health, but also impact bones differently in men and woman. These findings provide some insight into the conflicting data of gonadal effects on bone cells and the skeleton in DS. Although we have shown that the low bone mass phenotype in DS is due to low bone turnover [12], previous studies by other researchers have suggested high bone turnover due to increased bone resorption as the main source of osteopenia as seen in DS [34]. However, most of these studies did not consider the age-dependent effect of gonadal dysregulation in their cohort studies. Thus, it is just as likely that both events occur, but in a context- and time- dependent manner in both skeletal development and homeostasis.

In chapter IV, I will further investigate the pathophysiology of these dynamic processes and factors that regulate bone cells, thus bone turnover. In the chapter, we will begin to separate out the trisomic effects that potentially disturb development and those that alter cellular function

in adult life. Additionally, I will also describe the effect of anabolic bone therapies in a murine model of DS.

## References

1. Parker SE, Mai CT, Canfield MA, Rickard R, Wang Y, Meyer RE, et al. Updated National Birth Prevalence estimates for selected birth defects in the United States, 2004-2006. *Birth Defects Res A Clin Mol Teratol.* 2010;88(12):1008-16.
2. Presson AP, Partyka G, Jensen KM, Devine OJ, Rasmussen SA, McCabe LL, et al. Current estimate of Down Syndrome population prevalence in the United States. *J Pediatr.* 2013;163(4):1163-8.
3. Schreinemachers DM, Cross PK, Hook EB. Rates of trisomies 21, 18, 13 and other chromosome abnormalities in about 20 000 prenatal studies compared with estimated rates in live births. *Hum Genet.* 1982;61(4):318-24.
4. Kamalakar A, Harris JR, McKelvey KD, Suva LJ. Aneuploidy and skeletal health. *Curr Osteoporos Rep.* 2014;12(3):376-82.
5. Coppus AM, Evenhuis HM, Verberne GJ, Visser FE, Oostra BA, Eikelenboom P, et al. Survival in elderly persons with Down syndrome. *J Am Geriatr Soc.* 2008;56(12):2311-6.
6. Glasson EJ, Sullivan SG, Hussain R, Petterson BA, Montgomery PD, Bittles AH. The changing survival profile of people with Down's syndrome: implications for genetic counselling. *Clin Genet.* 2002;62(5):390-3.
7. Zigman WB. Atypical aging in Down syndrome. *Dev Disabil Res Rev.* 2013;18(1):51-67.
8. Schragger S, Kloss C, Ju AW. Prevalence of fractures in women with intellectual disabilities: a chart review. *J Intellect Disabil Res.* 2007;51(Pt 4):253-9.
9. Geijer JR, Stanish HI, Draheim CC, Dengel DR. Bone mineral density in adults with Down syndrome, intellectual disability, and nondisabled adults. *Am J Intellect Dev Disabil.* 2014;119(2):107-14.



10. Kao CH, Chen CC, Wang SJ, Yeh SH. Bone mineral density in children with Down's syndrome detected by dual photon absorptiometry. *Nucl Med Commun.* 1992;13(10):773-5.
11. Hawli Y, Nasrallah M, El-Hajj Fuleihan G. Endocrine and musculoskeletal abnormalities in patients with Down syndrome. *Nat Rev Endocrinol.* 2009;5(6):327-34.
12. McKelvey KD, Fowler TW, Akel NS, Kelsay JA, Gaddy D, Wenger GR, et al. Low bone turnover and low bone density in a cohort of adults with Down syndrome. *Osteoporos Int.* 2013;24(4):1333-8.
13. Rueda N, Florez J, Martinez-Cue C. Mouse models of Down syndrome as a tool to unravel the causes of mental disabilities. *Neural Plast.* 2012;2012:584071.
14. Fowler TW, McKelvey KD, Akel NS, Vander Schilden J, Bacon AW, Bracey JW, et al. Low bone turnover and low BMD in Down syndrome: effect of intermittent PTH treatment. *PLoS One.* 2012;7(8):e42967.
15. Blazek JD, Gaddy A, Meyer R, Roper RJ, Li J. Disruption of bone development and homeostasis by trisomy in Ts65Dn Down syndrome mice. *Bone.* 2011;48(2):275-80.
16. Leffler A, Ludwig M, Schmitt O, Busch LC. Germ cell migration and early development of the gonads in the trisomy 16 mouse--an animal model for Down's syndrome. *Ann Anat.* 1999;181(3):247-52.
17. Starbuck JM, Dutka T, Ratliff TS, Reeves RH, Richtsmeier JT. Overlapping trisomies for human chromosome 21 orthologs produce similar effects on skull and brain morphology of Dp(16)1Yey and Ts65Dn mice. *Am J Med Genet A.* 2014;164A(8):1981-90.
18. Williams DK, Parham SG, Schryver E, Akel NS, Shelton RS, Webber J, et al. Sclerostin Antibody Treatment Stimulates Bone Formation to Normalize Bone Mass in Male Down Syndrome Mice. *JBMR Plus.* 2018;2(1):47-54.
19. Costa R, De Miguel R, Garcia C, de Asua DR, Castaneda S, Moldenhauer F, et al. Bone Mass Assessment in a Cohort of Adults With Down Syndrome: A Cross-Sectional Study. *Intellect Dev Disabil.* 2017;55(5):315-24.
20. van Allen MI, Fung J, Jurenka SB. Health care concerns and guidelines for adults with Down syndrome. *Am J Med Genet.* 1999;89(2):100-10.

21. Guijarro M, Valero C, Paule B, Gonzalez-Macias J, Riancho JA. Bone mass in young adults with Down syndrome. *J Intellect Disabil Res.* 2008;52(Pt 3):182-9.
22. Bittles AH, Glasson EJ. Clinical, social, and ethical implications of changing life expectancy in Down syndrome. *Dev Med Child Neurol.* 2004;46(4):282-6.
23. Cipriani G, Danti S, Carlesi C, Di Fiorino M. Aging With Down Syndrome: The Dual Diagnosis: Alzheimer's Disease and Down Syndrome. *Am J Alzheimers Dis Other Demen.* 2018:1533317518761093.
24. Angelopoulou N, Souftas V, Sakadamis A, Matziari C, Papameletiou V, Mandroukas K. Gonadal function in young women with Down syndrome. *Int J Gynaecol Obstet.* 1999;67(1):15-21.
25. Vaananen HK, Harkonen PL. Estrogen and bone metabolism. *Maturitas.* 1996;23 Suppl:S65-9.
26. Nicks KM, Fowler TW, Gaddy D. Reproductive hormones and bone. *Curr Osteoporos Rep.* 2010;8(2):60-7.
27. Keck-Wherley J, Grover D, Bhattacharyya S, Xu X, Holman D, Lombardini ED, et al. Abnormal microRNA expression in Ts65Dn hippocampus and whole blood: contributions to Down syndrome phenotypes. *Dev Neurosci.* 2011;33(5):451-67.
28. Hill CA, Sussan TE, Reeves RH, Richtsmeier JT. Complex contributions of Ets2 to craniofacial and thymus phenotypes of trisomic "Down syndrome" mice. *Am J Med Genet A.* 2009;149A(10):2158-65.
29. Delabar JM, Aflalo-Rattenbac R, Creau N. Developmental defects in trisomy 21 and mouse models. *ScientificWorldJournal.* 2006;6:1945-64.
30. Letourneau A, Santoni FA, Bonilla X, Sailani MR, Gonzalez D, Kind J, et al. Domains of genome-wide gene expression dysregulation in Down's syndrome. *Nature.* 2014;508(7496):345-50.
31. Richtsmeier JT, Baxter LL, Reeves RH. Parallels of craniofacial maldevelopment in Down syndrome and Ts65Dn mice. *Dev Dyn.* 2000;217(2):137-45.

32. Roper RJ, Reeves RH. Understanding the basis for Down syndrome phenotypes. *PLoS Genet.* 2006;2(3):e50.
33. Gonzalez-Aguero A, Vicente-Rodriguez G, Moreno LA, Casajus JA. Bone mass in male and female children and adolescents with Down syndrome. *Osteoporos Int.* 2011;22(7):2151-7.
34. Sakadamis A, Angelopoulou N, Matziari C, Papameletiou V, Souftas V. Bone mass, gonadal function and biochemical assessment in young men with trisomy 21. *Eur J Obstet Gynecol Reprod Biol.* 2002;100(2):208-12.
35. Baptista F, Varela A, Sardinha LB. Bone mineral mass in males and females with and without Down syndrome. *Osteoporos Int.* 2005;16(4):380-8.
36. Kanis JA. Bone density measurements and osteoporosis. *J Intern Med.* 1997;241(3):173-5.
37. Kanis JA, Johnell O, Oden A, De Laet C, Mellstrom D. Epidemiology of osteoporosis and fracture in men. *Calcif Tissue Int.* 2004;75(2):90-9.
38. Seeman E, Bianchi G, Adami S, Kanis J, Khosla S, Orwoll E. Osteoporosis in men--consensus is premature. *Calcif Tissue Int.* 2004;75(2):120-2.
39. Clement-Lacroix P, Ormandy C, Lepescheux L, Ammann P, Damotte D, Goffin V, et al. Osteoblasts are a new target for prolactin: analysis of bone formation in prolactin receptor knockout mice. *Endocrinology.* 1999;140(1):96-105.
40. Krishnamra N, Seemoung J. Effects of acute and long-term administration of prolactin on bone <sup>45</sup>Ca uptake, calcium deposit, and calcium resorption in weaned, young, and mature rats. *Can J Physiol Pharmacol.* 1996;74(10):1157-65.
41. Hsiang YH, Berkovitz GD, Bland GL, Migeon CJ, Warren AC. Gonadal function in patients with Down syndrome. *Am J Med Genet.* 1987;27(2):449-58.
42. Gaddy-Kurten D, Coker JK, Abe E, Jilka RL, Manolagas SC. Inhibin suppresses and activin stimulates osteoblastogenesis and osteoclastogenesis in murine bone marrow cultures. *Endocrinology.* 2002;143(1):74-83.

43. Perrien DS, Akel NS, Edwards PK, Carver AA, Bendre MS, Swain FL, et al. Inhibin A is an endocrine stimulator of bone mass and strength. *Endocrinology*. 2007;148(4):1654-65.
44. Perrien DS, Nicks KM, Liu L, Akel NS, Bacon AW, Skinner RA, et al. Inhibin A enhances bone formation during distraction osteogenesis. *J Orthop Res*. 2012;30(2):288-95.
45. Angelopoulou N, Souftas V, Sakadamis A, Mandroukas K. Bone mineral density in adults with Down's syndrome. *Eur Radiol*. 1999;9(4):648-51.

CHAPTER IV  
MECHANISMS OF LOW BONE MASS PHENOTYPE AND THERAPEUTIC TREATMENT  
IN TS65DN MALE MICE

**Introduction**

Down syndrome (DS), the trisomy of human chromosome (Hsa) 21, is the most common symptomatic chromosomal abnormality compatible with survival into adulthood [1]. The likelihood of trisomy 21 is strongly associated with maternal age [2], although trisomy 21 originates either maternally or paternally [3-5]. Indeed, individuals with DS present with a plethora of multifaceted endocrine, metabolic, behavioral and musculoskeletal syndromes with over 80 clinically-defined phenotypes affecting virtually all organ systems [6]. People with DS have some degree of cognitive impairment, various endocrine disorders and decreased fertility as well as an abnormal pattern of long bone skeletal growth during adolescence [7]. In addition, individuals with DS exhibit a profound dysregulation of the adult appendicular skeleton, that we and others have reported [8-11]. It is clear that children and adults with DS exhibit a significant reduction in bone mineral density (BMD) [8-13], and an imbalance between the processes of bone resorption and formation during bone accrual and bone remodeling [8]. The combination of these cellular activities contribute to the high incidence of osteopenia and osteoporosis in adults with DS [14, 15].

Unlike other low bone mass scenarios, the low BMD of DS is not associated with increased bone turnover, but is instead the result of decreased bone turnover [8], and attributed to

-----  
Part of this chapter is reprinted with permission from “Sclerostin Antibody Treatment Stimulates Bone Formation to Normalize Bone Mass in Male Down Syndrome Mice” by Williams, DK, Parham, SG, Schryver, E, Akel, NS, Shelton, RS, Webber, J, Swain, FL, Schmidt, J, Suva, LJ, and Gaddy, D.2018. JBMR Plus. 2:48-55. Copyright 2018 by JBMR Plus

reduced osteoclast and osteoblast numbers as previously shown in Ts65Dn male mice [16], a well-characterized and recognized murine model of Down syndrome [17, 18]. The low bone turnover phenotype exists despite the sustained and profound hypogonadism [10, 19], as discussed in Chapter I. However, the molecular mechanism(s) underlying this cellular defect is not well understood. In this setting, anti-resorptive treatments are inappropriate, since the reason for bone loss is not increased bone turnover as in post-menopausal osteoporosis. Therefore, in the case of individuals with DS and low bone turnover, the need for bone anabolic agents that can enhance bone mass, increase bone strength and decrease fracture risk become particularly important. We have shown previously that intermittent parathyroid hormone (PTH) treatment of Ts65Dn DS mice induces a profound and significant elevation of bone mass and strength [16]. Despite the well-documented efficacy of PTH as a bone anabolic therapy [20-22], the use of PTH has distinct limitations. Treatment with PTH is limited to 24 months because of concerns regarding a potential link to osteosarcoma [23] and PTH is approved only for the treatment of osteoporosis in men and post-menopausal women who are at high risk for a fracture, have existing fractures and not for use in younger adults [24]. Despite these limitations, it is also important to recognize that no connection with the occurrence of osteosarcoma in humans currently exists between elevated serum PTH in hyperparathyroidism or PTH treatment [25]. In the case of adults with DS, there is a distinct opportunity and unmet need for the use of potent bone anabolic agents to increase bone quality and decrease fracture risk and potentially incidence.

Currently, the bone anabolic target receiving the greatest pharmaceutical attention is the inhibition of the sclerostin pathway, which is discussed in greater detail in Chapter I. Sclerostin, the product of the *SOST* gene, produced primarily by osteocytes, is a potent negative regulator of

bone formation via inhibition of the Wnt signaling pathway [26]. Our laboratory has shown no differences in circulating serum sclerostin levels in individuals with Down syndrome compared with non-DS patients; suggesting that an anti-sclerostin biological therapy could be beneficial for improving bone mass in DS. Although a promising treatment candidate that significantly increases bone mineral density and bone formation with decreased bone resorption in postmenopausal women with low bone mass [27], the potential utility of anti-sclerostin therapy to increase bone mass in challenging patient populations such as DS is unknown. Additionally, a better understanding of the mechanistic underpinnings of this rare and unusual low bone turnover and low bone mass phenotype is required.

In order to determine the potential utility of this anabolic therapeutic approach and gain insight into other potential therapeutic targets in DS, the effect of anti-sclerostin therapy on bone and the differential gene expression profiles in DS, specifically Ts65Dn DS mice, was determined in the experiments described in this chapter. Ts65Dn was chosen for this treatment study due to its more pronounced DS bone phenotype compared with Dp16, and its similar age-dependent decrease in bone turnover to human DS. Sclerostin antibody (SclAb) treatment significantly stimulated bone mass in wild type mice and normalized bone mass in Ts65Dn DS mice, via a mechanism that was osteoblast-mediated with little or no impact on inherent osteoclastogenesis. The data suggest that bone anabolic therapies such as SclAb is an appropriate therapy in healthy adult DS patients with low BMD and at increased risk of fracture.

## **Sclerostin Antibody Treatment Stimulate Bone Formation and Normalize Bone Mass in Male Down Syndrome**

### Study Design

Using baseline body mass to minimize inter-group differences, 8-week old male

Ts(1716)65Dn (Ts65Dn) mice and wild-type (WT) mice (Jackson Laboratory, Bar Harbor, ME) were randomly assigned to treatment (SclAb) or control vehicle-treated (VEH) (n=4-6/group each) for a total of four groups with all animals housed individually. Group **1**) WT (VEH); **2**) WT-SclAb; **3**) Ts65 (VEH); **4**) Ts65-SclAb. The groups received either vehicle (isotonic vehicle buffer) or SclAb (100 mg/kg/week, both kindly provided by Dr. Michaela Kniessel, Novartis) as weekly i.v. injections in the morning on day 0, 7, 14 and 21 as previously described [28, 29] before sacrifice and tissue collection on day 28 (**Figure 12**). Measurements of body weight occurred at the same time per week to allow individual calculation of SclAb dose. All mice were maintained on a 12/12 hour light/dark cycle, had *ad libitum* access to standard laboratory rodent chow and water, and were sacrificed by CO<sub>2</sub> inhalation at the end of the experiment (mice at 12 weeks of age). In this study, only male mice were used due to the lack of any commercial source of Ts65Dn female mice reported to be due to the importance of female mice in colony maintenance at Jackson Laboratory. All animal procedures were approved by and performed in accordance with the guidelines of the University of Arkansas for Medical Sciences (UAMS) Institutional Animal Care and Use Committee (IACUC).



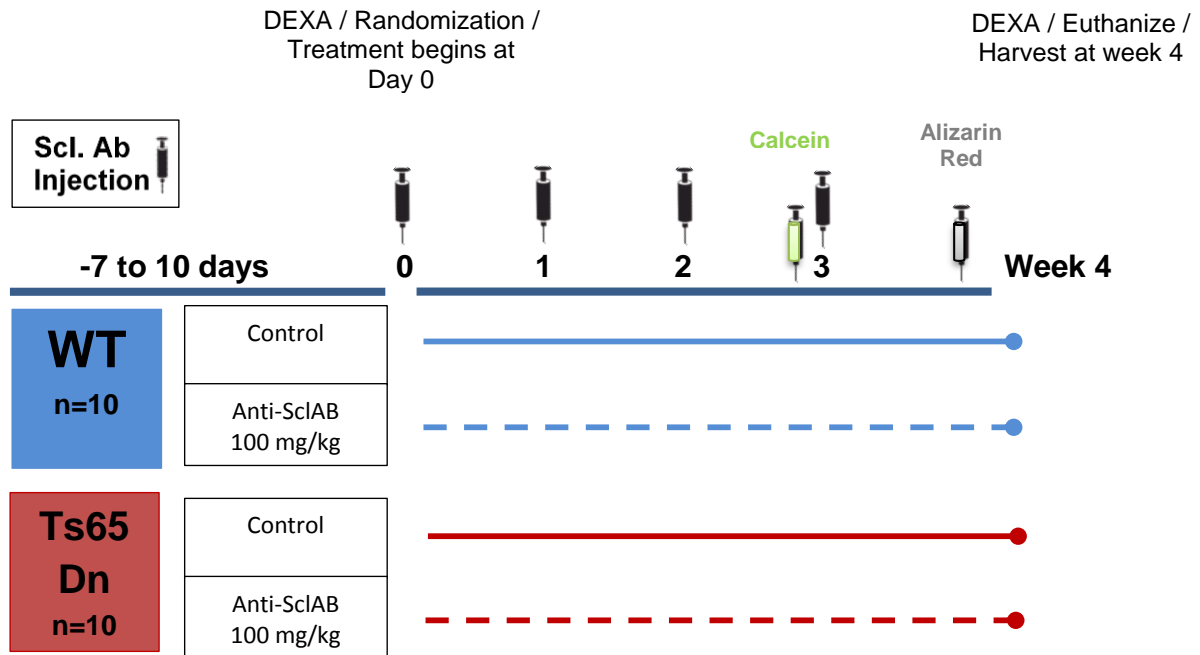


**Figure 12. Schematic of study design for the treatment of male Ts65Dn mice with SclAB.**

8 week old Ts65Dn DS mice were randomly assigned to four treatment groups with 5 mice per group – WT control (vehicle treated), WT anti-SclAB (100 mg/kg), Ts65DN Control (vehicle treated), or Ts65Dn anti-SclAB (100 mg/kg). All treatment injections were given intravenously. Measurements by DXA was taken pre and post treatment (time of euthanasia). Calcein (15 mg/kg) and alizarin red complexome (40 mg/kg) were given i.p. 8 and 2 days, respectively. Serum, long bones, spines, and skulls were harvested at time of euthanasia (4 weeks).

## Results

### Normalization of BMD by sclerostin antibody treatment at multiple sites in Ts65Dn Mice

At baseline and as we and others have reported [16, 30], Ts65Dn mice body weight was significantly less than WT ( $p < 0.001$ ) and the genotype-specific differences in body weight remained apparent at the end of the experiment (4 weeks) ( $p = 0.01$ ) [16] (**Figure 13F**). As shown previously [16], BMD of vehicle treated Ts65Dn mice was significantly reduced from WT vehicle treated mice at both baseline and after 4 weeks ( $p < 0.001$  vs. WT at baseline;  $p < 0.05$  at 4 weeks). BMD was assessed at baseline following 4 weeks of SclAb treatment (100

mg/kg/week) at whole body, spine, tibia, and femur (**Figure 13A-E**). BMD was significantly increased in both WT ( $p < 0.001$  vs. vehicle treated WT) and Ts65 mice ( $p < 0.001$  vs. vehicle treated Ts65Dn) in multiple sites after 4 weeks of treatment. Remarkably, at both the whole body and proximal tibia, the low bone mass phenotype of Ts65Dn mice normalized after 4 weeks of SclAb treatment and was not different from vehicle treated WT mice (**Figure 13A, B**). In contrast, Ts65Dn spine BMD was significantly increased compared to WT controls 4 weeks after SclAb treatment (**Figure 13D**). At the primarily cortical bone site of the tibia and femur midshaft, SclAb treatment significantly increased cortical BMD in both genotypes but Ts65Dn cortical BMD was normalized to WT levels (**Figure 13C, E**). The overall extent and rate of increase in BMD at all sites in the SclAb treated animals was similar in both genotypes.

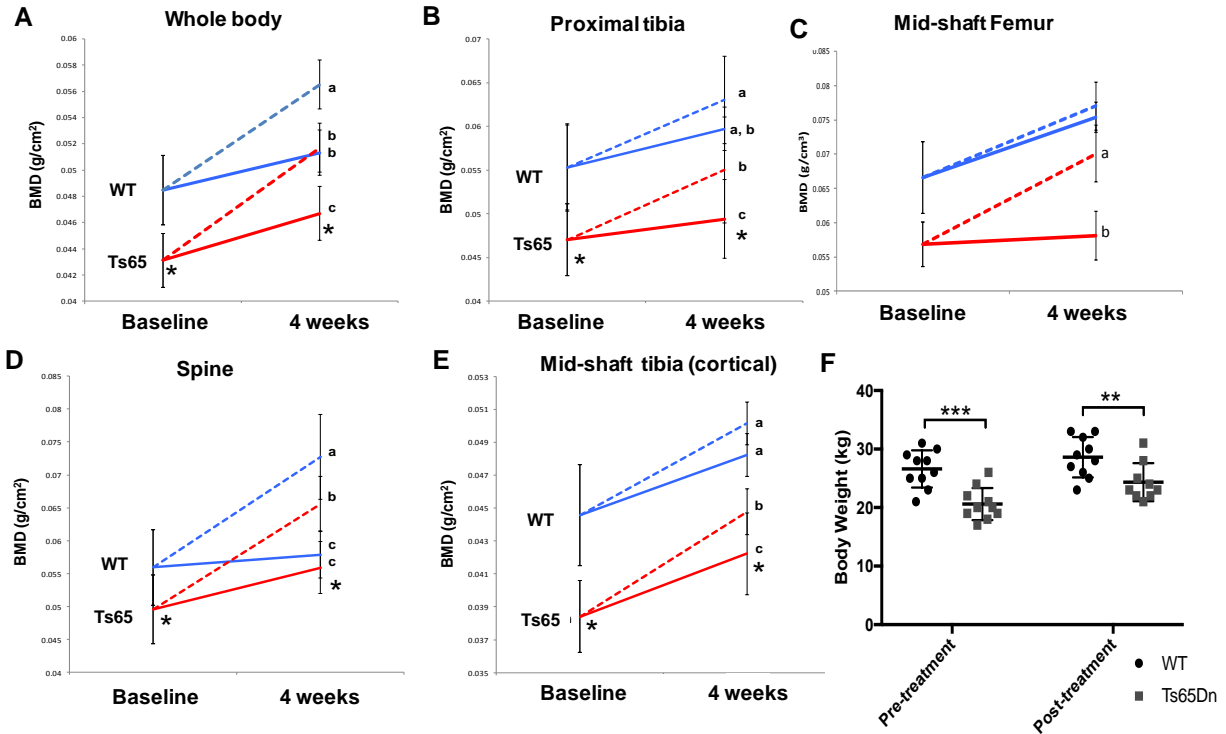


**Figure 13. Sclerostin Antibody increased BMD in Ts65Dn and WT mice.** BMD was measured via DXA at baseline and post treatment (week 4) at the whole body (A), proximal tibia (B), femur mid-shaft (cortical) (C), spine (D) and tibia mid-shaft (cortical) (E) sites. Vehicle treated (Solid line), SclAb treated (dashed line). Body weight of pre and post-treatment (F). Different letters are significantly different from each other at  $p < 0.05$ . \* Indicates Ts65Dn vehicle treated significantly different from WT vehicle treated at both baseline and at 4 weeks (\* $p < 0.05$ ; \*\*  $p < 0.01$ ; \*\*\*  $p < 0.001$ ). Reprinted with permission from [81].

### Effect of sclerostin antibody on bone microarchitecture and geometry

The effect of SclAb treatment on trabecular bone architecture and cortical geometry was assessed by *ex vivo* MicroCT, using methods that we have previously reported and as described in Chapter II. Overall SclAb treatment improved both trabecular bone microarchitecture (Figure 14) and cortical bone geometry (Table 5) in WT and Ts65Dn mice. Trabecular bone microarchitecture was significantly enhanced in both WT and Ts65Dn mice treated with SclAb compared to vehicle-treated mice. MicroCT renderings (Figure 14A) as well as quantitation showed significant SclAb treatment differences within genotype of BV/TV ( $p = 0.025$  WT;

p=0.008 Ts65; **Figure 14B**), Tb.N. (p=0.019 WT; p=0.02 Ts65; **Figure 14C**), Tb.Th (p=0.035 WT; p=0.02 Ts65; **Figure 14D**) and Tb.Sp. (p=0.004 WT; p=0.022 Ts65; **Figure 14E**).

In cortical bone the SclAb-mediated effects were anabolic but not as consistently robust (**Table 5**). The bone marrow microenvironment is a very active site of the skeleton that includes many cell types that can alter bone formation and bone mass [31, 32]. Therefore, the differences in the robust nature of SclAb effects in trabecular bone compared to cortical bone could be explained by changes in the bone marrow microenvironment. Following SclAb treatment, cortical thickness (Ct.Th.) was significantly increased in both genotypes, and in Ts65Dn treated animals was restored to near WT levels (**Table 5**). Medullary area (MA) was significantly lower in Ts65Dn animals compared with WT (p=0.045) as we have previously shown [16]. This parameter was significantly reduced in both WT and Ts65Dn mice by SclAb treatment (**Table 5**), consistent with increased cortical thickness and suggesting an increase in bone strength. In WT animals, treatment with SclAb also led to significantly increased total cross sectional area (Tt. CSA). In sum, these cortical changes were less profound than the changes observed in trabecular bone, but appear to be due to endosteal bone apposition, as mice treated with SclAb had significantly increased cortical thickness (Ct.Th.) and decreased midshaft medullary area (MA) and diameter (MD) (**Table 5**). Lack of changes in other cortical parameters could be attributed to a reduction in cellular activity in those particular regions of the skeleton, thus osteogenic potential.

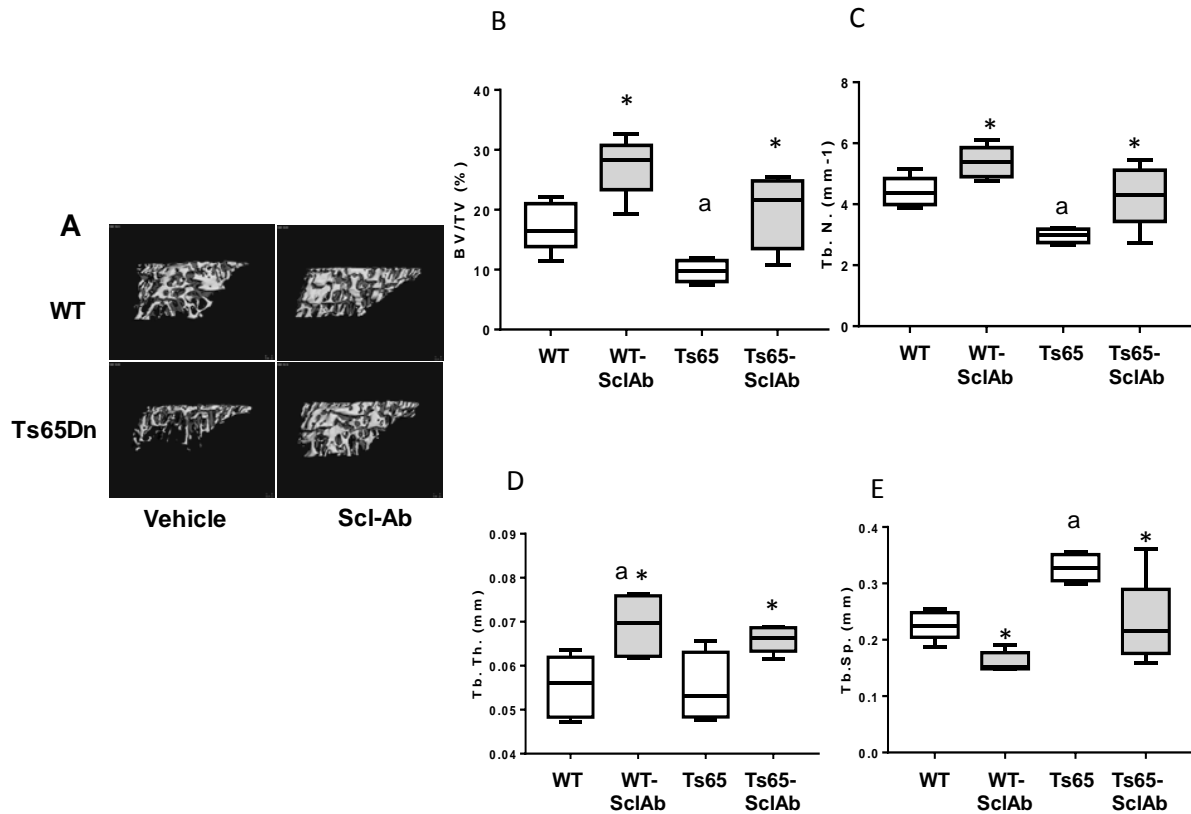


**Figure 14. Sclerostin antibody treatment significantly improved bone microarchitecture assessed by microCT.** Sclerostin antibody treatment significantly improved bone microarchitecture assessed by microCT. (A) MicroCT renderings of the proximal tibia. (B) Measurement of BV/TV (%). \* shows a significantly higher BV/TV in SclAb–treated mice compared to vehicle-treated genotype controls (WT-SclAb vs. WT  $p=0.0169$ ; Ts65-SclAb vs. Ts65  $p=0.028$ ). a: significantly different BV/TV compared to vehicle-treated WT (WT vs Ts65  $p=0.0187$ ). No difference in BV/TV is observed between WT and Ts65-SclAb ( $p=0.8415$ ) (C) Measurement of Tb.N. ( $\text{mm}^{-1}$ ). \* shows a significantly higher Tb.N. in SclAb–treated mice compared to vehicle-treated genotype controls (WT-SclAb vs. WT  $p=0.0159$ ; Ts65-SclAb vs. Ts65  $p=0.041$ ). a: significantly different Tb.N. compared to vehicle-treated WT (WT vs Ts65  $p=0.0227$ ; ). No difference in Tb.N. is observed between WT and Ts65 SclAb ( $p=0.9887$ ) (D). Measurement of Tb.Th. (mm). \* shows a significantly increased Tb.Th. in SclAb–treated mice compared to vehicle-treated genotype controls (WT-SclAb vs. WT  $p=0.0167$ ; Ts65-SclAb vs. Ts65  $p=0.020$ ). No difference in Tb.Th. is observed between WT and Ts65Dn at the genotype level ( $p=0.9996$ ) (E) Measurement of Tb.Sp. (mm). \* shows a significantly decreased Tb.Sp. in SclAb–treated mice compared to vehicle-treated genotype controls (WT-SclAb vs. WT  $p=0.0015$ ; Ts65-SclAb vs. Ts65  $p=0.022$ ). a: significantly different Tb.Th. compared to vehicle-treated WT ( $p=0.0178$ ). No difference in Tb.Sp. is observed between WT and Ts65 SclAb ( $p=0.9994$ ). Reprinted with permission from [81].

**Table 5.** Effect of sclerostin antibody treatment on cortical bone geometry of the tibia assessed by microCT (mean  $\pm$  S.D.) [81]

Parameter	WT		Ts65Dn		ANOVA		
	Vehicle	SclAb	Vehicle	SclAb	p (a)	p (b)	P (c)
<b>Ct.Th. (mm)</b>	0.270 $\pm$ 0.002	<b>0.293<math>\pm</math>0.006<sup>a</sup></b>	<b>0.205<math>\pm</math>0.003<sup>c</sup></b>	<b>0.265<math>\pm</math>0.005<sup>b</sup></b>	<b>0.035</b>	<b>0.0002</b>	<b>&lt;0.0001</b>
<b>MA (mm<sup>2</sup>)</b>	0.122 $\pm$ 0.01	<b>0.095<math>\pm</math>0.005<sup>a</sup></b>	<b>0.101<math>\pm</math>0.005<sup>c</sup></b>	<b>0.079<math>\pm</math>0.01<sup>b</sup></b>	<b>0.002</b>	<b>0.01</b>	<b>0.045</b>
<b>Endos. Pm. (mm)</b>	0.674 $\pm$ 0.089	0.728 $\pm$ 0.09	0.777 $\pm$ 0.06	0.706 $\pm$ 0.04	0.8	0.6	0.9
<b>MD (mm)</b>	0.355 $\pm$ 0.019	<b>0.298<math>\pm</math>0.03<sup>a</sup></b>	<b>0.277<math>\pm</math>0.015<sup>c</sup></b>	<b>0.231<math>\pm</math>0.03<sup>b</sup></b>	<b>0.015</b>	<b>0.016</b>	<b>0.016</b>
<b>Tt.CSA (mm<sup>2</sup>)</b>	0.419 $\pm$ 0.02	<b>0.484<math>\pm</math>0.05<sup>a</sup></b>	<b>0.316<math>\pm</math>0.008<sup>c</sup></b>	0.366 $\pm$ 0.03	<b>0.0379</b>	0.16	<b>0.0018</b>
<b>Ps.Pm. (mm)</b>	1.576 $\pm$ 0.11	1.394 $\pm$ 0.169	1.293 $\pm$ 0.055	1.284 $\pm$ 0.09	0.4	0.9	0.088
<b>AvD. Midshaft (mm)</b>	0.600 $\pm$ 0.025	0.588 $\pm$ 0.03	0.545 $\pm$ 0.05	0.534 $\pm$ 0.02	0.9	0.9	0.1

a: p<0.05 WT-VEH vs. WT-SclAb

b: p<0.05 Ts65Dn Vehicle control vs. Ts65Dn SclAb

c: p<0.05 WT Vehicle control vs. Ts65Dn Vehicle

Abbreviations: Ct.Th. (cortical thickness); MA (medullary area); Endos. Pm (endosteal perimeter); MD (medullary diameter); Tt.CSA (total cross sectional area); Ps.Pm (periosteal perimeter); AvD. Midshaft (average diameter of midshaft)

Reprinted with permission from [81].

## **Sclerostin antibody treatment increases osteoblast parameters without altering osteoclast parameters**

Sclerostin antibody effects on bone formation and cellular differentiation was assessed by histological and histomorphometric evaluation. To determine the rate of bone formation due to SclAb, calcein (15 mg/kg) and alizarin red complexome (40 mg/kg) were injected were i.p. 8 and 2 days, respectively, in Ts65Dn and WT mice. Evaluation of mineralizing surface per bone surface (MS/BS), mineral apposition rate (MAR) of double fluorochrome-labeled murine tibiae were measured in unstained ultraviolet light using Osteomeasure software, which was used to calculate bone formation rates per bone surface (BFR/BS) as described in Chapter II. (**Figure 15**). This analysis confirmed the low bone formation rates in Ts65Dn compared with WT mice as reported previously [16] and identified that bone formation (as measured by mineral apposition rate (MAR) and bone formation rate) was significantly increased with SclAb treatment (**Figure 15E, F**). MAR was significantly decreased in Ts65Dn mice compared to WT mice at baseline (**Figure 15E**) ( $p=0.042$ ) [16]. Following treatment with SclAb bone formation parameters BFR/BS and MAR were both significantly elevated in both genotypes (**Figure 15E, F**). Interestingly, SclAb treated Ts65Dn animals had a significantly increased mineralizing surface to bone surface (MS/BS) ( $p<0.0001$ ) that was not seen in SclAb treated WT animals, perhaps due to the SclAb-related stimulation of the low osteoblast activity inherent in Ts65Dn mice and not regulated in WT animals.

To determine the cellular details of the SclAb treatment effect, evaluation of non-decalcified double fluorochrome labeled murine tibiae was performed using Osteomeasure software. SclAb treatment significantly increased osteoblast surface/bone surface (Ob.S/BS) in WT ( $19 \pm 4\%$  vs. SclAb  $34 \pm 5\%$ ;  $p=0.0014$ ) and in Ts65Dn mice ( $14 \pm 4\%$  vs. SclAb  $24 \pm 3\%$ ;

p=0.045). However, SclAb treatment had no significant effect on osteoclast surface (Oc.S/BS) in either WT ( $0.9 \pm 1\%$  vs. SclAb  $1.1 \pm 0.8\%$ ; p=0.8) or Ts65Dn mice ( $2 \pm 2\%$  vs. SclAb  $3 \pm 2\%$ ; p=0.9), suggesting the profound anabolism of SclAb observed in both genotypes was independent of any detectable changes in osteoclast parameters *in vivo*.

Next, using *ex vivo* bone marrow cultures as described in the methods chapter, the same osteoblast-specific effects of SclAb treatment were observed. As in prior reports [16] the recruitment of bone marrow cells into the osteoblast lineage measured as alkaline phosphatase positive (AP+) colonies/total colonies or the osteoclast lineage as TRAP positive multinucleated cells (**Figure 16**) were less in Ts65Dn at baseline. However, SclAb treatment significantly increased AP+ colonies/total colonies in both genotypes (**Figure 16A**) with no demonstrable effect on osteoclastogenesis (**Figure 16B**). Interestingly, the effect of SclAb on TS65Dn on AP+ colonies/total colonies was able to stimulate recruitment beyond WT or even WT treated with SclAb, perhaps indicative of the extent to which osteoblast lineage is suppressed in Ts65Dn and that can be activated by SclAb treatment. Interestingly, such a profound effect was not observed in PTH-treated Ts65Dn animals [16], perhaps indicative of differences in anabolic potency and/or mechanism of action between the two agents.



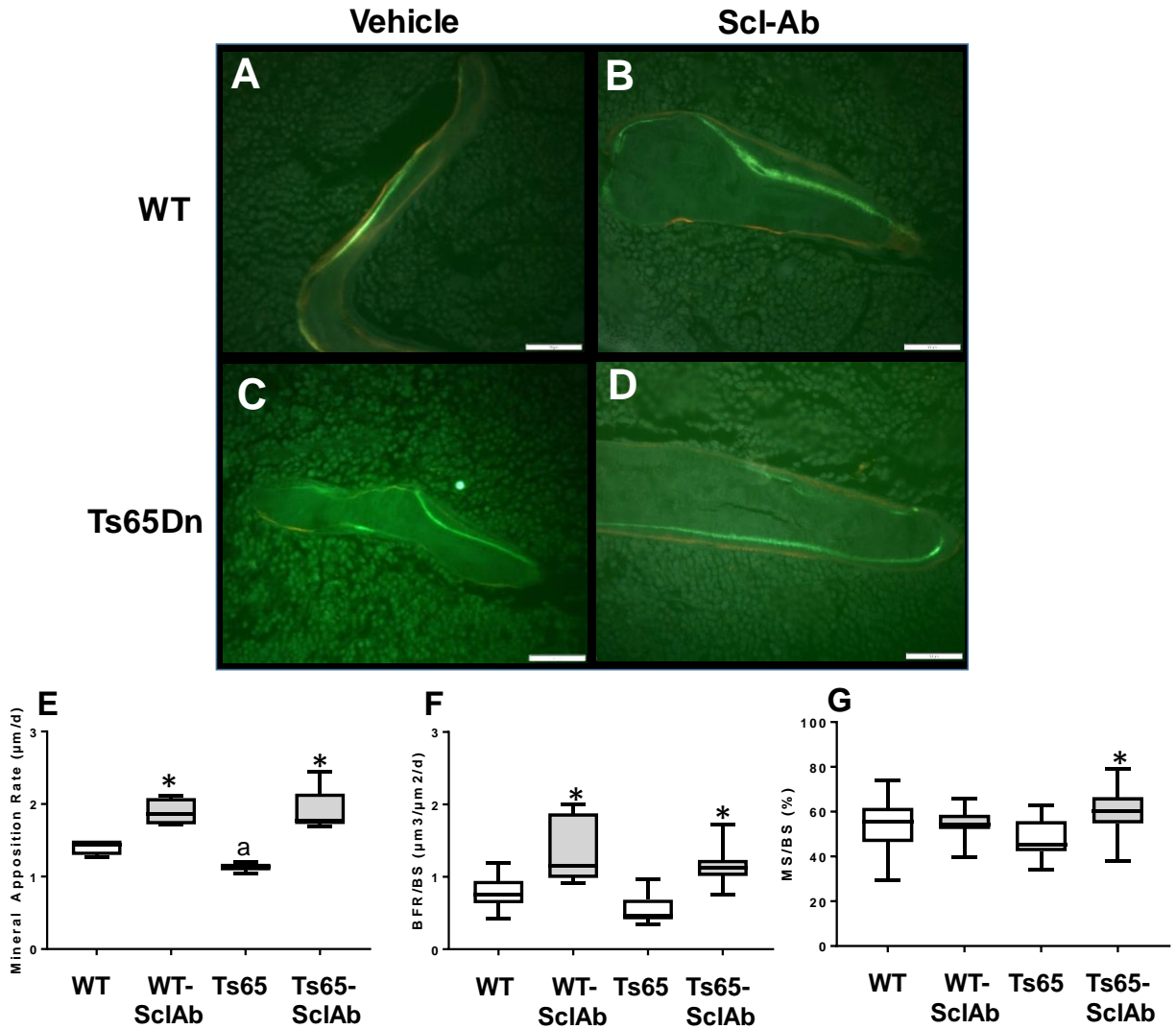


**Figure 15. Representative images of dual fluorochrome labeling of trabecular bone surfaces in (A)** WT Control (Vehicle); **(B)** WT-SclAb; **(C)** Ts65Dn (Vehicle); **(D)** Ts65Dn-SclAb. The increased distance between labels in mice treated with SclAb indicates bone anabolism. Images were acquired under fluorescent light using a 40x objective. Bar = 50  $\mu\text{m}$ . Effect of vehicle (open bars) and SclAb treatment (gray bars) treatment on **(E)** mineral apposition rate (MAR,  $\mu\text{m}/\text{day}$ ), **(F)** bone formation rate/bone surface (BFR/BS,  $\mu\text{m}^3/\mu\text{m}^2/\text{d}$ ), and **(G)** mineral surface/bone surface (MS/BS, %) in WT and Ts65Dn DS mice. \*  $p < 0.05$  shows significant differences in SclAb-treated mice compared to vehicle-treated genotype controls. a: significant difference in vehicle-treated Ts65 compared to vehicle-treated WT  $p < 0.05$ . (MAR WT-SclAb vs. WT  $p = 0.0093$ ; Ts65 vs. Ts65-SclAb  $p < 0.0001$ ), (BFR/BS WT-SclAb BFR/BS vs. WT  $p < 0.0001$ ; Ts65 vs. Ts65-SclAb  $p = 0.0007$ ), (MS/BS WT-SclAb vs. WT  $p = 0.9$ ; Ts65 vs. Ts65-SclAb  $p < 0.0001$ ). Reprinted with permission from [81].

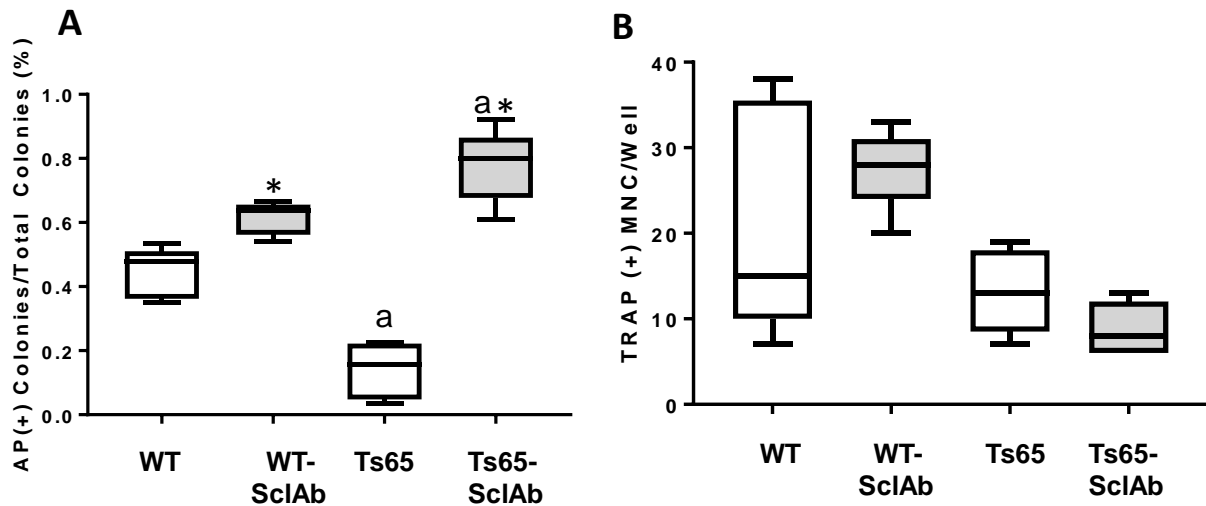


**Figure 16. Sclerostin antibody increases osteoblast recruitment but not osteoclastogenesis.** *Ex vivo* bone marrow cultures of bone marrow from vehicle and SclAb treated WT and Ts65Dn mice. (A) Alkaline phosphatase positive (AP+) / Total colonies are significantly less in Ts65Dn than WT at baseline ( $p=0.0002$ ). (AP+) / Total colonies were significantly increased in both genotypes by SclAb treatment, indicative of increased recruitment into osteogenic lineage and differentiation of precursors by SclAb treatment. \* Significantly different from genotype control (WT-SclAb vs. WT  $p=0.039$ ; Ts65-SclAb vs. Ts65  $p<0.0001$ ) a shows significantly different AP+/Total compared to vehicle-treated WT at  $p<0.05$  (Ts65-SclAb vs. WT  $p<0.0001$ ). (B) Whole bone marrow cultured towards osteoclasts and TRAP+MNC/well enumerated. SclAb treatment has no significant effect on osteoclastogenesis.

## Discussion

In general, social and consenting issues and the apparent lack of mechanistic understanding in disease progression complicate pharmacologic intervention in at risk populations, such as people with DS [33]. This is particularly relevant in the context of low bone mass, where people with DS are at increased risk of fracture [34]. At present, there are no medical treatments approved for use in DS adults with low bone mass and increased risk of fracture. Therefore, low BMD in DS is currently managed by a combination of calcium and vitamin D supplements, physiotherapy, nutritional interventions, exercise and off-label (and contraindicated) oral bisphosphonate use [1]. These interventions are important and can be

effective, but there remains an urgent need for alternative treatments that increase bone mass and strength in this vulnerable and underserved population.

As shown in this chapter, weekly treatment with SclAb not only stimulated bone mass in WT and Ts65Dn DS mice, but returned bone mass and bone microarchitecture in Ts65Dn DS mice to normal age-matched WT levels at multiple skeletal sites. The data suggest that the anabolic effect of SclAb treatment that is well documented in high bone turnover scenarios such as osteoporosis [27] and osteogenesis imperfecta [35, 36] was able to enhance bone mass, bone quality and bone formation in the face of the low bone turnover inherent in DS. The microarchitectural changes in the trabecular and cortical compartments are entirely consistent with increased bone strength following SclAb treatment, although this was not specifically assessed in this work. However, we and others have shown that the architectural changes observed here in murine long bones are entirely consistent with significant improvements in bone strength [26]. Furthermore, dynamic histomorphometry from the trabecular bone compartment demonstrated that the increased bone volume was due to increased bone formation indices, with no apparent impact on any osteoclastic parameters in either genotype. The potent anabolic response was also captured in *ex vivo* bone marrow cultures from vehicle and SclAb treated animals that showed increased recruitment into the osteogenic lineage with no significant effects on osteoclastogenesis.

The significant improvements in bone mineral density, trabecular bone microarchitecture and cortical geometry as well as increased bone formation rate in SclAb-treated animals are reminiscent of those previously reported by Fowler et al. [16] in WT and Ts65Dn mice treated with PTH. However, unlike PTH, there is little data to suggest that SclAb therapy would be inappropriate for the treatment of low bone mass in people with DS. Indeed, there is data from a

recent randomized Phase 2a clinical trial in adults with moderate osteogenesis imperfecta [35] that demonstrated safe and powerful anabolic effects in a younger adult population than previous SclAb clinical trials. In particular, the bone-modeling-based concept of anti-sclerostin treatment may provide a promising approach to cover longer treatment periods as part of a long-term medication strategy important for younger patients that enables phases of bone regeneration and formation, without changes in bone resorption that could be of significant benefit in the setting of low bone turnover.

As with most preclinical studies, this study has several limitations, including the use of a single dosing regimen of SclAb, assessment of a single 4 week time point, no active comparator and although sufficiently powered, only 4-6 animals per group. Thus, we may have missed early increases in bone resorption parameters associated with SclAb treatment and not seen changes in osteoclast number or activity that occur with age in Ts65Dn mice [16]. Future studies of longer duration with additional time points, increased animal numbers and active comparators that assess the extent to which bone mass is maintained in the low bone turnover setting would be highly informative and valuable. Such studies will provide important insight into the mechanisms that are responsible for the skeletal responses to SclAb in DS. However, despite these limitations, the current study provides the first evidence that SclAb is an effective treatment option for people with DS and low bone mass and potentially in other low bone turnover scenarios. Further investigation to determine the efficacy of SclAb in people with DS and low bone turnover will be required for eventual clinical application.

In sum, these exciting data open up potential opportunities for ongoing research efforts. In the next few pages, I will integrate these findings with other published literature and unpublished studies from our laboratory that may help better understand the mechanisms

underlying bone health in Ts65Dn and identify future directions for anabolic treatments in people with DS. As with all such research ideas, examination *in vitro* and in pre-clinical studies are required before translation to patient care is feasible.





## **Effects of Trisomy 21 on Gene Expression in the Bone and Bone Marrow**

### **Microenvironment**

#### Hypothesis and Study Design

Gene expression profiles by messenger RNA sequencing (RNASeq) were obtained from the femurs (including bone marrow) of 6-7 month old Ts65Dn male DS mice and age-matched littermate controls to study the transcriptome of the bone and bone marrow microenvironment. These data were collected in order to provide insight into the conflicting literature regarding gene dosage effect on DS phenotypes due the trisomic genes found on *Hsa21* in DS or mouse chromosome 16 in Ts65Dn mice as discussed in greater depth in Chapter I. We hypothesized that overexpression of trisomic Mmu 16 genes in the bone of Ts65Dn mice may involve overexpression of RCAN1, which can regulate bone homeostasis via NFATc1 signaling [39]. Thus, overexpression of RCAN1 could be a major contributor to the bone deficits observed in DS (**Table 6**). Additionally, we anticipated the upregulation of genes that function to inhibit osteoclast and osteoblast differentiation or the downregulation of genes associated with bone formation and bone resorption (e.g.: RANKL, M-CSF (**Table 6**) due to the overexpression of RCAN1. Thus, normalized gene expression (FPKM, fragments per kilobase per million) was compared between whole femurs from Ts65Dn male mice and age-matched littermate controls.

**Table 6.** Expected Outcomes for Differential Gene Expression Profile of Ts65Dn mice

<p><b>Hypothesis 1:</b> Since osteoclast- and osteoblastogenesis are decreased in DS and RCAN1 is an inhibitor of NFATc1 via calcineurin inactivation, we expected to see an increase in the expression of RCAN1 and a decrease in genes downstream of calcineurin as well as NFATc1 dependent genes.</p>	
 RCAN1	 <p><b>Ocl:</b> NFATc1, AP1, CREB, MITF, PU.1 ; NFATc1-dependent genes (<b>Ocl:</b> Cathepsin K, TRAP, Calcitonin Receptor – <b>OB:</b> osteocalcin, osteopontin, osteonectin, Type I collagen )</p>
<p><b>Hypothesis 2:</b> Since DS is a low bone turnover disease, we may also identify up-regulation of additional genes that function to inhibit osteoclast- and osteoblastogenesis or down-regulation of genes associated with bone formation and resorption.</p>	
 <p><b>Formation:</b> DKK1 <b>Resorption:</b> OPG</p>	 <p><b>Formation:</b> Wnt, <math>\beta</math>-catenin <b>Resorption:</b> RANKL, M-CSF</p>

## Results

### **Differential Gene Expression Profile by RNASeq**

Data analysis revealed more than 4600 statistically significant differentially expressed genes. Of the differentially expressed genes identified, 3% (152 genes) were found on chromosome 16 and less than half (45%, 69 genes) were up-regulated – some of which were not *Hsa21* syntenic genes. Moreover, RCAN1 was not differentially expressed, as we had proposed. However, my original hypothesis did consider **1)** the complexity of bone development and homeostasis (i.e. regulation of the skeletal system is an integrative process that includes numerous organ systems); **2)** the expression patterns of the trisomic genes at a particular time (age; 7 months) and space (skeletal system), and **3)** the downstream effect, either direct or indirect, on other genes [40] and cell types – especially given the extreme heterogeneity of the skeleton.

As a result, analysis of the 4648 differentially expressed genes continued. Manual curation of the data was initially performed. The large data set was first sorted by magnitude

(largest to smallest) of differential gene expression represented as the log<sub>2</sub> (Fold Change) or log<sub>2</sub> (FC) to determine other gene(s) that could contribute to the bone phenotype in Ts65Dn. At first glance, the genes with the highest log<sub>2</sub> (FC) gene expression were genes encoding histone proteins (*Hist1h2bb*, *Hist1h3f*, *Hist1h2bl*, *Hist1h1a*, *Hist1h4d*, *Hist1h2ak*, *Hist1h4f*, *Hist2h4*, *Hist1h3c*), which are important components of nucleosomes that limit DNA accessibility to the cellular DNA replication machinery [41, 42]. Additional functions of these proteins as listed by UniProtKB (<https://www.uniprot.org/uniprot/P33778>) include transcription regulation, DNA repair, and DNA replication and chromosome stability. The increased expression of these regulators of DNA transcription is entirely consistent with data that confirmed the role of chromatin modifications in gene expression changes in skin fibroblasts obtained from twins (Down syndrome vs. non-Down syndrome) [43].

Next, genes with a log<sub>2</sub> Fold Change less than -2 or greater than 2 were analyzed using the Mouse Genome Informatics (MGI) Batch Query Tool [44] to determine the function of gene targets most significantly affected by trisomy in Ts65Dn male mice. This analysis facilitates the study of human disease by integrating genetic, genomic, and biological data of mammalian species. Functional annotation revealed many gene targets for skeletal pathology seen in Ts65Dn, as their disruption by gain-or-loss of function mutations exert effects to the musculoskeletal system. However, dopamine receptor D2 (*Drd2*) with an expression fold change of 12.91 (q=0.000346) piqued my interest most as a potential upstream mediator, either directly or indirectly, of bone health in DS. DRD2 disruption is linked to abnormal pituitary gland morphology [45], reduced fertility [46] and gonadal size [47], and abnormal growth hormone levels that alter body size [48]. Dopamine binding to DRD2 inhibits protein kinase B (AKT) activity via  $\beta$ -arrestin2, which leads to subsequent activation of glycogen synthase

kinase-3 (GSK-3) and its downstream gene targets [49]. Additionally, the deletion of DRD2 in mice led to increased expression of inflammatory factors such as TNF $\alpha$  [50] and an increase in the production of reactive oxygen species [51] in the kidney.

Integrative analysis using the Database for Annotation, Visualization and Integrated Discovery (DAVID) web accessible bioinformatics software was next utilized to gain further insight into the biological mechanisms potentially responsible for the bone phenotype in adult Ts65Dn male mice [52, 53]. The gene ontology (GO) analysis [54] revealed the reduced expression of genes involved in the immune system (adjusted p value =  $1.1 \times 10^{-31}$ ), innate immune response (adjusted p-value =  $1.4 \times 10^{-15}$ ), inflammatory response (adjusted p value =  $5.6 \times 10^{-9}$ ) and intracellular signal transduction (adjusted p value =  $1.8 \times 10^{-8}$ ), potentially due to increases in nucleosome assembly genes (adjusted p-value =  $3.4 \times 10^{-3}$ ) as previously shown in a DS and non-DS twins pair [43]. The reduced expression of genes associated with bone resorption (adjusted p value =  $8.5 \times 10^{-3}$ ) due to possibly decreased expression of positive regulators of NF-kappaB transcription factor activity (adjusted p-value =  $3.5 \times 10^{-3}$ ) was also observed. Conversely, GO analysis revealed the increased expression of DNA transcription (adjusted p-value =  $1.6 \times 10^{-11}$ ), which is consistent with the large number of differentially expressed genes in this data set, and the associated regulation of DNA transcription (adjusted p-value =  $2.7 \times 10^{-9}$ ). Genes associated with osteoblast differentiation (adjusted p-value =  $2.8 \times 10^{-5}$ ) (**Table 7**) and ossification (adjusted p-value =  $5.6 \times 10^{-6}$ ) (**Table 8**) were also significantly upregulated.



**Table 7.** GO analysis of upregulated genes associated with osteoblast differentiation

Gene Name	Gene ID	Log2(FC)
B cell receptor associated protein 29(Bcap29)	ENSMUSG00000020650	1.57
DEAD (Asp-Glu-Ala-Asp) box polypeptide 21(Ddx21)	ENSMUSG00000020075	0.58
DEAH (Asp-Glu-Ala-His) box polypeptide 9(Dhx9)	ENSMUSG00000042699	0.85
GTP binding protein 4(Gtpbp4)	ENSMUSG00000021149	0.7
H3 histone, family 3B(H3f3b)	ENSMUSG00000016559	0.46
Indian hedgehog(Ihh)	ENSMUSG00000006538	1.06
SRY (sex determining region Y)-box 8(Sox8)	ENSMUSG00000024176	1.13
UFM1 specific ligase 1(Ufl1)	ENSMUSG00000040359	1.05
WW domain containing transcription regulator 1(Wwtr1)	ENSMUSG00000027803	1.43
actinin alpha 3(Actn3)	ENSMUSG00000006457	1.82
anti-silencing function 1A histone chaperone(Asf1a)	ENSMUSG00000019857	1.19
bone morphogenetic protein 2(Bmp2)	ENSMUSG00000027358	0.71
coiled-coil domain containing 47(Ccdc47)	ENSMUSG00000078622	0.95
collagen, type VI, alpha 1(Col6a1)	ENSMUSG00000001119	0.46
core binding factor beta(Cbfb)	ENSMUSG00000031885	0.56
cysteine rich protein 61(Cyr61)	ENSMUSG00000028195	3
fidgetin-like 1(Fignl1)	ENSMUSG00000035455	0.51
gap junction protein, alpha 1(Gja1)	ENSMUSG00000050953	0.66
growth differentiation factor 10(Gdf10)	ENSMUSG00000021943	0.68
heterogeneous nuclear ribonucleoprotein U(Hnrnpu)	ENSMUSG00000039630	1.13
insulin-like growth factor binding protein 3(Igfbp3)	ENSMUSG00000020427	0.86
integrin binding sialoprotein(Ibsp)	ENSMUSG00000029306	0.88
intraflagellar transport 80(Ift80)	ENSMUSG00000027778	1.24
jun B proto-oncogene(Junb)	ENSMUSG00000052837	0.49
lymphoid enhancer binding factor 1(Lef1)	ENSMUSG00000027985	1.37
myocilin(Myoc)	ENSMUSG00000026697	2.3
myocyte enhancer factor 2C(Mef2c)	ENSMUSG00000005583	1.3
retinol dehydrogenase 14 (all-trans and 9-cis)(Rdh14)	ENSMUSG00000020621	0.79
ribosomal L1 domain containing 1(Rsl1d1)	ENSMUSG00000005846	0.71
runt related transcription factor 2(Runx2)	ENSMUSG00000039153	0.65
secreted phosphoprotein 1(Spp1)	ENSMUSG00000029304	1.06
synaptotagmin binding, cytoplasmic RNA interacting protein(Syncrip)	ENSMUSG00000032423	0.9
transforming growth factor, beta receptor III(Tgfb3)	ENSMUSG00000029287	1.24
twist basic helix-loop-helix transcription factor 1(Twist1)	ENSMUSG00000035799	1.23
versican(Vcan)	ENSMUSG00000021614	1.69

**Table 8.** GO analysis of upregulated genes associated with ossification

<b>Gene Name</b>	<b>Ensembl Gene ID</b>	<b>Log2(FC)</b>
C-type lectin domain family 3, member b(Clec3b)	ENSMUSG00000025784	0.66
DEAH (Asp-Glu-Ala-His) box polypeptide 36(Dhx36)	ENSMUSG00000027770	1.57
Indian hedgehog(Ihh)	ENSMUSG00000006538	1.06
SRY (sex determining region Y)-box 9(Sox9)	ENSMUSG00000000567	1.81
SUN domain containing ossification factor(Suco)	ENSMUSG00000040297	0.76
bone morphogenetic protein 2(Bmp2)	ENSMUSG00000027358	0.71
bone morphogenetic protein 5(Bmp5)	ENSMUSG00000032179	1.37
calcium-sensing receptor(Casr)	ENSMUSG000000051980	2.82
chordin-like 1(Chrdl1)	ENSMUSG000000031283	0.71
collagen, type XI, alpha 1(Col11a1)	ENSMUSG000000027966	1.02
connective tissue growth factor(Ctgf)	ENSMUSG00000019997	1.83
core binding factor beta(Cbfb)	ENSMUSG000000031885	0.56
dentin matrix protein 1(Dmp1)	ENSMUSG000000029307	2.48
discoïdin domain receptor family, member 2(Ddr2)	ENSMUSG000000026674	0.59
forkhead box C1(Foxc1)	ENSMUSG000000050295	1.6
forkhead box C2(Foxc2)	ENSMUSG000000046714	1.82
frizzled class receptor 9(Fzd9)	ENSMUSG000000049551	1.23
glycoprotein m6b(Gpm6b)	ENSMUSG000000031342	1.12
growth differentiation factor 10(Gdf10)	ENSMUSG000000021943	0.68
integrin binding sialoprotein(Ibsp)	ENSMUSG000000029306	0.88
matrix Gla protein(Mgp)	ENSMUSG000000030218	0.98
mitogen-activated protein kinase 8(Mapk8)	ENSMUSG000000021936	1.14
natriuretic peptide receptor 2(Npr2)	ENSMUSG000000028469	0.64
osteocrin(Ostn)	ENSMUSG000000052276	2
pleiotrophin(Ptn)	ENSMUSG000000029838	3.87
runt related transcription factor 1(Runx1)	ENSMUSG000000022952	0.47
sclerostin(Sost)	ENSMUSG000000001494	0.76
secreted phosphoprotein 1(Spp1)	ENSMUSG000000029304	1.06
stanniocalcin 1(Stc1)	ENSMUSG000000014813	2
trans-acting transcription factor 3(Sp3)	ENSMUSG000000027109	1.58
tumor necrosis factor (ligand) superfamily, member 11(Tnfsf11)	ENSMUSG000000022015	1.79
twist basic helix-loop-helix transcription factor 1(Twist1)	ENSMUSG000000035799	1.23
twisted gastrulation BMP signaling modulator 1(Twsg1)	ENSMUSG000000024098	0.96

The increase in osteoblastogenesis-associated gene expression was accompanied by the increased expression of genes found in skeletal system development (adjusted p-value =  $3.3 \times 10^{-2}$ ), including many of the genes associated with osteoblast differentiation and ossification such as *RUNX1*, and *RUNX2*, in addition, to hormone regulators such as follistatin (*FST*). Interestingly, the gene expression increases in osteoblast differentiation and skeletal system development was counter-balanced by the increased expression of genes associated with negative regulation of canonical WNT signaling pathway (adjusted p-value = 0.5). As mentioned in chapter I, canonical WNT signaling is a major component of bone formation and osteogenesis [55] that has been postulated to be almost exclusively expressed in osteocytes in the adult skeleton and regulated by a variety of hormonal and mechanical influences [31, 56]. Loss of function studies of the WNT-receptor LDL receptor related protein 5 (LRP5) also suggest a predominant role of LRP5-WNT signaling in osteocyte-specific regulation of bone homeostasis [31, 57]. Additionally, tissue expression analysis of the differentially expressed genes analyzed by DAVID suggested that these genes are more commonly associated with macrophages (adjusted p-value =  $3.1 \times 10^{-29}$ ) and the thymus (adjusted p-value =  $4.3 \times 10^{-21}$ ), suggesting significant regulation of cells of the hematopoietic cell (HSC) lineage. As expected, gene expression changes associated with bone marrow (adjusted p-value =  $1.8 \times 10^{-15}$ ) and bone (adjusted p-value =  $3.4 \times 10^{-15}$ ) tissue had very high significance supporting the observations by DAVID GO analysis [58].

### **Dysregulation of Signaling Pathways Associated with Bone Homeostasis and Bone Disease in Ts65Dn**

Signaling pathway analysis by DAVID [58] revealed altered expression in more than 123 different signaling pathways. Upregulated expression of pathway genes involved in

transcriptional misregulation in cancer (adjusted p-value =  $8.6 \times 10^{-6}$ ), proteoglycans in cancer (adjusted p-value =  $1.2 \times 10^{-4}$ ), cell cycle (adjusted p-value =  $1.1 \times 10^{-4}$ ), and immunosuppression such as the transforming growth factor beta (TGF $\beta$ ) signaling pathway (adjusted p-value =  $1.8 \times 10^{-2}$ ) suggest a highly proliferative bone marrow environment conducive to bone marrow-derived (liquid) cancer progression, yet resistant to solid tumors [59-61]. Modifications in signaling pathways that function to regulate the basic multicellular unit (BMU) such as WNT signaling (adjusted p-value =  $8.6 \times 10^{-2}$ ), NF $\kappa$ B signaling (adjusted p-value =  $6.6 \times 10^{-4}$ ), and osteoclast differentiation (adjusted p-value =  $1.1 \times 10^{-10}$ ) were also observed. The down regulation of the lysosomal pathway (adjusted p-value of  $9.7 \times 10^{-11}$ ) was among the top 2 pathways significantly altered and supported the downregulation of osteoclast differentiation signaling pathway. Indeed, decreased lysosomal gene expression is entirely consistent with the decreased osteoclastogenesis and bone resorption inherent in Ts65Dn mice. Endocytosis (adjusted p-value =  $4.2 \times 10^{-7}$ ) and phagosome (adjusted p-value =  $1.7 \times 10^{-5}$ ) signaling of downregulated genes in conjunction with decreased lysosome signaling suggesting defects in mechanisms responsible for protein packaging and degradation in addition to recycling of intracellular components were also observed and are consistent with the bone phenotype. Failure in these signaling pathways have been associated with significantly decreased lumbar and total hip BMD [62]. These observations of lysosome and phagosome malfunction are entirely consistent with the GO analysis highlighting autophagy (adjusted p-value = 0.02) [63] as a potential mechanism for the dysregulation of bone homeostasis and decreased bone mass observed in Ts65Dn male mice and DS; and could suggest an accelerated skeletal-aging phenotype in Ts65Dn due at least in part to autophagy suppression [64]. Such observations if confirmed in humans with DS may provide insight into the age-related declines of DS.

## **Molecular Mechanisms of the Dysregulated Bone Homeostasis in Ts65Dn Male Mice**

### *WNT Signaling*

To elucidate the mechanism underlying changes in gene expression profiles of key signaling pathways involved in regulation of bone cells and thus bone homeostasis, the differential expression patterns for these signaling pathways were mapped to Pathway Mapper from the KEGG PATHWAY Database [65-67]. Given the crucial role of WNT signaling in maintaining bone homeostasis via osteoblast proliferation and maturation, and its effects on hematopoiesis [31], we initially mapped the gene patterns of this pathway (**Figure 17**). WNT signaling, more specifically the non-canonical signaling pathway, showed increased expression (red) of genes that encode for the WNT proteins –WNT1, WNT6, and WNT5a in Ts65Dn bones. As mentioned previously, WNTs play an important role in bone formation and bone homeostasis [31] and when overexpressed, can lead to increased risk of cancer [32, 68, 69]. WNT6, specifically, has been shown to play an important role in the formation and maturation of different embryonic tissues including the fetal heart [70]. Over expressing WNT6 causes underdevelopment of heart muscle [70] and decreased muscle mass [71] due to defects in mesenchymal progenitor cells that decrease cell differentiation. WNT6 overexpression has also been shown to block adipogenesis and stimulate osteoblastogenesis [72]. On the other hand, WNT5a signaling functions as a negative feedback loop in bone turnover, where secretion of this WNT protein by osteoblasts leads to hematopoietic stem cell renewal and subsequently increased osteoclast differentiation [73]. WNT5a is also expressed by adult leukemic cells to stimulate osteoclast differentiation. Gain of function mutations in osteocyte-specific WNT1 were shown to stimulate bone formation by increasing the activity and number of osteoblasts via the MTOR

pathway [36] and diagrammed in **Figure 18**. The MTOR-dependent osteoblastogenesis was also observed *in vitro*, in which hypoxia stimulation to cultured osteoblasts increased mRNA and protein levels of BMP2 via HIF-1 alpha and MTOR pathways [74]. Moreover, upregulation of these WNT proteins has also been implicated in oncogenesis in multiple tissues [75-77].

In addition to the WNT proteins, gene expression of the WNT-receptors were also altered in Ts65Dn male mice. Expression of LDL receptor related protein 6 (LRP6) and Frizzled, which are known for their profound effect in increasing bone mass and strength [31], were upregulated (**Figure 17**). Conversely, *LRP5* expression was decreased (**Figure 17**). Based on the idea that *LRP5* expression is osteocyte-specific to regulate bone homeostasis[57], the reduction in *LRP5* suggests decreased sensitivity to mechanical loading possibly due to reduced numbers of osteocytes in the bone matrix [57, 63, 78]. Reduced mechano-sensitivity of osteocytes could explain the increases in *SOST* – the gene that encodes sclerostin, a potent inhibitor of WNT signaling [29]. Additionally, the increased expression of downstream WNT signaling factors such as oncogenes, *c-myc* and *c-jun*, suggest a role of the WNT signaling pathway in the highly proliferative nature of the bone marrow microenvironment in Ts65Dn mice [79] and possibly human DS [80]. Therefore, based on these *in silico* analysis and the *in vivo* data presented in this chapter, WNT signaling is a potential therapeutic target to normalize bone mass in DS [29, 37, 81] as well as to potentially minimize/treat the increased risk of hematopoietic cancers such as acute myeloid leukemia (AML), which is common in DS [32, 68, 69].

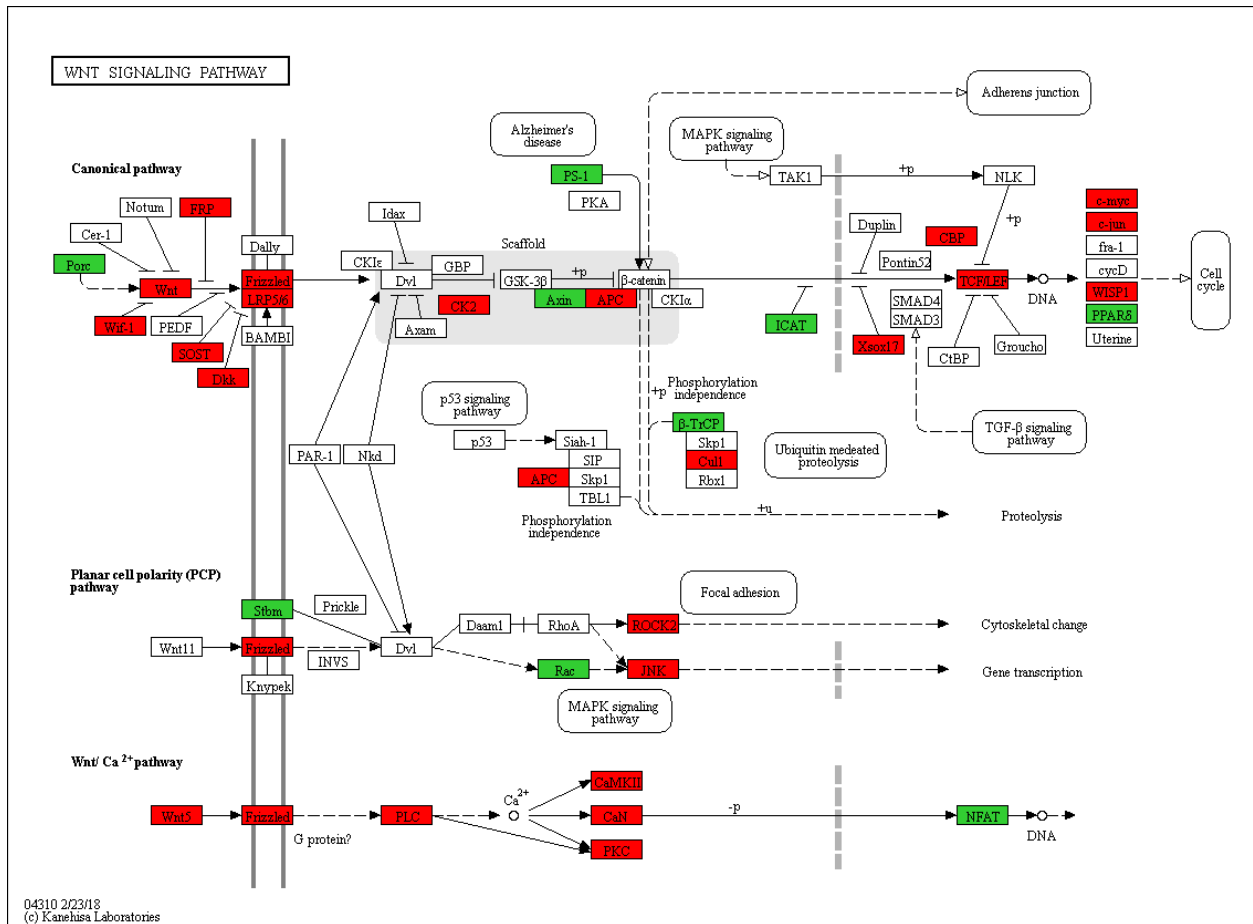


**Figure 17. Differential gene expression profile of the WNT signaling pathway.** Comparative mRNA expression of femurs from adult 7-month old male Ts65Dn mice to WT littermate controls show upregulated expression in WNT proteins – WNT1, WNT5a, and WNT6. Gene expression of regulators of canonical WNT signaling were also upregulated. Genes shown in red indicate upregulation and genes in green downregulation in Ts65Dn DS mice.

The anabolic effect of WNT signaling on bone is blunted by the expression of other genes, in addition to SOST, that encode regulators of this pathway - specifically Dickkopf-3 (Dkk-3) [82] and secreted frizzled-related proteins (*sFRP*) 2, 4, and 5. SFRP proteins regulate canonical and non-canonical pathways, thus regulation of bone mass and bone homeostasis [31]. Additionally, deletion of SFRP proteins, more specifically SFRP1, was shown to protect against

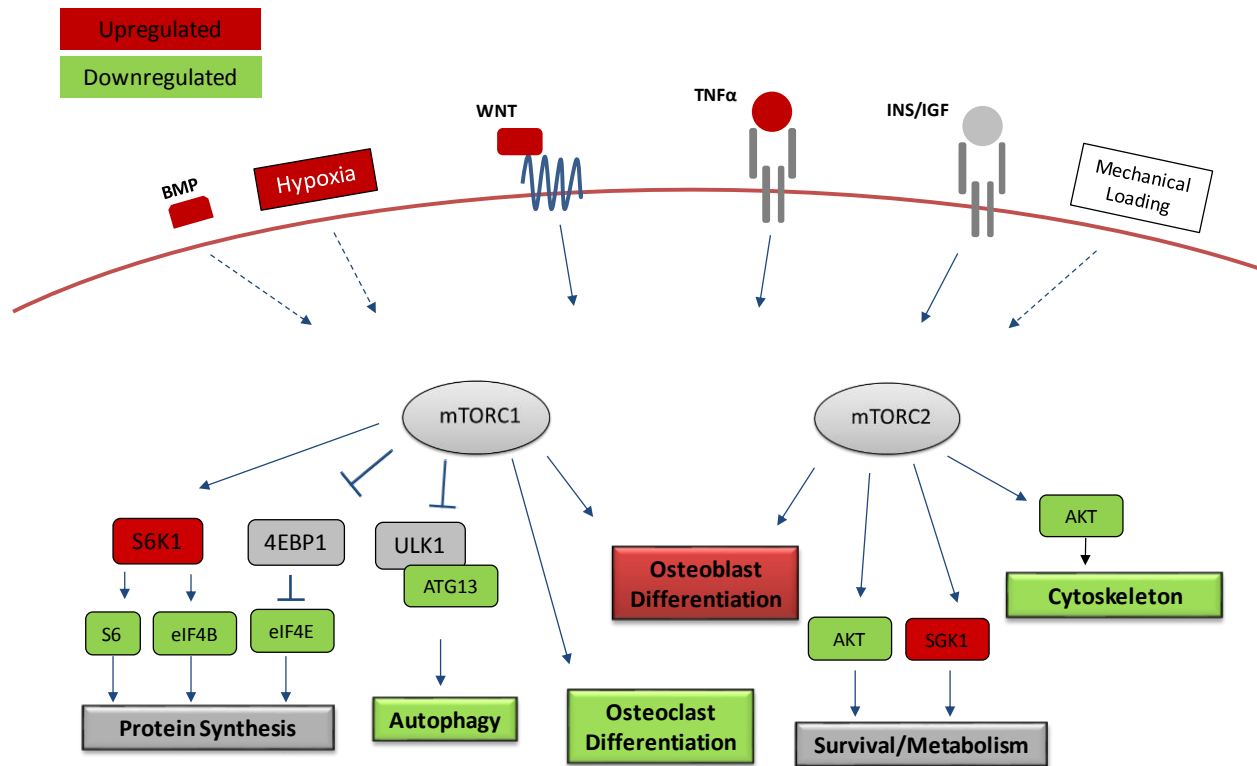


**Figure 18. MTOR signaling effect on bone and the BM microenvironment.** A schematic of the mTOR signaling pathway in bone cells and the differential gene expression profile of Ts65Dn male compared WT. mTOR pathway plays an important role in regulating development and homeostasis of skeletal tissue and it is activated by growth factors and other mechanisms. mTORc1 promotes anabolic processes such as osteoblast differentiation and activity, while mTORc1 signaling is suggested to inhibit osteoclastogenesis. mTORc2 signaling also plays a role in osteoblast differentiation. Genes or biological events in red are upregulated and downregulated in green in Ts65Dn. Grey indicates no change gene expression. Adapted from [74, 83].



osteoblast and osteocyte apoptosis, suggesting that their overexpression could lead to osteoblast and osteocyte cell death. The increased mRNA expression of the LRP4/5/6 inhibitor and thus inhibitor of WNT signaling, sclerostin, observed in femurs of Ts65Dn mice was somewhat surprising given our previous data which showed no noticeable changes in circulating serum sclerostin levels in Ts65Dn or human DS [8], compared to relevant controls. However, it is important to recognize the limited utility of commercial sclerostin ELISA assays, and the fact that serum and bone-marrow sclerostin levels are not correlated [84]. Thus, a reasonable interpretation of these data is that sclerostin actions are bone-specific or localized to the skeleton – further reinforcing its effectiveness as a possible bone therapeutic in Ts65Dn mice, as discussed in earlier in this chapter, and human DS. Additionally, SOST overexpression suggests reduced mechanical load due to decreased bone resorption by osteoclasts.

#### *TGF $\beta$ signaling pathway*

I next mapped the differentially expressed genes to the KEGG Database TGF $\beta$  signaling pathway (**Figure 19**), given the known and important role of TGF $\beta$  in the skeleton [85].

Upregulation of members of the TGF- $\beta$  ligand superfamily, including *TGF $\beta$ 2* and activin was observed. In addition to its role in gonadal growth and embryo differentiation, activin, which is also stored in bone, can regulate bone turnover and bone mass [86]. Post-embryogenesis stimulation of the activin signaling pathway has been shown to exert both pro- and anti-oncogenic effects [58, 87, 88]. In addition, TGF $\beta$  signaling is further intensified by increased expression of TGF $\beta$ -receptor 1 (*TGF $\beta$ R1*) and *ACTVR1A*. Regulation of the increased TGF $\beta$  was also supported by the observed upregulation of the TGF $\beta$  target decorin (*DCN*), an inhibitor of TGF $\beta$  [89, 90]. *DCN* has been shown to reduce tissue fibrosis [91] and alter migration of myoblast and other cells of connective tissues [92, 93] by modifying TGF $\beta$  signaling. The

apparent regulation of TGF $\beta$  regulators was confirmed by the observed effects of thrombospondin-1 (*THBS*) on latent transforming growth factor beta binding protein 1 (LTBP1), which plays a critical roles in controlling TGF $\beta$ 1 activity [94].

Upregulation of other TGF $\beta$  superfamily members was also detected. Expression of bone morphogenetic proteins (BMPs) – *BMP2* and *BMP5* [95], and their receptor (*BMPRII*) was increased (**Figure 19**). The BMP signaling pathway is well-recognized mediator of endochondral bone formation [95] and osteoblast differentiation [96]. The increased expression of BMPs and their cognate receptors appeared to be associated with the increased expression of neuroblastoma suppressor of tumorigenicity 1 (*NBL1* or *DAN*) – an inhibitor of BMP2 and BMP4 signaling [97, 98] as well as the decreased expression of downstream effector SMADs by increased expression in SMAD6/7 [88]. Many studies have linked dysregulated BMP expression with tumorigenesis, including the development of chronic myelogenous leukemia, lymphoid leukemia [68], and bone metastasis of breast cancer [99, 100]. Additionally, expression of the miR-17-92 family of microRNA clusters (MiR17HG) was increased more than 2 fold [Log<sub>2</sub>(FC) = 2.57] and is a known MYC-dependent oncogene, which can inhibit downstream TGF- $\beta$  effectors to promote tumor growth and angiogenesis [101]. Overexpression of miR-17~92 in mice led to a lymphoproliferative disease due expansion of the B-cell and T-cell compartments without the development of solid tumors [102], which is consistent with the finding of downregulated genes associated with B cell receptor signaling pathway (adjusted p-value =  $5.9 \times 10^{-5}$ ) and T cell receptor signaling pathway (adjusted p-value =  $1.1 \times 10^{-5}$ ) as noted by DAVID signaling software of KEGG pathways. More notably, alterations of the miR-17~92 cluster in human pathogenesis is not limited to cancer, but have been linked to developmental

abnormalities of the skeleton in Feingold syndrome [103] and other skeletal anomalies such as short stature [104].

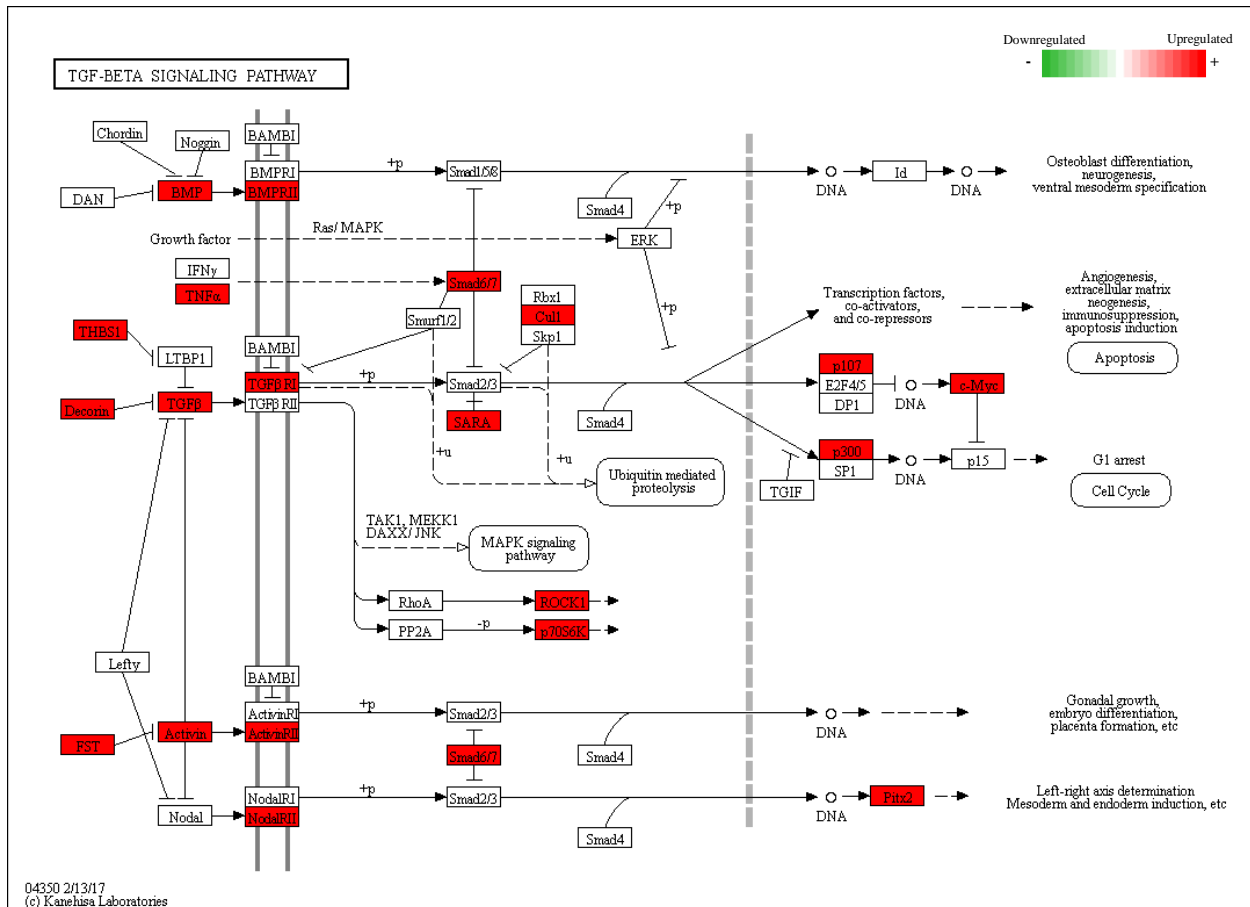


**Figure 19. Differential gene expression profile of TGF- $\beta$  signaling pathway.** Genes in green indicate upregulation and genes in red downregulation. TGF- $\beta$  superfamily members play an important in many biological processes including osteoblast differentiation, angiogenesis, and immunosuppression. mRNA expression of factors such as TGF- $\beta$ 2, BMP2, BMP5, and Activin were upregulated. Genes in red are upregulated and genes in green are downregulated in Ts65Dn mice.

Lastly, I examined the differential gene expression profiles associated with osteoclast differentiation (**Figure 20**). In contrast to the WNT signaling pathway, genes associated with osteoclast differentiation were significantly reduced as noted by DAVID signaling pathway analysis. The TNF receptor Associated Factor (TRAF) proteins, *TRAF2*, *TRAF4* and *TRAF6* - which are major factors in NF $\kappa$ B signaling were downregulated. Many osteoclast-specific genes such as tartrate resistant acid phosphatase (TRAP) and Cathepsin k (CTSK) were downregulated. These findings confirmed the decreased number of TRAP<sup>+</sup> osteoclasts seen in Ts65Dn male mice [16] and in this chapter. Increased expression of the TNF receptor superfamily member 11b (*TNFRSF11b*) gene that encodes Osteoprotegerin (OPG), the osteoblast and osteocyte-secreted inhibitor of osteoclastogenesis, support the finding of decreased osteoclast numbers. These very relevant findings provide further insight into the low numbers of osteoclast in Ts65Dn male mice and a potential mechanism. This expression profile would also explain the lack of efficacy of SclAb treatment on osteoclast parameters, even in the presence of the significantly increased osteoblast differentiation [81] as reported in this chapter. It seems that not even the increased TGF $\beta$  detected was sufficient to rescue the strong suppression of osteoclast differentiation and activity elicited by significantly elevated OPG levels [85] or some other mechanism. In conjunction with the findings of increased WNT signaling, increased signaling of the TGF $\beta$  signaling and its superfamily members (BMP, Activin), the observation of decreased differentiation of cells from HSC lineage (osteoclasts, B cells, T cells) suggests the increased signaling of pathways regulating pluripotency of stem cells (**Figure 21**) as important contributors to the pleotropic effects (skeletal and otherwise) observed in Ts65Dn mice.

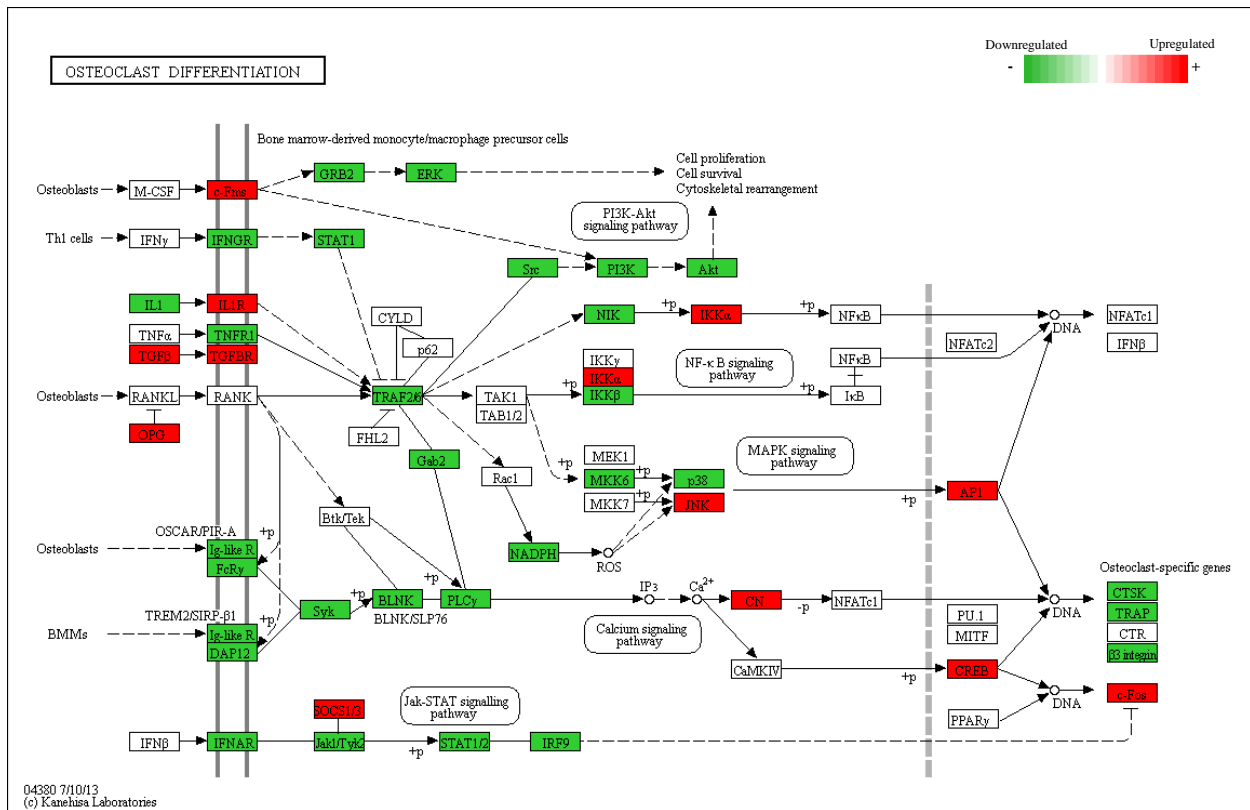


**Figure 20. Differential gene expression profile of the Osteoclast differentiation pathway.** Genes vital for osteoclast differentiation such as TRAF2 and TRAF6 were downregulated although TGF- $\beta$  signals were upregulated. Upregulation of OPG, a potent inhibitor of osteoclast differentiation, was also found to be upregulated. Genes in red indicate upregulation and genes in green indicate downregulation.

## Conclusions and Future Directions

Trisomy of Hsa21 leads to numerous complications in multiple organ systems, including the musculoskeletal system [12, 105-107]. We have previously shown that the mechanism underlying the bone defect in DS [8] and a mouse model of DS, Ts65Dn [16], is due to decreased bone turnover. We hypothesized that the decreased bone turnover due to a reduced number of osteoblasts and osteoclasts was a consequence of an intracellular cellular defect due to overexpression of RCAN1 – one of the genes found on the Down syndrome critical region (DSCR) [108, 109]. Overexpression of these genes are arguably the main causes of DS phenotypes [110] [108, 110, 111] as discussed in Chapter I. However, RNAseq analysis of

differentially expressed genes taken from femurs of 7-month old Ts65Dn male mice and aged-matched littermates did not show any changes in RCAN1 expression. Furthermore, the differential expression profiles revealed over 4500 genes, half of which were not even upregulated.

**Table 9.** Differentially expressed genes on mouse chromosome 16 in Ts65Dn mice.

Gene name	Log2 (FC)	Gene name	Log2 (FC)	Gene name	Log2 (FC)	Gene name	Log2 (FC)
Chodl	3.6	Sh3bgr	1.01	1700021K19Rik	-0.58	King1	-0.98
Casr	2.82	Zbtb11	0.99	Dopey2	-0.61	Tiam1	-1.03
Rbfox1	2.23	Trmt10c	0.98	Dyrk1a	-0.61	Smim11	-1.04
Abi3bp	2.06	Hes1	0.95	Gramd1c	-0.62	Prdm15	-1.04
ORF63	2.04	Usp25	0.95	Poglut1	-0.63	Stfa2l1	-1.07
Ostn	2	Fbxo40	0.94	Rtn4r	-0.64	Rwdd2b	-1.08
Itgb2l	1.98	Senp7	0.94	Mefv	-0.64	Tmem50b	-1.09
Lrrc15	1.95	Igll1	0.92	Ppm1f	-0.66	Cep19	-1.1
Ube2v2	1.84	Popdc2	0.86	King2	-0.66	Stfa2	-1.12
Adamts1	1.81	Srl	0.85	B4galt4	-0.66	Mrps6	-1.13
Myh11	1.8	Mcm4	0.82	Litaf	-0.67	Pigx	-1.14
C330027C09Rik	1.8	Klhl24	0.81	Vps8	-0.67	Adcy5	-1.14
Lrrc58	1.77	Jam2	0.81	Abcc1	-0.68	Il10rb	-1.14
Pvrl3	1.74	Spice1	0.79	Klhl6	-0.68	Ciita	-1.15
Dzip3	1.66	Arl13b	0.79	Adprh	-0.68	Cd96	-1.18
Nrip1	1.59	Samsn1	0.74	Muc13	-0.69	Wrb	-1.18
2310015D24Rik	1.57	Btla	0.72	Rogdi	-0.7	5330426P16Rik	-1.24
Ppl	1.57	Rsl1d1	0.71	Rpl35a	-0.72	Dgkg	-1.25
Zfp654	1.55	Ccdc50	0.7	Marf1	-0.73	Cd200r3	-1.29
Atp13a3	1.49	Zfp148	0.69	Cct8	-0.73	Gm5483	-1.32
B3gnt5	1.47	Ccdc80	0.68	Retnlg	-0.74	Tm4sf19	-1.33
Dnm1l	1.3	Prkdc	0.66	App	-0.74	Ifnar2	-1.33
Hrasls	1.29	Crebbp	0.66	Crkl	-0.75	Rtp4	-1.34
Robo1	1.28	Boc	0.64	Naa60	-0.75	Sdf2l1	-1.36
Vpreb1	1.25	Col8a1	0.61	Bace2	-0.76	Stfa3	-1.37
Filip1l	1.25	St3gal6	0.52	Lrrc33	-0.77	Cbr3	-1.42
Tbc1d23	1.24	Usp7	0.47	Nagpa	-0.8	Dscr3	-1.54
Bbx	1.23	Runx1	0.47	Psmg1	-0.82	2310005G13Rik	-1.6
Zc3h7a	1.2	Tfr3	0.46	C2cd2	-0.83	Stfa1	-1.79
Naa50	1.2	Bach1	-0.45	Ptplb	-0.86	Bex6	-1.81
Mfi2	1.17	Med15	-0.47	Dtx3l	-0.86	BC100530	-2.62
Apod	1.16	Slx4	-0.47	Adcy9	-0.86	Gm5416	-10.87
A630089N07Rik	1.16	Umps	-0.51	Ifnar1	-0.87		
Nfkbiz	1.14	Hcls1	-0.51	Cryzl1	-0.91		
2310010M20Rik	1.1	Dgcr2	-0.52	Mx1	-0.92		
Iqcb1	1.07	Urb1	-0.53	5-Sep	-0.93		
Cldn5	1.04	Ets2	-0.54	Ifngr2	-0.93		
Fytd1	1.03	Gart	-0.55	Snx29	-0.95		
Cpox	1.01	Mrpl39	-0.57	Pdia5	-0.96		
Slc5a3	1.01	Cebpd	-0.58	Hlcs	-0.96		

As with many inherited genetic diseases, the disease phenotypes and severity vary greatly amongst patients with the same genetic defect [112-115], although general similarities amongst clinical phenotypes exist [116]. Thus, the sole contribution of one gene or even one mechanism in disease pathology, including tissue-specific pathologies, is not probable; but, more likely a consequence of altering expression of multiple genes and their downstream effectors in a specific tissue during a certain period time, either during development or homeostasis [40] and in a particular gender.

Therefore, in this section, I will outline potential mechanisms responsible for the decreased bone mass due to decreased bone formation observed age mature Ts65Dn male mice (**Figure 21**). I hypothesize that the bone defect, at least in adult male Ts65Dn mice, is due to changes in the skeleton due to an aging mechanism, as DS has been referred to as an “accelerated aging” disease [117, 118], and/or alterations in the bone marrow microenvironment due to proliferative disease [79, 80]. In addition, I propose several molecular factors driving 2 of these phenotypes, including the WNT signaling and TGF $\beta$  signaling pathways.

In addition to providing insight into the potential mechanisms underlying bone health in DS, this analysis provides candidate molecular targets (**Figure 21**) of skeletal disease progression that could/should be verified and evaluated in future studies. Gene knock-out experiments in mice could provide insight into the role of DRD2 in bone. Additionally, potential loss of function experiments using ATG13, a protein responsible for osteoclast/osteocyte autophagy (*in vitro* and/or specifically *in vivo*), could provide insight on the autophagy-related bone loss in adult Ts65Dn male mice. In fact, osteocyte-specific ATG7 null mice show decreased bone mass that was contributed by reduced osteoclast and osteoblast numbers that mimicked aging of the skeleton in 6 month old mice (accelerated aging) [63, 64]. However, the



cell specific-loss of the ATG13 should be confirmed, which could be done by q-PCR of individual cells in the BMU. Enumeration of osteocytes and empty lacunae, in femurs and tibiae of adult Ts65Dn mice could also shine light onto the decreased expression of LRP5 and determine if it was caused by a reduction in osteocyte numbers, decreased sensitivity to mechanical load, or both. Indeed, decreased osteocyte numbers would contribute to myeloproliferation and has been shown in multiple myeloma [119] Myeloproliferative diseases such as AML are common in pediatric DS [120]. These clonal hematological disorders arise from a transformation in a hematopoietic stem cell [121]. Thus, the molecular mechanisms for the bone defects in DS could be consequences of these proliferative diseases. I further hypothesize that upregulation of WNT proteins and TGF $\beta$  superfamily factors (i.e. TGF $\beta$ 2, BMPs, and activin) disrupts HSC homeostasis by maintaining their self-renewal potential, quiescent state, or both [59]. In the highly metabolically active and proliferative bone marrow environment, these cells could easily activate over time until they eventually lose their stem-like characteristics as seen in aging [64]. Such an accelerated phenotype could contribute to the decrease in osteoclast differentiation and numbers as early as 3 months in Ts65Dn mice [16]. I speculate that the mechanism for this disrupted HSC state is exerted by secreted factors from cells in the bone marrow microenvironment including osteoblasts (i.e. WNT5a) [73, 75]. Such a situation would also explain the decreased expression of genes associated with B-Cell and T-Cell signaling, further suggesting decreased differentiation of these HSC lineage cells. Decreased B-cell and T-cell differentiation could also exert additional effects on the BM microenvironment such as decreased maintenance of mature osteoclasts and decreased osteogenic effects, respectively [16, 81].

It is also likely that inhibitors of osteoblastogenesis in the bone environment, play a major role in bone defects observed in Ts65Dn mice. As mentioned previously, differential increases in *SOST*, *WIF1*, and *sFRP* genes were observed. These molecules are known inhibitors of WNT signaling, and thus osteoblastogenesis [31]. However, the efficacy of WNT inhibitors including *WIF1* and certain *sFRP*, has been associated with cancer progression [122], but through a HSC quiescent-specific mechanism [123]; further suggesting a role in altering the bone marrow microenvironment. Transcriptional silencing of another WNT inhibitor, DKK-3, is associated with cancer progression in acute lymphoblastic leukemia [120]. Conversely, DKK-3 deletion correlated with improved prognosis and lower lymphoid metastasis in head and neck carcinomas [124]. Therefore, determining the cells responsible for DKK-3 expression and epigenetic regulation of this tumor suppressor or pro-oncogene could be beneficial in understanding its role in the proliferative nature of the bone marrow microenvironment, and thus bone and other defects in DS.

As with all *in silico* analyses, the quality of the analyses are only as reliable as the quality of input RNA and the rigor of the RNAseq output. It is also worth noting that the extraction of RNA from whole bones including bone marrow may have diluted or completely washed out differentially expressed genes that would have otherwise been seen when comparing individual cell types (i.e. genes expressed specifically by osteoblasts, osteoclasts, or other bone marrow derived cells), due to heterogeneous environment of bone. However even with this caveat, the data presented here provide significant insight into the dysregulation of the bone and bone marrow microenvironment in Ts65Dn male DS mice.

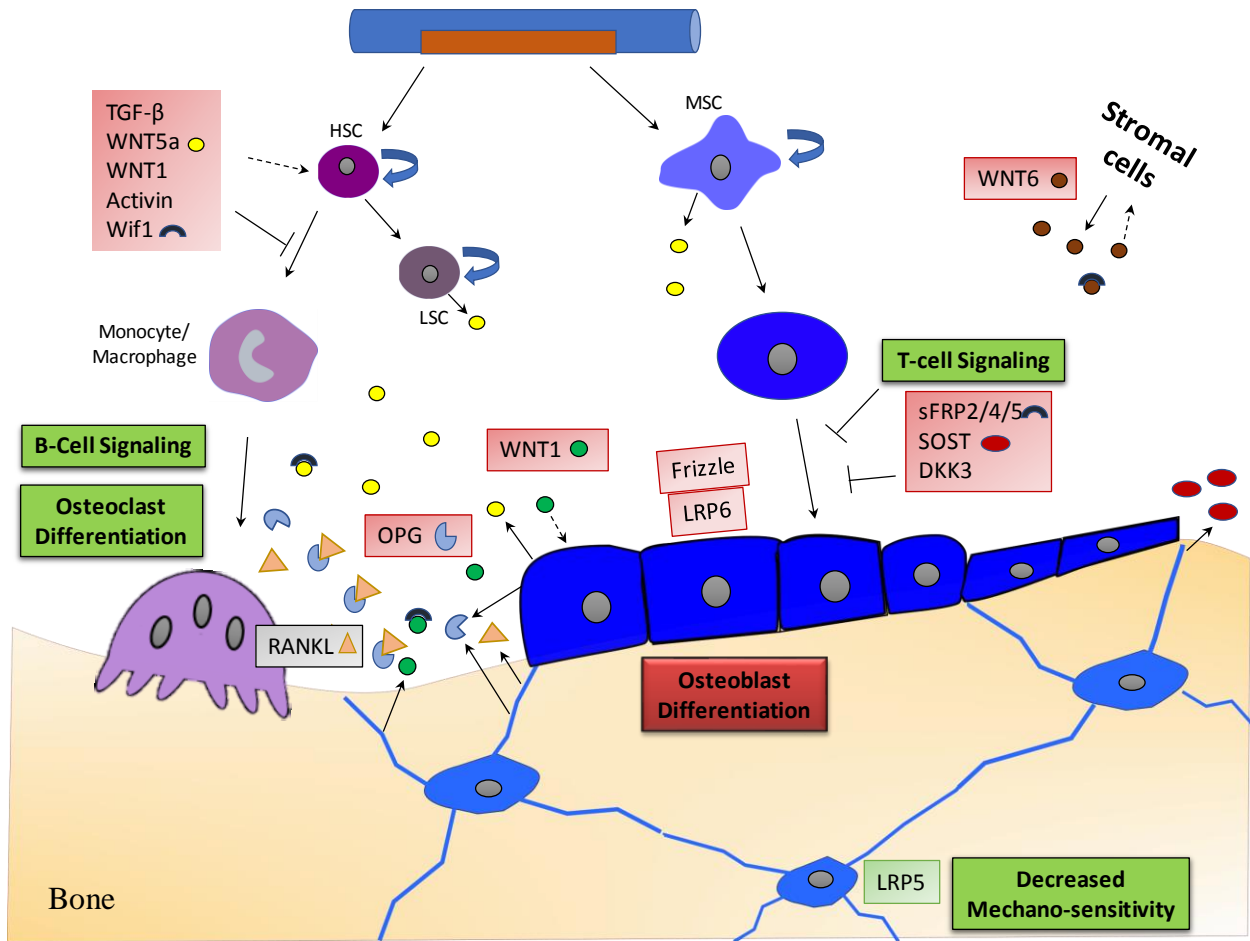


**Figure 21. Schematic of the mechanisms and molecular factors associated with the low bone mass phenotype in Ts65Dn male mice.** The differential gene expression profiles of Ts65Dn compared WT in conjunction with the GO analysis and Signal Pathway analysis are illustrated here. Genes or biological processes in red are upregulated and downregulated in green in Ts65Dn mice.

In conclusion, the development and maintenance of the mammalian skeleton involves many complex processes that include different cell types and factors secreted by these cells, and dysregulation of any of these processes can significantly impact bone health and homeostasis. Therefore, trisomic gene expression, the regulation of these genes, and the regulation of their regulators further complicate our understanding of the pathological processes associated with bone growth and maintenance in DS. A recent study describing the chronic auto-inflammatory effects of DS due to overexpression of the four interferon receptors encoded by human

chromosome 21 [125] is redefining the way DS is viewed. It is clear that DS is not any single disorder, it is not a neurologic, behavioral, immune or musculoskeletal or disorder, rather DS is a complex integration of a spectrum of diseases mediated by intricate and complex gene expression patterns that may be unique to each individual. Given the integrative physiology of the skeleton with other systems including the immune and endocrine systems, the specific male-dominated low bone mass phenotype in DS, may define the phenotype as a rare bone disease. Such an identification could have profound consequences on ongoing studies of the skeletal consequences of DS and may open the way to experimental treatments in the context of a rare disease. Only time and more experimentation will tell.

## References

1. Kamalakar A, Harris JR, McKelvey KD, Suva LJ. Aneuploidy and skeletal health. *Curr Osteoporos Rep.* 2014;12(3):376-82.
2. Huether CA, Ivanovich J, Goodwin BS, Krivchenia EL, Hertzberg VS, Edmonds LD, et al. Maternal age specific risk rate estimates for Down syndrome among live births in whites and other races from Ohio and metropolitan Atlanta, 1970-1989. *J Med Genet.* 1998;35(6):482-90.
3. Petersen MB, Antonarakis SE, Hassold TJ, Freeman SB, Sherman SL, Avramopoulos D, et al. Paternal nondisjunction in trisomy 21: excess of male patients. *Hum Mol Genet.* 1993;2(10):1691-5.
4. Hsu LY, Gertner M, Leiter E, Hirschhorn K. Paternal trisomy 21 mosaicism and Down's syndrome. *Am J Hum Genet.* 1971;23(6):592-601.
5. Verma RS, Dosik H. Trisomy 21 in a child due to paternal nondisjunction as determined by RFA technique. *Jinrui Idengaku Zasshi.* 1978;23(1):17-21.
6. Hawli Y, Nasrallah M, El-Hajj Fuleihan G. Endocrine and musculoskeletal abnormalities in patients with Down syndrome. *Nat Rev Endocrinol.* 2009;5(6):327-34.

7. Blazek JD, Abeysekera I, Li J, Roper RJ. Rescue of the abnormal skeletal phenotype in Ts65Dn Down syndrome mice using genetic and therapeutic modulation of trisomic Dyrk1a. *Hum Mol Genet.* 2015;24(20):5687-96.
8. McKelvey KD, Fowler TW, Akel NS, Kelsay JA, Gaddy D, Wenger GR, et al. Low bone turnover and low bone density in a cohort of adults with Down syndrome. *Osteoporos Int.* 2013;24(4):1333-8.
9. Angelopoulou N, Souftas V, Sakadamis A, Mandroukas K. Bone mineral density in adults with Down's syndrome. *Eur Radiol.* 1999;9(4):648-51.
10. Sakadamis A, Angelopoulou N, Matziari C, Papameletiou V, Souftas V. Bone mass, gonadal function and biochemical assessment in young men with trisomy 21. *Eur J Obstet Gynecol Reprod Biol.* 2002;100(2):208-12.
11. Baptista F, Varela A, Sardinha LB. Bone mineral mass in males and females with and without Down syndrome. *Osteoporos Int.* 2005;16(4):380-8.
12. Guijarro M, Valero C, Paule B, Gonzalez-Macias J, Riancho JA. Bone mass in young adults with Down syndrome. *J Intellect Disabil Res.* 2008;52(Pt 3):182-9.
13. Gonzalez-Aguero A, Vicente-Rodriguez G, Moreno LA, Casajus JA. Bone mass in male and female children and adolescents with Down syndrome. *Osteoporos Int.* 2011;22(7):2151-7.
14. van Allen MI, Fung J, Jurenka SB. Health care concerns and guidelines for adults with Down syndrome. *Am J Med Genet.* 1999;89(2):100-10.
15. Carfi A, Antocicco M, Brandi V, Cipriani C, Fiore F, Mascia D, et al. Characteristics of adults with down syndrome: prevalence of age-related conditions. *Front Med (Lausanne).* 2014;1:51.
16. Fowler TW, McKelvey KD, Akel NS, Vander Schilden J, Bacon AW, Bracey JW, et al. Low bone turnover and low BMD in Down syndrome: effect of intermittent PTH treatment. *PLoS One.* 2012;7(8):e42967.
17. Xing Z, Li Y, Pao A, Bennett AS, Tycko B, Mobley WC, et al. Mouse-based genetic modeling and analysis of Down syndrome. *Br Med Bull.* 2016;120(1):111-22.

18. Do C, Xing Z, Yu YE, Tycko B. Trans-acting epigenetic effects of chromosomal aneuploidies: lessons from Down syndrome and mouse models. *Epigenomics*. 2017;9(2):189-207.
19. Angelopoulou N, Souftas V, Sakadamis A, Matziari C, Papameletiou V, Mandroukas K. Gonadal function in young women with Down syndrome. *Int J Gynaecol Obstet*. 1999;67(1):15-21.
20. Devogelaer JP, Boutsen Y, Manicourt DH. Biologicals in osteoporosis: teriparatide and parathyroid hormone in women and men. *Curr Osteoporos Rep*. 2010;8(3):154-61.
21. Kamimura M, Taguchi A, Nakamura Y, Koiwai H, Ikegami S, Uchiyama S, et al. Pretreatment of daily teriparatide enhances the increase of bone mineral density in cortical bones by denosumab therapy. *Ther Clin Risk Manag*. 2018;14:637-42.
22. Nishiyama KK, Cohen A, Young P, Wang J, Lappe JM, Guo XE, et al. Teriparatide increases strength of the peripheral skeleton in premenopausal women with idiopathic osteoporosis: a pilot HR-pQCT study. *J Clin Endocrinol Metab*. 2014;99(7):2418-25.
23. Baron R, Hesse E. Update on bone anabolics in osteoporosis treatment: rationale, current status, and perspectives. *J Clin Endocrinol Metab*. 2012;97(2):311-25.
24. Hodsmann AB, Bauer DC, Dempster DW, Dian L, Hanley DA, Harris ST, et al. Parathyroid hormone and teriparatide for the treatment of osteoporosis: a review of the evidence and suggested guidelines for its use. *Endocr Rev*. 2005;26(5):688-703.
25. Subbiah V, Madsen VS, Raymond AK, Benjamin RS, Ludwig JA. Of mice and men: divergent risks of teriparatide-induced osteosarcoma. *Osteoporos Int*. 2010;21(6):1041-5.
26. Spatz JM, Ellman R, Cloutier AM, Louis L, van Vliet M, Suva LJ, et al. Sclerostin antibody inhibits skeletal deterioration due to reduced mechanical loading. *J Bone Miner Res*. 2013;28(4):865-74.
27. McClung MR, Grauer A, Boonen S, Bolognese MA, Brown JP, Diez-Perez A, et al. Romosozumab in postmenopausal women with low bone mineral density. *N Engl J Med*. 2014;370(5):412-20.

28. Chandra A, Lin T, Young T, Tong W, Ma X, Tseng WJ, et al. Suppression of Sclerostin Alleviates Radiation-Induced Bone Loss by Protecting Bone-Forming Cells and Their Progenitors Through Distinct Mechanisms. *J Bone Miner Res.* 2017;32(2):360-72.
29. McDonald MM, Reagan MR, Youlten SE, Mohanty ST, Seckinger A, Terry RL, et al. Inhibiting the osteocyte-specific protein sclerostin increases bone mass and fracture resistance in multiple myeloma. *Blood.* 2017;129(26):3452-64.
30. Blazek JD, Gaddy A, Meyer R, Roper RJ, Li J. Disruption of bone development and homeostasis by trisomy in Ts65Dn Down syndrome mice. *Bone.* 2011;48(2):275-80.
31. Baron R, Kneissel M. WNT signaling in bone homeostasis and disease: from human mutations to treatments. *Nat Med.* 2013;19(2):179-92.
32. Sinnberg T, Levesque MP, Krochmann J, Cheng PF, Ikenberg K, Meraz-Torres F, et al. Wnt-signaling enhances neural crest migration of melanoma cells and induces an invasive phenotype. *Mol Cancer.* 2018;17(1):59.
33. Wellman-Labadie O, Zhou Y. The US Orphan Drug Act: rare disease research stimulator or commercial opportunity? *Health Policy.* 2010;95(2-3):216-28.
34. Schragger S, Kloss C, Ju AW. Prevalence of fractures in women with intellectual disabilities: a chart review. *J Intellect Disabil Res.* 2007;51(Pt 4):253-9.
35. Glorieux FH, Devogelaer JP, Durigova M, Goemaere S, Hemsley S, Jakob F, et al. BPS804 Anti-Sclerostin Antibody in Adults With Moderate Osteogenesis Imperfecta: Results of a Randomized Phase 2a Trial. *J Bone Miner Res.* 2017;32(7):1496-504.
36. Joeng KS, Lee YC, Lim J, Chen Y, Jiang MM, Munivez E, et al. Osteocyte-specific WNT1 regulates osteoblast function during bone homeostasis. *J Clin Invest.* 2017;127(7):2678-88.
37. Roschger A, Roschger P, Keplingter P, Klaushofer K, Abdullah S, Kneissel M, et al. Effect of sclerostin antibody treatment in a mouse model of severe osteogenesis imperfecta. *Bone.* 2014;66:182-8.

38. Li X, Ominsky MS, Warmington KS, Morony S, Gong J, Cao J, et al. Sclerostin antibody treatment increases bone formation, bone mass, and bone strength in a rat model of postmenopausal osteoporosis. *J Bone Miner Res.* 2009;24(4):578-88.
39. Kim JH, Kim K, Kim I, Seong S, Jeong BC, Nam KI, et al. RCANs regulate the convergent roles of NFATc1 in bone homeostasis. *Sci Rep.* 2016;6:38526.
40. Roper RJ, Reeves RH. Understanding the basis for Down syndrome phenotypes. *PLoS Genet.* 2006;2(3):e50.
41. Petrucci LA, Pettersson F, Del Rincon SV, Guilbert C, Licht JD, Miller WH, Jr. Expression of leukemia-associated fusion proteins increases sensitivity to histone deacetylase inhibitor-induced DNA damage and apoptosis. *Mol Cancer Ther.* 2013;12(8):1591-604.
42. Wang P, Byrum S, Fowler FC, Pal S, Tackett AJ, Tyler JK. Proteomic identification of histone post-translational modifications and proteins enriched at a DNA double-strand break. *Nucleic Acids Res.* 2017;45(19):10923-40.
43. Letourneau A, Santoni FA, Bonilla X, Sailani MR, Gonzalez D, Kind J, et al. Domains of genome-wide gene expression dysregulation in Down's syndrome. *Nature.* 2014;508(7496):345-50.
44. Blake JA, Bult CJ, Kadin JA, Richardson JE, Eppig JT, Mouse Genome Database G. The Mouse Genome Database (MGD): premier model organism resource for mammalian genomics and genetics. *Nucleic Acids Res.* 2011;39(Database issue):D842-8.
45. Kelly MA, Rubinstein M, Asa SL, Zhang G, Saez C, Bunzow JR, et al. Pituitary lactotroph hyperplasia and chronic hyperprolactinemia in dopamine D2 receptor-deficient mice. *Neuron.* 1997;19(1):103-13.
46. Saiardi A, Bozzi Y, Baik JH, Borrelli E. Antiproliferative role of dopamine: loss of D2 receptors causes hormonal dysfunction and pituitary hyperplasia. *Neuron.* 1997;19(1):115-26.
47. Baik JH, Picetti R, Saiardi A, Thiriet G, Dierich A, Depaulis A, et al. Parkinsonian-like locomotor impairment in mice lacking dopamine D2 receptors. *Nature.* 1995;377(6548):424-8.



48. Noain D, Perez-Millan MI, Bello EP, Luque GM, Casas Cordero R, Gelman DM, et al. Central dopamine D2 receptors regulate growth-hormone-dependent body growth and pheromone signaling to conspecific males. *J Neurosci*. 2013;33(13):5834-42.
49. Beaulieu JM, Gainetdinov RR, Caron MG. The Akt-GSK-3 signaling cascade in the actions of dopamine. *Trends Pharmacol Sci*. 2007;28(4):166-72.
50. Zhang Y, Cuevas S, Asico LD, Escano C, Yang Y, Pascua AM, et al. Deficient dopamine D2 receptor function causes renal inflammation independently of high blood pressure. *PLoS One*. 2012;7(6):e38745.
51. Armando I, Wang X, Villar VA, Jones JE, Asico LD, Escano C, et al. Reactive oxygen species-dependent hypertension in dopamine D2 receptor-deficient mice. *Hypertension*. 2007;49(3):672-8.
52. Luo Q, Li X, Xu C, Zeng L, Ye J, Guo Y, et al. Integrative analysis of long non-coding RNAs and messenger RNA expression profiles in systemic lupus erythematosus. *Mol Med Rep*. 2018;17(3):3489-96.
53. Cole S, Walsh A, Yin X, Wechalekar MD, Smith MD, Proudman SM, et al. Integrative analysis reveals CD38 as a therapeutic target for plasma cell-rich pre-disease and established rheumatoid arthritis and systemic lupus erythematosus. *Arthritis Res Ther*. 2018;20(1):85.
54. Huang da W, Sherman BT, Lempicki RA. Bioinformatics enrichment tools: paths toward the comprehensive functional analysis of large gene lists. *Nucleic Acids Res*. 2009;37(1):1-13.
55. Bennett CN, Longo KA, Wright WS, Suva LJ, Lane TF, Hankenson KD, et al. Regulation of osteoblastogenesis and bone mass by Wnt10b. *Proc Natl Acad Sci U S A*. 2005;102(9):3324-9.
56. Hens JR, Wilson KM, Dann P, Chen X, Horowitz MC, Wysolmerski JJ. TOPGAL mice show that the canonical Wnt signaling pathway is active during bone development and growth and is activated by mechanical loading in vitro. *J Bone Miner Res*. 2005;20(7):1103-13.

57. Cui Y, Niziolek PJ, MacDonald BT, Zylstra CR, Alenina N, Robinson DR, et al. Lrp5 functions in bone to regulate bone mass. *Nat Med.* 2011;17(6):684-91.
58. Huang DW, Sherman BT, Lempicki RA. Systematic and integrative analysis of large gene lists using DAVID bioinformatics resources. *Nature Protocols.* 2008;4:44.
59. Staudacher JJ, Bauer J, Jana A, Tian J, Carroll T, Mancinelli G, et al. Activin signaling is an essential component of the TGF-beta induced pro-metastatic phenotype in colorectal cancer. *Sci Rep.* 2017;7(1):5569.
60. Millan JL. Alkaline phosphatase as a reporter of cancerous transformation. *Clin Chim Acta.* 1992;209(1-2):123-9.
61. Makhoul I, Montgomery CO, Gaddy D, Suva LJ. The best of both worlds - managing the cancer, saving the bone. *Nat Rev Endocrinol.* 2016;12(1):29-42.
62. Herrera S, Perez-Lopez J, Molto-Abad M, Guerri-Fernandez R, Cabezudo E, Novelli S, et al. Assessment of Bone Health in Patients With Type 1 Gaucher Disease Using Impact Microindentation. *J Bone Miner Res.* 2017;32(7):1575-81.
63. Piemontese M, Onal M, Xiong J, Han L, Thostenson JD, Almeida M, et al. Low bone mass and changes in the osteocyte network in mice lacking autophagy in the osteoblast lineage. *Sci Rep.* 2016;6:24262.
64. Onal M, Piemontese M, Xiong J, Wang Y, Han L, Ye S, et al. Suppression of autophagy in osteocytes mimics skeletal aging. *J Biol Chem.* 2013;288(24):17432-40.
65. Fujibuchi W, Kanehisa M. Prediction of gene expression specificity by promoter sequence patterns. *DNA Res.* 1997;4(2):81-90.
66. Kanehisa M. Linking databases and organisms: GenomeNet resources in Japan. *Trends Biochem Sci.* 1997;22(11):442-4.
67. Kanehisa M. A database for post-genome analysis. *Trends Genet.* 1997;13(9):375-6.

68. Zylbersztejn F, Flores-Violante M, Voeltzel T, Nicolini FE, Lefort S, Maguer-Satta V. The BMP pathway: A unique tool to decode the origin and progression of leukemia. *Exp Hematol*. 2018;61:36-44.
69. Zhang Z, Wang J, Zeng X, Li D, Ding M, Guan R, et al. Two-stage study of lung cancer risk modification by a functional variant in the 3'-untranslated region of SMAD5 based on the bone morphogenetic protein pathway. *Mol Clin Oncol*. 2018;8(1):38-46.
70. Lavery DL, Martin J, Turnbull YD, Hoppler S. Wnt6 signaling regulates heart muscle development during organogenesis. *Dev Biol*. 2008;323(2):177-88.
71. Beaton H, Andrews D, Parsons M, Murphy M, Gaffney A, Kavanagh D, et al. Wnt6 regulates epithelial cell differentiation and is dysregulated in renal fibrosis. *Am J Physiol Renal Physiol*. 2016;311(1):F35-45.
72. Cawthorn WP, Bree AJ, Yao Y, Du B, Hemati N, Martinez-Santibanez G, et al. Wnt6, Wnt10a and Wnt10b inhibit adipogenesis and stimulate osteoblastogenesis through a beta-catenin-dependent mechanism. *Bone*. 2012;50(2):477-89.
73. Arabzadeh S, Hossein G, Salehi-Dulabi Z, Zarnani AH. WNT5A-ROR2 is induced by inflammatory mediators and is involved in the migration of human ovarian cancer cell line SKOV-3. *Cell Mol Biol Lett*. 2016;21:9.
74. Tseng WP, Yang SN, Lai CH, Tang CH. Hypoxia induces BMP-2 expression via ILK, Akt, mTOR, and HIF-1 pathways in osteoblasts. *J Cell Physiol*. 2010;223(3):810-8.
75. Bellon M, Ko NL, Lee MJ, Yao Y, Waldmann TA, Trepel JB, et al. Adult T-cell leukemia cells overexpress Wnt5a and promote osteoclast differentiation. *Blood*. 2013;121(25):5045-54.
76. Huang CL, Liu D, Ishikawa S, Nakashima T, Nakashima N, Yokomise H, et al. Wnt1 overexpression promotes tumour progression in non-small cell lung cancer. *Eur J Cancer*. 2008;44(17):2680-8.
77. Yuan G, Regel I, Lian F, Friedrich T, Hitkova I, Hofheinz RD, et al. WNT6 is a novel target gene of caveolin-1 promoting chemoresistance to epirubicin in human gastric cancer cells. *Oncogene*. 2013;32(3):375-87.

78. Suva LJ, Gaddy D, Perrien DS, Thomas RL, Findlay DM. Regulation of bone mass by mechanical loading: microarchitecture and genetics. *Curr Osteoporos Rep.* 2005;3(2):46-51.
79. Kirsammer G, Jilani S, Liu H, Davis E, Gurbuxani S, Le Beau MM, et al. Highly penetrant myeloproliferative disease in the Ts65Dn mouse model of Down syndrome. *Blood.* 2008;111(2):767-75.
80. Roy A, Roberts I, Norton A, Vyas P. Acute megakaryoblastic leukaemia (AMKL) and transient myeloproliferative disorder (TMD) in Down syndrome: a multi-step model of myeloid leukaemogenesis. *Br J Haematol.* 2009;147(1):3-12.
81. Williams DK, Parham SG, Schryver E, Akel NS, Shelton RS, Webber J, et al. Sclerostin Antibody Treatment Stimulates Bone Formation to Normalize Bone Mass in Male Down Syndrome Mice. *JBMR Plus.* 2018;2(1):47-54.
82. Clines GA, Mohammad KS, Bao Y, Stephens OW, Suva LJ, Shaughnessy JD, Jr., et al. Dickkopf homolog 1 mediates endothelin-1-stimulated new bone formation. *Mol Endocrinol.* 2007;21(2):486-98.
83. Chen J, Long F. mTOR signaling in skeletal development and disease. *Bone Res.* 2018;6:1.
84. Clarke BL, Drake MT. Clinical utility of serum sclerostin measurements. *Bonekey Rep.* 2013;2:361.
85. Itonaga I, Sabokbar A, Sun SG, Kudo O, Danks L, Ferguson D, et al. Transforming growth factor-beta induces osteoclast formation in the absence of RANKL. *Bone.* 2004;34(1):57-64.
86. Gaddy-Kurten D, Coker JK, Abe E, Jilka RL, Manolagas SC. Inhibin suppresses and activin stimulates osteoblastogenesis and osteoclastogenesis in murine bone marrow cultures. *Endocrinology.* 2002;143(1):74-83.
87. Massague J, Chen YG. Controlling TGF-beta signaling. *Genes Dev.* 2000;14(6):627-44.
88. Massague J, Wotton D. Transcriptional control by the TGF-beta/Smad signaling system. *EMBO J.* 2000;19(8):1745-54.

89. Grafe I, Yang T, Alexander S, Homan EP, Lietman C, Jiang MM, et al. Excessive transforming growth factor-beta signaling is a common mechanism in osteogenesis imperfecta. *Nat Med.* 2014;20(6):670-5.
90. Ibrahim I, Serrano MJ, Ruest LB, Svoboda KKH. Biglycan and Decorin Expression and Distribution in Palatal Adhesion. *J Dent Res.* 2017;96(12):1445-50.
91. Yan W, Wang P, Zhao CX, Tang J, Xiao X, Wang DW. Decorin gene delivery inhibits cardiac fibrosis in spontaneously hypertensive rats by modulation of transforming growth factor-beta/Smad and p38 mitogen-activated protein kinase signaling pathways. *Hum Gene Ther.* 2009;20(10):1190-200.
92. Augoff K, Grabowski K, Rabczynski J, Kolondra A, Tabola R, Sikorski AF. Expression of decorin in esophageal cancer in relation to the expression of three isoforms of transforming growth factor-beta (TGF-beta1, -beta2, and -beta3) and matrix metalloproteinase-2 activity. *Cancer Invest.* 2009;27(4):443-52.
93. Goetsch KP, Niesler CU. The extracellular matrix regulates the effect of decorin and transforming growth factor beta-2 (TGF-beta2) on myoblast migration. *Biochem Biophys Res Commun.* 2016;479(2):351-7.
94. Wang X, Dong C, Li N, Ma Q, Yun Z, Cai C, et al. Modulation of TGFbeta activity by latent TGFbetabinding protein 1 in human osteoarthritis fibroblastlike synoviocytes. *Mol Med Rep.* 2018;17(1):1893-900.
95. Salazar VS, Gamer LW, Rosen V. BMP signalling in skeletal development, disease and repair. *Nat Rev Endocrinol.* 2016;12(4):203-21.
96. Hassan MQ, Tare RS, Lee SH, Mandeville M, Morasso MI, Javed A, et al. BMP2 commitment to the osteogenic lineage involves activation of Runx2 by DLX3 and a homeodomain transcriptional network. *J Biol Chem.* 2006;281(52):40515-26.
97. Hung WT, Wu FJ, Wang CJ, Luo CW. DAN (NBL1) specifically antagonizes BMP2 and BMP4 and modulates the actions of GDF9, BMP2, and BMP4 in the rat ovary. *Biol Reprod.* 2012;86(5):158, 1-9.
98. Nolan K, Kattamuri C, Luedeke DM, Angerman EB, Rankin SA, Stevens ML, et al. Structure of neuroblastoma suppressor of tumorigenicity 1 (NBL1): insights for the

- functional variability across bone morphogenetic protein (BMP) antagonists. *J Biol Chem.* 2015;290(8):4759-71.
99. Liu Y, Zhang RX, Yuan W, Chen HQ, Tian DD, Li H, et al. Knockdown of Bone Morphogenetic Proteins Type 1a Receptor (BMPRIa) in Breast Cancer Cells Protects Bone from Breast Cancer-Induced Osteolysis by Suppressing RANKL Expression. *Cell Physiol Biochem.* 2018;45(5):1759-71.
  100. Xia S, Ji R, Xu Y, Ni X, Dong Y, Zhan W. Twisted Gastrulation BMP Signaling Modulator 1 Regulates Papillary Thyroid Cancer Cell Motility and Proliferation. *J Cancer.* 2017;8(14):2816-27.
  101. Dews M, Fox JL, Hultine S, Sundaram P, Wang W, Liu YY, et al. The myc-miR-17~92 axis blunts TGF $\beta$  signaling and production of multiple TGF $\beta$ -dependent antiangiogenic factors. *Cancer Res.* 2010;70(20):8233-46.
  102. Xiao C, Srinivasan L, Calado DP, Patterson HC, Zhang B, Wang J, et al. Lymphoproliferative disease and autoimmunity in mice with increased miR-17-92 expression in lymphocytes. *Nat Immunol.* 2008;9(4):405-14.
  103. van Bokhoven H, Celli J, van Reeuwijk J, Rinne T, Glaudemans B, van Beusekom E, et al. MYCN haploinsufficiency is associated with reduced brain size and intestinal atresias in Feingold syndrome. *Nat Genet.* 2005;37(5):465-7.
  104. Concepcion CP, Bonetti C, Ventura A. The microRNA-17-92 family of microRNA clusters in development and disease. *Cancer J.* 2012;18(3):262-7.
  105. Blazek JD, Malik AM, Tischbein M, Arbones ML, Moore CS, Roper RJ. Abnormal mineralization of the Ts65Dn Down syndrome mouse appendicular skeleton begins during embryonic development in a Dyrk1a-independent manner. *Mech Dev.* 2015;136:133-42.
  106. Olson LE, Mohan S. Bone density phenotypes in mice aneuploid for the Down syndrome critical region. *Am J Med Genet A.* 2011;155(10):2436-45.
  107. Costa R, De Miguel R, Garcia C, de Asua DR, Castaneda S, Moldenhauer F, et al. Bone Mass Assessment in a Cohort of Adults With Down Syndrome: A Cross-Sectional Study. *Intellect Dev Disabil.* 2017;55(5):315-24.

108. Kim YS, Cho KO, Lee HJ, Kim SY, Sato Y, Cho YJ. Down syndrome candidate region 1 increases the stability of the IkappaBalpha protein: implications for its anti-inflammatory effects. *J Biol Chem*. 2006;281(51):39051-61.
109. Ryeom S, Baek KH, Zaslavsky A. Down's syndrome: protection against cancer and the therapeutic potential of DSCR1. *Future Oncol*. 2009;5(8):1185-8.
110. Olson LE, Richtsmeier JT, Leszl J, Reeves RH. A chromosome 21 critical region does not cause specific Down syndrome phenotypes. *Science*. 2004;306(5696):687-90.
111. Reynolds LE, Watson AR, Baker M, Jones TA, D'Amico G, Robinson SD, et al. Tumour angiogenesis is reduced in the Tc1 mouse model of Down's syndrome. *Nature*. 2010;465(7299):813-7.
112. Michaelides M, Jeffery G, Moore AT. Developmental macular disorders: phenotypes and underlying molecular genetic basis. *Br J Ophthalmol*. 2012;96(7):917-24.
113. Hodapp RM, Dykens EM. Genetic disorders of intellectual disability: expanding our concepts of phenotypes and of family outcomes. *J Genet Couns*. 2012;21(6):761-9.
114. Higuchi S, Matsushita S, Masaki T, Yokoyama A, Kimura M, Suzuki G, et al. Influence of genetic variations of ethanol-metabolizing enzymes on phenotypes of alcohol-related disorders. *Ann N Y Acad Sci*. 2004;1025:472-80.
115. Szatmari P, Maziade M, Zwaigenbaum L, Merette C, Roy MA, Joobor R, et al. Informative phenotypes for genetic studies of psychiatric disorders. *Am J Med Genet B Neuropsychiatr Genet*. 2007;144B(5):581-8.
116. Leoyklang P, Suphapeetiporn K, Srichomthong C, Tongkobpetch S, Fietze S, Dorward H, et al. Disorders with similar clinical phenotypes reveal underlying genetic interaction: SATB2 acts as an activator of the UPF3B gene. *Hum Genet*. 2013;132(12):1383-93.
117. Buxhoeveden D, Casanova MF. Accelerated maturation in brains of patients with Down syndrome. *J Intellect Disabil Res*. 2004;48(Pt 7):704-5.
118. Devenny DA, Wegiel J, Schupf N, Jenkins E, Zigman W, Krinsky-McHale SJ, et al. Dementia of the Alzheimer's type and accelerated aging in Down syndrome. *Sci Aging Knowledge Environ*. 2005;2005(14):dn1.

119. Lin N, Li Y, Tian H. [Advance of study on evaluating index for multiple myeloma prognosis -- review]. *Zhongguo Shi Yan Xue Ye Xue Za Zhi*. 2009;17(1):255-60.
120. Roman-Gomez J, Jimenez-Velasco A, Agirre X, Castillejo JA, Navarro G, Barrios M, et al. Transcriptional silencing of the Dickkopfs-3 (Dkk-3) gene by CpG hypermethylation in acute lymphoblastic leukaemia. *Br J Cancer*. 2004;91(4):707-13.
121. Campbell PJ, Green AR. The myeloproliferative disorders. *N Engl J Med*. 2006;355(23):2452-66.
122. Song W, Qian L, Jing G, Jie F, Xiaosong S, Chunhui L, et al. Aberrant expression of the sFRP and WIF1 genes in invasive non-functioning pituitary adenomas. *Mol Cell Endocrinol*. 2018.
123. Tang Y, Simoneau AR, Liao WX, Yi G, Hope C, Liu F, et al. WIF1, a Wnt pathway inhibitor, regulates SKP2 and c-myc expression leading to G1 arrest and growth inhibition of human invasive urinary bladder cancer cells. *Mol Cancer Ther*. 2009;8(2):458-68.
124. Katase N, Gunduz M, Beder L, Gunduz E, Lefeuvre M, Hatipoglu OF, et al. Deletion at Dickkopf (dkk)-3 locus (11p15.2) is related with lower lymph node metastasis and better prognosis in head and neck squamous cell carcinomas. *Oncol Res*. 2008;17(6):273-82.
125. Sullivan KD, Evans D, Pandey A, Hraha TH, Smith KP, Markham N, et al. Trisomy 21 causes changes in the circulating proteome indicative of chronic autoinflammation. *Sci Rep*. 2017;7(1):14818.



## CHAPTER V

# GENETICALLY ENGINEERED SHEEP WITH A MISSENSE MUTATION IN ALKALINE PHOSPHATASE GENE RECAPITULATE HUMAN HYPOPHOSPHATASIA

### **Introduction**

Hypophosphatasia (HPP) is a rare genetic disorder with a remarkable range of severity (OMIM 241500, 241510, 146300). The wide clinical spectrum of the disease is organized into a nosology that includes several major clinical forms (odonto, adult, mild and severe childhood, infantile, perinatal, pseudo, and benign prenatal) spanning less severe phenotypes such as dental complications with no skeletal defects to severe manifestations such as death *in utero* [1]. HPP is biochemically characterized by low serum activity levels of the tissue-nonspecific isoenzyme of alkaline phosphatase (TNSALP) [1]. This biochemical hallmark reflects loss-of-function mutations in the coding *ALPL* gene; currently 349 (mostly missense) HPP-inducing mutations have been identified ([http://www.sesep.uvsq.fr/03\\_hypo\\_mutations.php](http://www.sesep.uvsq.fr/03_hypo_mutations.php)) [1, 2]. TNSALP is highly expressed in the skeleton, liver, kidney, and developing teeth [1], though expression of the membrane-bound homodimeric phosphohydrolase is ubiquitous. In HPP, defective mineralization of bones (resulting in rickets/osteomalacia) and teeth (resulting in dental defects and premature tooth loss) can be explained by accumulation of TNSALP substrate, inorganic pyrophosphate (PP<sub>i</sub>), a potent inhibitor of mineralization as discussed in chapter I [1].

Case reports of patients with HPP have been instrumental in advancing the understanding of disease etiology and knowledge of clinical presentations while documenting its wide-ranging severity [3-7]. However, as with many human diseases, HPP animal models to date have been engineered exclusively in rodents, specifically *ALPL* knockout and transgenic mice [8-12].

Enzymatic knockout or transgenic models, such as the HPP mice models, are limited by their inability to maintain physiologically relevant enzymatic activity levels or random insertions of transgenes often lead to variable enzyme expression levels. This can be problematic when investigating disease mechanism(s) in a disorder such as HPP, where more than 70% of the *ALPL* mutations are missense. Although useful for modeling many of the metabolic and skeletal defects, murine models harboring *ALPL* mutations do not faithfully represent the broad spectrum of human HPP clinical presentations, which is partly due to the limiting physical and physiological differences such as size and gene expression and regulation. Additionally, mice with HPP do not lose their teeth, and severe forms of *ALPL* knockout models result in premature death [8] – restricting mechanistic investigations to short-term experiments. While a bone-targeted recombinant TNSALP (Asfotase Alfa) is being used to successfully treat the metabolic skeletal defects in severely affected pediatric HPP patients [13], a thorough understanding of the broad spectrum of pathophysiological effects of HPP is lacking and would prove beneficial for assessing prognosis and treatment for any given patient [7].

Our goal in the studies described in this chapter was to generate the first large animal model of HPP. *Ovis aries* (sheep) bone structure and remodeling, tooth development and replacement, as well as genetic and physiological composition are more analogous to humans than are mice [14-20]. Importantly, the sheep TNSALP protein sequence is highly conserved with humans (>90% identity) (**Figure 22**). For CRISPR/Cas9 introduction of a single mutation into the sheep genome, an HPP-causing *ALPL* mutation (p.Ile359Met; c.1077C>G) associated with severe infantile HPP in humans [13] was identified. To date, there have been no reports of genetically engineered point mutations in sheep using CRISPR/Cas9. Crispo et al [21] generated a myostatin gene (*MSTN*)-null mutation in sheep resulting from frameshift mutations causing

premature-stop codons [21]. In addition, others have generated deletions of entire genes such as FGF5 [22], yet reports of the successful generation of missense point mutations are limited to goats [23] and as yet, none have been generated with the goal of modeling human disease.

This thesis chapter presents the first successful use of CRISPR/Cas9 to efficiently edit the sheep *ALPL* gene, and create a specific point mutation that closely resembles the musculoskeletal and tooth phenotype observed in human HPP. This accomplishment represents a major advance in the development of a relevant large (domestic) animal model for the examination of HPP's pathophysiology and extraordinarily wide-ranging severity.

## **Results**

### Confirmation of *ALPL* exon 10 mutation-specific locus

The human *ALPL* coding exon 10 sequence was compared to the *Ovis aries* (sheep) genome using NCBI (**Figure 22**). A highly conserved region (90% identity) on chromosome 2 of the sheep genome was located via nucleotide BLAST analysis. Based on the knowledge that more than 70% of HPP cases are caused by missense single point mutations in *ALPL*, the human *ALPL* exon 10 translated sequence was aligned to the sheep sequence and revealed a highly conserved amino acid sequence (90% identity) (**Figure 22**), including conservation of the orthologous isoleucine to methionine (p.Ile359Met; c.1077C>G). The HPP mutation target locus (p.Ile359Met; c.1077C>G) has been reported to cause both mild [24] and severe HPP [13]. In the case of the severe form, the patient was compound heterozygous for the c.1077C>G and a perinatal mutation [13].

Human	1	MISFFLVLAIGTCLTNSLVPEKEKDPKYWRDQAQETLKYALELQKLNNTVAKNVIMFLGDGMGVSTVTAARILKQQLHHN	80
Sheep	1	MISFFLVLAIGTCLASSLVPEKEKDPKYWRDQAQETLKNALRLQTLNNTVAKNVIMFLGDGMGVSTVTAARILKQQLHHN	80
Mouse	1	MISFFLVLAIGTCLTNSFVPEKERDPSYWRQQAQETLKNALKLQKLNNTVAKNVIMFLGDGMGVSTVTAARILKQQLHHN	80
Human	81	PGEETRLEMDKFPFVALSKTYNTNAQVPDSAGTATAYLCGVKANEGTVGVSAATERSRCNTTQGNEVTSILRWAKDAGKS	160
Sheep	81	PGEETKLEMDKFPYVALSKTYNTNAQVPDSAGTATAYLCGVKANEGTVGVSAATQRSQCNTTQGNEVTSILRWAKDAGKS	160
Mouse	81	TGEETRLEMDKFPFVALSKTYNTNAQVPDSAGTATAYLCGVKANEGTVGVSAATERTRCNTTQGNEVTSILRWAKDAGKS	160
Human	161	VGIVTTTRVNHATPSAAYAHSADRDWYSDNEMPEALSQGCKDIAYQLMHNIRDIDVIMGGGRKMYPKNKT DVEYESDE	240
Sheep	161	VGIVTTTRVNHATPSASYAHSADRDWYSDNEMPEALSQGCKDIAYQLMHNVKDIEVIMGGGRKMYPKNRTDVEYELDE	240
Mouse	161	VGIVTTTRVNHATPSAAYAHSADRDWYSDNEMPEALSQGCKDIAYQLMHNIKDIDVIMGGGRKMYPKNRTDVEYELDE	240
Human	241	KARGTRL DGLDLVDTWKSFKPRHKHSHFIWNRETELLTLDPHNV DYLGLFEPGDMQYELNRRNVTDPSLSEMVVVAIQIL	320
Sheep	241	KARGTRL DGLNLVDIWKSFKPKHKHSHYVWNRD LLDLDPHTVDYLLGLFEPGDMQYELNRRNVTDPSLSEMVEMAIRIL	320
Mouse	241	KARGTRL DGLDLISIWKSFKPRHKHSHYVWNRTELLALDPSRVDYLLGLFEPGDMQYELNRRNLTDP SLSEMVVALRIL	320
Human	321	RKNPKGFLLVEGGRIDHGHHEGKAKQALHEAVEMDRAIGQAGSLTSS EDTLT VVTADHSHVTFGGYT PRGNSIFGLAP	400
Sheep	321	NKNPKGFLLVEGGRIDHGHHEGKAKQALHEAVEMDQAIIGQAGAMTSVEDTLT VVTADHSHVTFGGYT PRGNSIFGLAP	400
Mouse	321	TKNLKGFLLVEGGRIDHGHHEGKAKQALHEAVEMDQAIIGKAGAMTSQKDTLT VVTADHSHVTFGGYT PRGNSIFGLAP	400
		Ile>Met	
Human	401	MLSDTDKKPFTAILYGNPGYKVVGGERENVSMDVYAHNNYQAQSAVPLRHETHGGEDVAVFSKGPMAHLLHGVHEQNYV	480
Sheep	401	MVSDTDKKPFTAILYGNPGYKVVGGERENVSMDVYAHNNYQA-----VAVFAKGPMAHLLHGVHEQNYI	465
Mouse	401	MVSDTDKKPFTAILYGNPGYKVV DGERENVSMDVYAHNNYQAQSAVPLRHETHGGEDVAVFAKGPMAHLLHGVHEQNYI	480
Human	481	PHVMAYAACIGANLGHCAPASSAGSLAA-----GPLLALALYPLSVLF-----	524
Sheep	466	PHVMAYAACIGANRDHCA---SASSPLPargprkpkksachppgSPLESSTAARSVAGLQpppppaapfwptg	534
Mouse	481	PHVMAYASCIGANLDHCAWAGSGSAPSP-----GALLLPLAVLSLRTL F-----	524

**Figure 22. Amino Acid sequence alignment of human, sheep and mouse alkaline phosphatase to reference sequence via NCBI BLAST.**

### Design of sgRNA and ssODN Repair Template Targeting Sheep *ALPL*

To genetically modify the sheep *ALPL* gene and create a single nucleotide knock-in mutation (c.1077C>G), two sgRNAs were designed (as previously described in chapter II) to target exon 10 of the sheep *ALPL* gene. These sgRNAs were assessed *in silico* to estimate potential off-target genomic effects and showed minimal potential effects. The Cas9 cleavage site for sgRNA #1 (GGCGGGCGCTATGACCTCCG PAM=TGG) and sgRNA #2 (GGACCAGGCCATCGGGCAGG PAM=CGG) were 5bp and 23bp (**Table 3**) downstream the target site of the c.1077C>G point mutation (**Figure 23**), respectively. A 91bp single stranded oligonucleotide (ssODN) repair template was designed in the sense direction with 45bp homology arms flanking the target site as described in Chapter II. The ssODN was designed to pair with the CRISPR constructs and stimulate homology directed repair to incorporate the point

mutation into the target region (**Figure 23**) [25]. The synthetic repair template also contained a mutation in the protospacer adjacent motif (PAM) sequence to limit subsequent Cas9 cleavage of the ssODN repair template once it is incorporated into the gene (**Figure 23**) [25]. The PAM sequence is the region(s) of the genome that is recognized by Cas9 to induce cleavage.

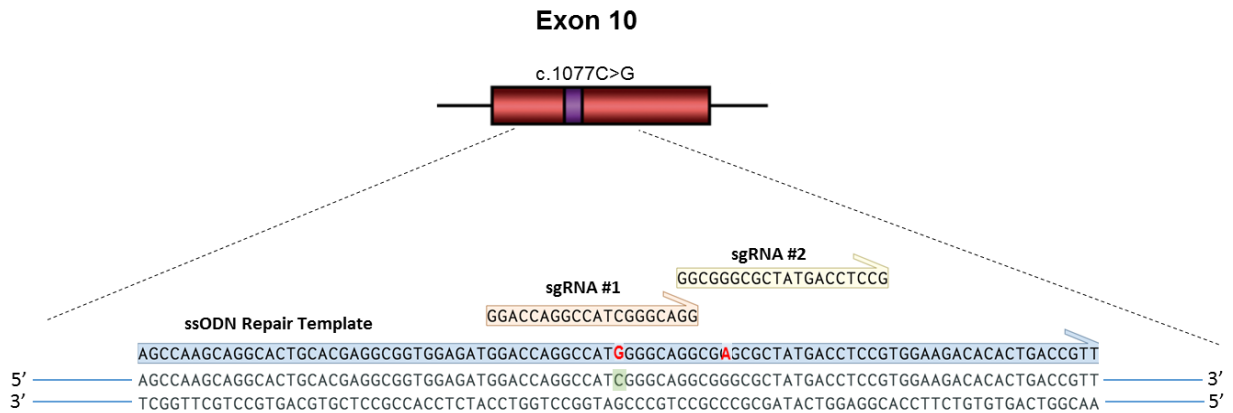


**Figure 23. Loci of CRISPR constructs relative to *ALPL* target mutation site.** Illustration of Exon 10 (red horizontal bar) and the approximate location of the target *ALPL* mutation for genetic manipulation (purple vertical bar). The relative location of sgRNA #1 (orange arrow), sgRNA #2 (yellow arrow), and the ssODN repair template (blue arrow) to the mutation site. The red letters indicate nucleotide manipulations in the repair template to be incorporated into the *ALPL* gene.

### Efficient targeting of the selected locus in sheep fibroblasts by CRISPR/Cas9

Functional validation of Cas9 activity and targeting efficiency for both sgRNAs was assessed by T7 endonuclease 1 (T7E1) activity [21]. The T7E1 cleaves at regions of mismatched DNA [26]. Thus, this enzyme has been repurposed as a simple screening method to determine regions of insertions or deletions (indels) incorporated into target cleavage sites of Cas9 (**Figure 24A**). In the case of Cas9 gene editing, are usually caused by non-homology end joining (NHEJ) [26]. To assess each sgRNAs/Cas9 targeting efficiency, CRISPR Cas9 all-in-one plasmids containing a green fluorescent protein (GFP) cassette with either sgRNA #1 or sgRNA #2 were

transfected into primary sheep fibroblasts using Lipofectamine 3000 as described in chapter II. After incubating for 48-72 h, genomic DNA was extracted and purified from sheep fibroblasts using Qiagen DNEasy kit and extracted DNA was PCR amplified using specific primers flanking exon 10 target site (**Table 2**); thereby creating a 959bp PCR product that was subsequently digested with T7E1 as previously described [21]. Electrophoresis of digested fragments by T7E1 demonstrated efficient targeting and cleavage by Cas9 at the target mutation site (**Figure 24B**). Cas9 cleavage at the target site was confirmed by Sanger sequencing [27] as a 12bp deletion at the target site was observed in the gene of a single sheep fibroblast cell (**Figure 24C**). Additionally, it is important to note that the additional fragments observed on the 2% agarose gel from the T7E1 assay were confirmed by Sanger sequencing to be silent (no effect on amino acid coding sequence) SNPs in sheep *ALPL* gene.

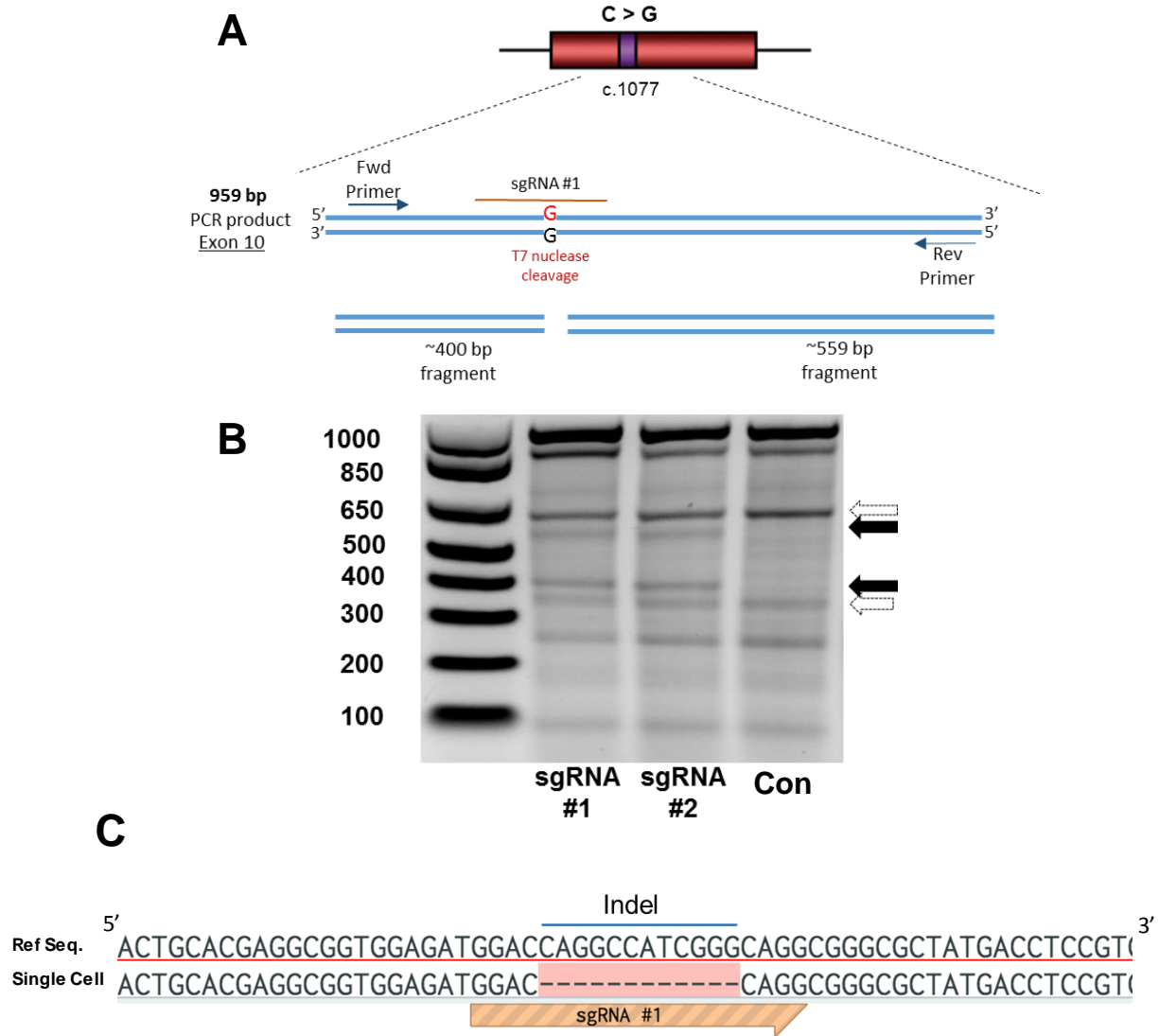


**Figure 24. Efficient targeting of *ALPL* gene by CRISPR Cas9 in primary sheep fibroblasts.** (A) Schematic of T7E1 potential cleavage activity in recognizing mutation incorporations in the Cas9 target regions. (B) Detection of Cas9 targeting efficiency by T7E1 analysis. Closed arrows on the 2% agarose gel indicate the expected fragment size of the Cas9 targeted-region for sgRNA #1 and #2. The open arrows indicate silent SNPs in the sheep *ALPL* gene confirmed by Sanger sequencing. (C) Confirmation of Cas9 cleavage activity by Sanger sequencing revealed a 12bp deletion at the target site in a single cell transfected with the CRISPR Cas9 constructs.

## Generation of *ALPL* Genetically Modified Lambs

A total of 88 one or two cell embryos were collected from 8 donor Rambouillet ewes as described in the detailed methods sections in chapter II. In sum, 74 *in vitro* genetically manipulated zygotes were generated targeting the *ALPL* exon 10 (c.1077) by microinjection of 10 ng *in vitro* transcribed sgRNA #1, 10 ng Cas9 mRNA, 30 ng Cas9 protein, and either 5ng or 50ng of the 91 bp ssODN repair template. Three to four individual embryos (injected n=41 and/or control n=11) per recipient were transferred immediately following microinjection into 17 recipient ewes. In addition, 21 microinjected embryos were also *in vitro* cultured (IVC) for analysis (**Table 10**). Of the IVC zygotes, a cleavage ratio of 95% was observed 24 h after culturing.

To determine gene editing efficiency and subsequent *ALPL* mutation analysis rate, hatched blastocysts (microinjected n=9; control n=1) from IVC zygotes were lysed, and whole genome amplified using Qiagen Repli-g Kit as previously described [28] and as described in chapter 2. The ~1kb of exon 10 PCR product flanking the c.1077C>G target was then generated using forward primer 5' ATGTTGGGCCCTTCCCTAA 3' and reverse primer 5' CAACATGACCCCTGGACCAA 3' (**Table 2**), and Sanger sequencing was performed. Sequence analysis of embryos revealed a high mutation rate of 66.6% (4/6), all exhibiting the desired *ALPL* c.1077C>G point mutations. It is important to note that the mutation incorporation rate is reported out of 6 instead of 10, due to 3 non-viable sequence reads from Sanger sequencing and 1 control embryo. Nine ewe pregnancies were confirmed by the measurement of Pregnancy-Associated Protein [29] on day 35 post-transfer, followed by ultrasound for further validation. Fifteen (15) lambs were born 145-152 days after transfer with a fetal loss rate of 40% (6/15) [7] (**Table 10**).

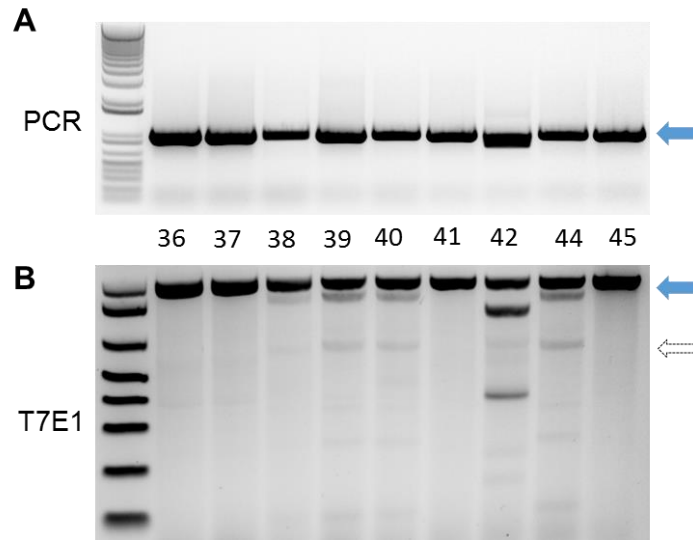


**Table 10.** Generation of *ALPL* gene-modified lambs with CRISPR/Cas9

Donor Ewes	Collected Embryos	Injected embryos	Recipient Ewes	Embryos Transferred	IVC Cultured Embryo Cleavage Rate (cleaved/IVC)	Pregnancy Rate	# of Lambs Conceived	Fetal Loss Rate	Mutant/ Live Newborn Lambs
8	88	74	17	52 (41 injected + 11 controls)	95% (20/21)	52.9% (9/17)	15	40% (6/15)	66.6% (6/9)

### Confirmation of *ALPL* Mutation Incorporation in Newborn Lambs

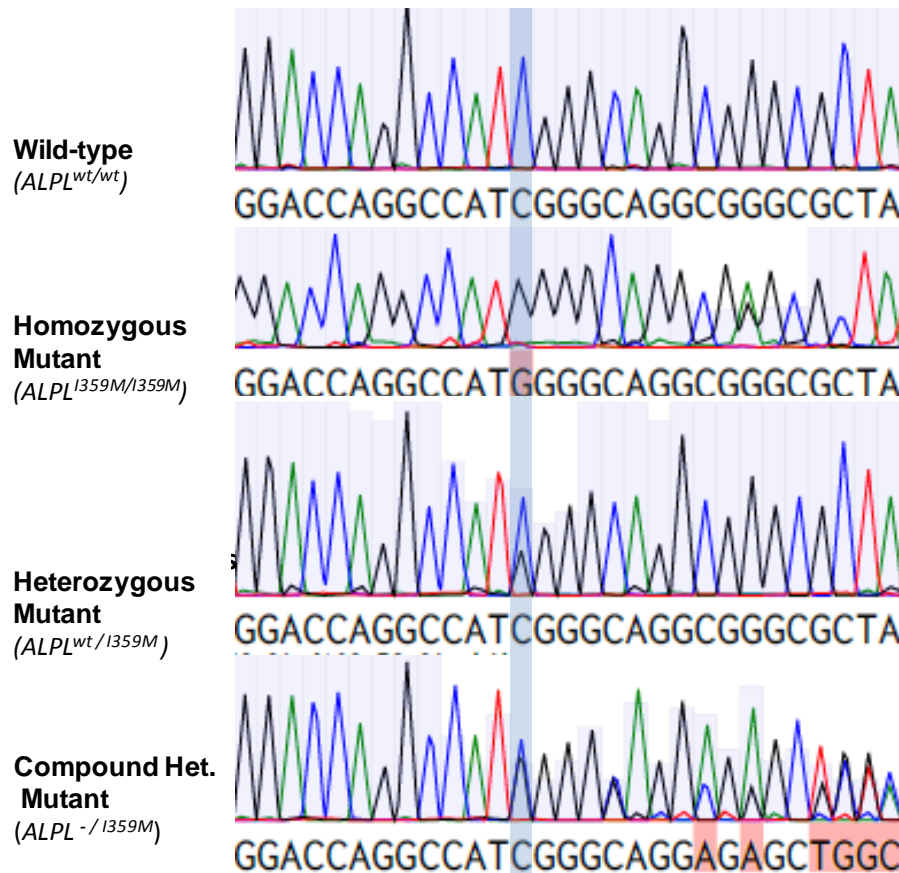
Newborn umbilical cord and whole blood were collected and genomic DNA extracted for analysis. Live newborn lamb DNA from all 9 live animal was analyzed by PCR (**Figure 25A**) and T7E1 (**Figure 25B**) as described in the detailed methods section in Chapter 2. In addition, DNA derived from all 9 live animals was analyzed by Sanger sequencing for the gene modifications [27] (**Figure 26A**). The preliminary examination of specific PCR products from each animal demonstrated an unexpected and aberrant band for lamb 42, with no detectable insertions or deletions for any of the other lambs. Subsequent Sanger sequencing of gel-extracted PCR amplicons revealed a gene editing rate of 66.6% (6/9) (Table 1). Overall, there were 3 wild type newborns (*ALPL*<sup>wt/wt</sup>), 4 heterozygous newborns with the p.Ile359Met mutation (*ALPL*<sup>wt/I359M</sup>), 1 homozygous newborn for the p.Ile359Met mutation (*ALPL*<sup>I359M/I359M</sup>), and 1 compound heterozygous newborn with a null-mutated allele and a p.Ile359Met allele (*ALPL*<sup>-/I359M</sup>) (**Figure 26A**). Representative images of each genotype are shown in **Figure 26B**.



**Figure 25. PCR and T7E1 genotype screening for transgenic lambs.** (A) PCR detection of sgRNA/Cas9 targeting modifications in newborn lambs, individually numbered at the bottom. (B) T7E1 screening of newborn genotypes. Blue closed arrows point to PCR product (959 bp) flanking target region. Open arrows are bands sizes for known SNPS in exon 10.

### ALPL Genetically-Modified Lambs Recapitulate Human HPP

Similar to HPP patients with the orthologous p.Ile359Met mutation [24] and consistent with the biochemical hallmark of human HPP [1], serum *ALP* activity was significantly reduced in *ALPL*<sup>wt/I359M</sup> (p<0.01) and dramatically reduced in *ALPL*<sup>I359M/I359M</sup> and *ALPL*<sup>-/I359M</sup> mutant lambs at 2 months of age compared to *ALPL*<sup>wt/wt</sup> animals (**Figure 26**) as measured by ELISA. Unsurprisingly, the *ALPL*<sup>-/I359M</sup> mutant animal had the lowest measured serum TNSALP activity (**Figure 26**), presumably associated with the incorporation of an INDEL into *ALPL*. Therefore, this animal was not subjected to further detailed phenotypic evaluation based on concerns with the interpretation being confounded due to the complexity of the compound heterozygous genotype specifically the INDEL incorporation which have been shown to severely impact function of target genes [21].

**A****B**

**Figure 26. Representative chromatographs and photos of transgenic lambs. (A)** Representative chromatographs from Sanger sequence analysis of newborn lambs from DNA extracted from sample umbilicus. **(B)** Photos of representative lambs with different *ALPL* genotypes.

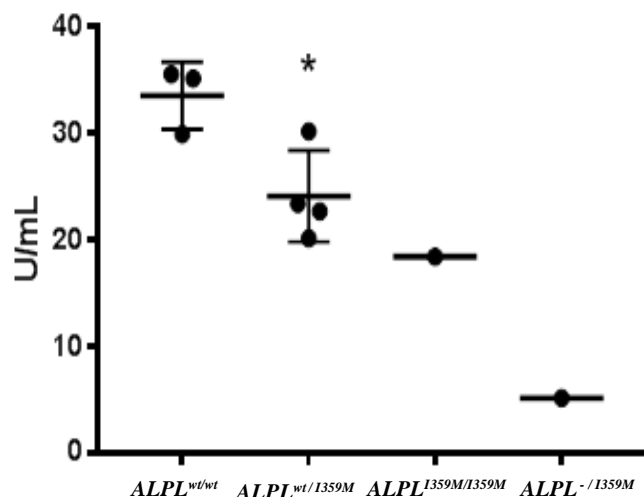


**Figure 27. Reduced serum Alkaline Phosphatase levels in 2 month old transgenic lambs.** Serum alkaline phosphatase activity measured by ELISA revealed a significant decrease in circulating ALP in  $ALPL^{wt/1359M}$  mutant compared to  $ALPL^{wt/wt}$  lambs.  $ALPL^{1359M/1359M}$  and  $ALPL^{-/1359M}$  mutant lambs were also dramatically reduced but significance was unable to be assessed due to low biological numbers.

$ALPL$  mutant lambs displayed variable phenotype expression at birth as noted by  $ALP$  activity (**Figure 27**), birth weights (**Figure 28**), radiographs (**Figure 29**), clinical reports, and daily observations. Several lambs suffered from respiratory difficulties diagnosed as pneumonia that led to fatalities in 2 mutant animals, similar to the respiratory insufficiency in infantile and perinatal HPP [30]. Birth weights much lower in  $ALPL$  mutant lambs than their wildtype counterparts but all animals grew at similar rates (**Figure 28**). At day 10, X-ray images by DXA of docked tails revealed decreased bone formation, markedly decreased mineralization, and apparent metaphyseal flaring in transgenic animal tail vertebrae compared to wildtype, entirely consistent with the clinical signs of HPP (**Figure 29A, B**). Metaphyseal flaring as observed in tail vertebrae of is also evident at the metaphysis of long bones given the significant increase in carpus joint diameter of  $ALPL^{wt/1359M}$  transgenic animals compared to the WT animals.

Additionally, the  $ALPL^{I359M/I359M}$  mutant lamb almost completely lacked secondary ossification centers (**Figure 29A**). Moreover, the variable presentation in  $ALPL^{wt/I359M}$  transgenic lambs as seen by the differences in animal size at birth (**Figure 28**) and tail bone radiographs (**Figure 29**) of animals with the same mutation suggests differences in severity. In Figure 27, metaphyseal flaring in transgenic lamb #1038 ( $ALPL^{wt/I359M}$ ) is clearly evident (**Figure 29A, B**). However, transgenic lamb #1036 ( $ALPL^{wt/I359M}$ ) does not have as much flaring, but present with very distinguishable tongues of radiolucency, indicative of hypomineralization as seen in long bones of patients with HPP [31].

With regard to the dental complications of human HPP, it is important to recall that the premature loss of deciduous teeth can occur at any age in less severe forms of HPP such as Odonto-HPP, but usually occur much earlier in more severe forms (i.e. infantile and perinatal HPP) of the disease [32, 33] (**Table 1**). In regards to the normal sheep dentition at birth, sheep have a maxillary dental pad and 8 primary incisors in the mandible (**Figure 30A, B**), which are replaced by secondary incisors by approximately 1 year [34]. Radiography and *in vivo* computed tomography (CT) at 2 months of age revealed a significant dental phenotype (**Figure 30C, D**). The appearance of the sheep dentition was entirely consistent with defects reported in human HPP, namely thin dentin and widened pulp spaces (similar to descriptions of “shell teeth”), thin roots, reduced mineralization indicated by generalized radiolucency in the jawbone, and reduced alveolar bone in interproximal spaces (**Figure 30C, D**) [9, 32, 35, 36].

In addition, muscle weakness is associated with human HPP as indicated by waddling gait and minimal ability for young patients to sustain a 6 minute walk test [37, 38]. though the underlying pathology is not well understood [1]. There are no studies to my knowledge assessing the muscle phenotype in HPP rodent models, potentially due to the short lifespan of  $ALPL$  null

mice [8]. To begin analyze the muscle phenotype in transgenic mutant animals, muscle biopsies were taken from gluteal muscle at 2 months of age as described in Chapter II and 500 nm histological sections were analyzed under light and electron microscopy. Mutant lambs exhibited aberrant muscle structure and ultrastructure compared to WT sheep, including more variable muscle fiber size (**Figure 31A**), altered mitochondrial cristae and increased fat droplets (**Figure 31B**). Moreover, these results to my knowledge provide the first preliminary analysis the muscle phenotype in an animal model of HPP.

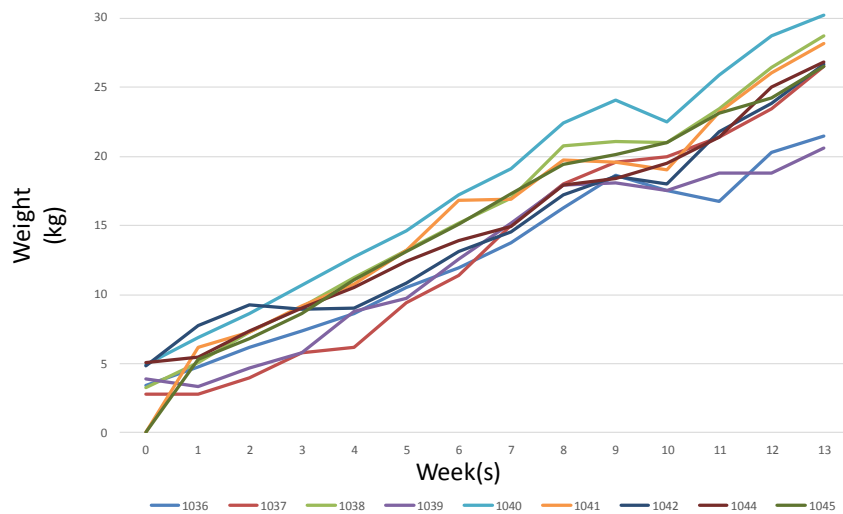


**Figure 28. Skeletal phenotype is not due to a “failure to thrive” phenotype.** Birth weights varied between newborn lambs. However, transgenic lambs were observed to weigh less than wildtype animals at birth. The growth curve for all lambs was pretty consistent indicating a steady development rate.

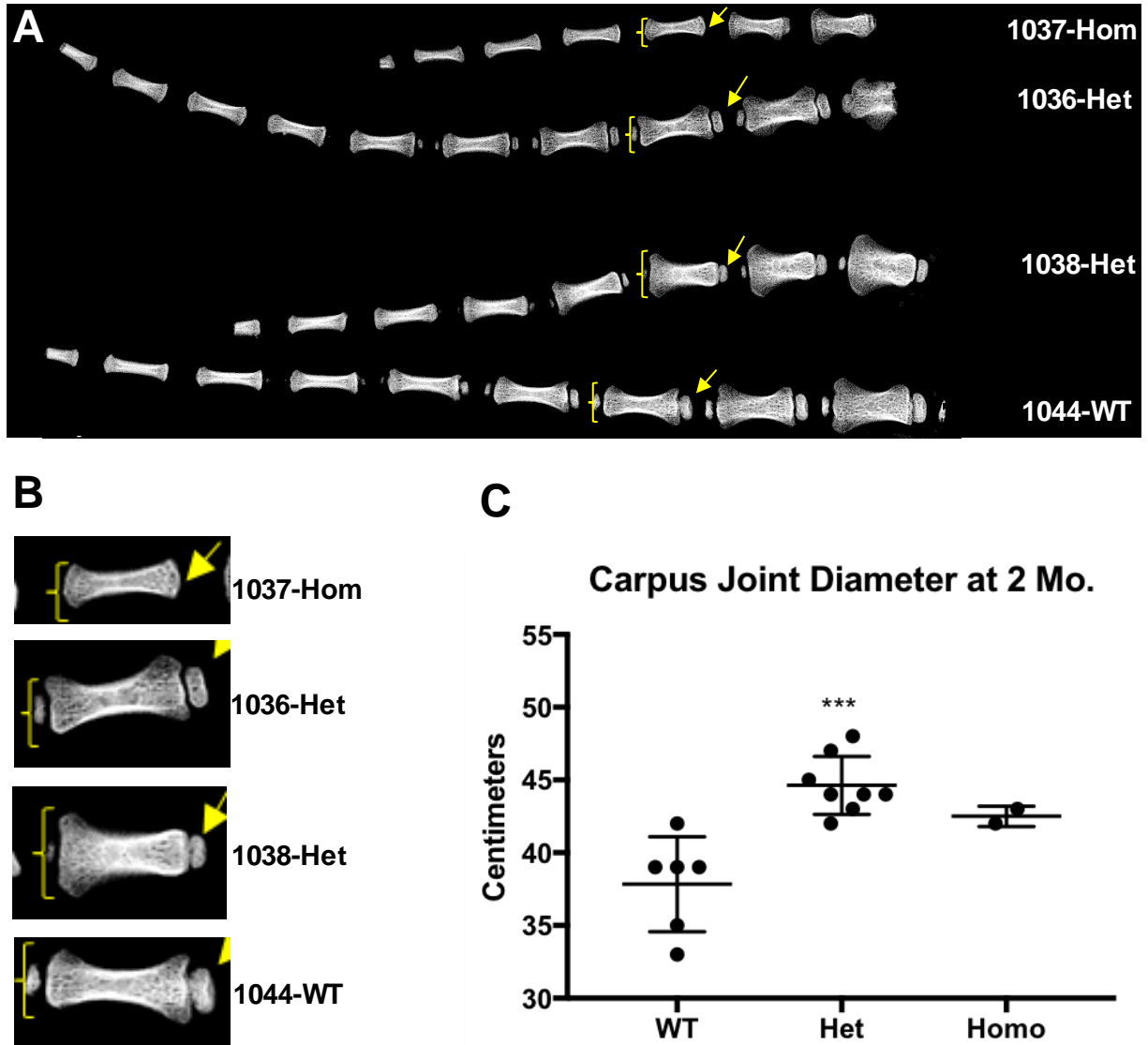


**Figure 29. Tail radiographs reveal skeletal phenotype in *ALPL* mutant lambs.** (A) Representative tail radiographs of day 10 lambs obtained by *ex vivo* DXA. Yellow brackets designate distal metaphyses; yellow arrows designate location of secondary ossification centers. (B) Inset magnification of individual tail vertebrae from B shows size and morphology differences in the 3 genotypes. Note different shape, size and extent of mineralization in the individual vertebrae. (C) Carpus joint diameter of transgenic lambs at 2 months of age. \* indicates statistical significance compared to WT animals.

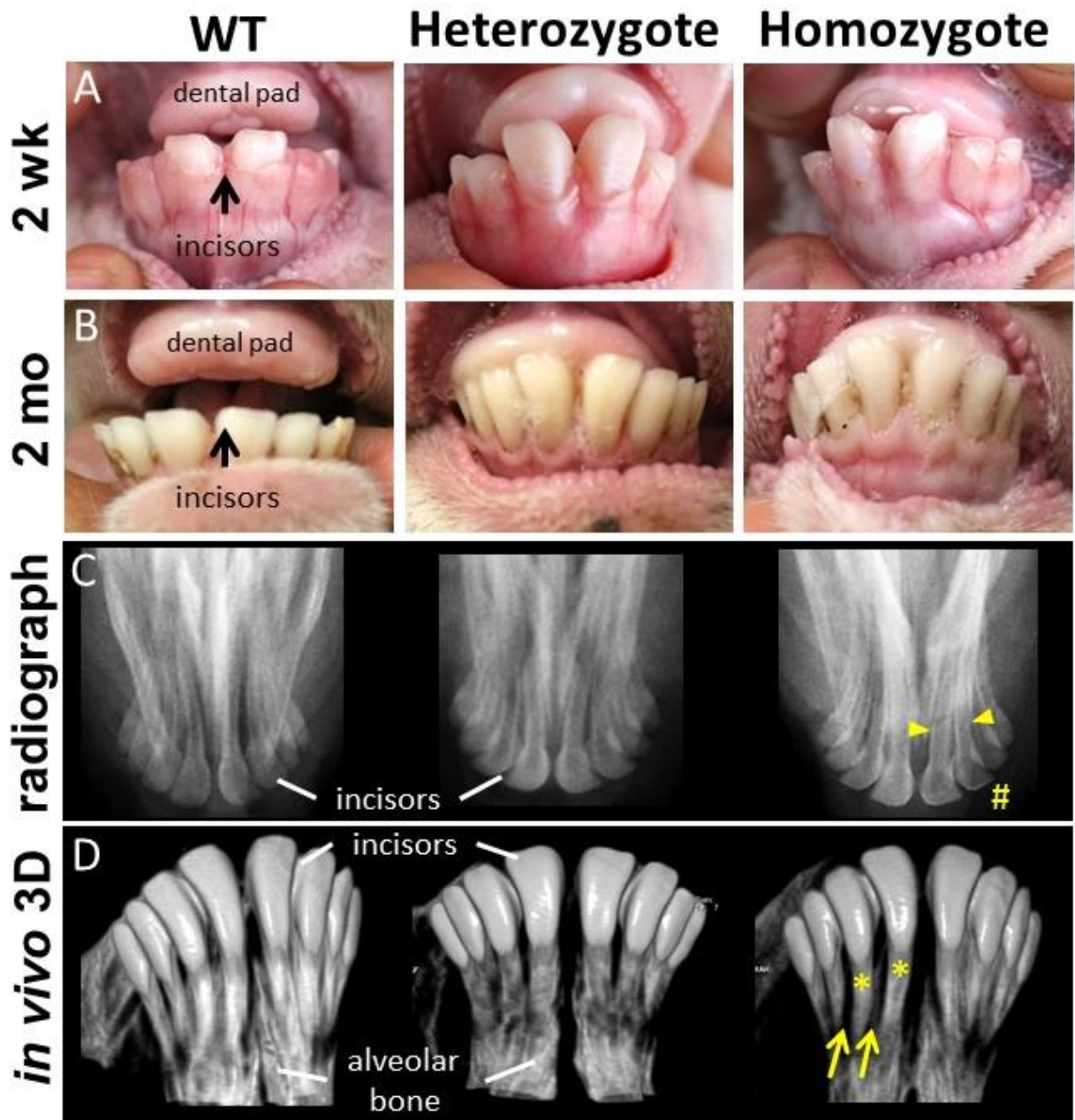


**Figure 30. Dental phenotype in ALPL c.1077C>G targeted sheep.** Oral photographs from wildtype, heterozygous, and homozygous lambs at (A) 2 weeks and (B) 2 months of age show the maxillary dental pad and mandibular incisors. (C) Oral radiographs of incisors at 2 months of age show thin root dentin in homozygous HPP sheep (yellow arrow). (D) 3D reconstructions of in vivo CT of mandibles at 2 months of age show thin roots (\*) and reduced or radiolucent alveolar bone around incisors (yellow arrow).



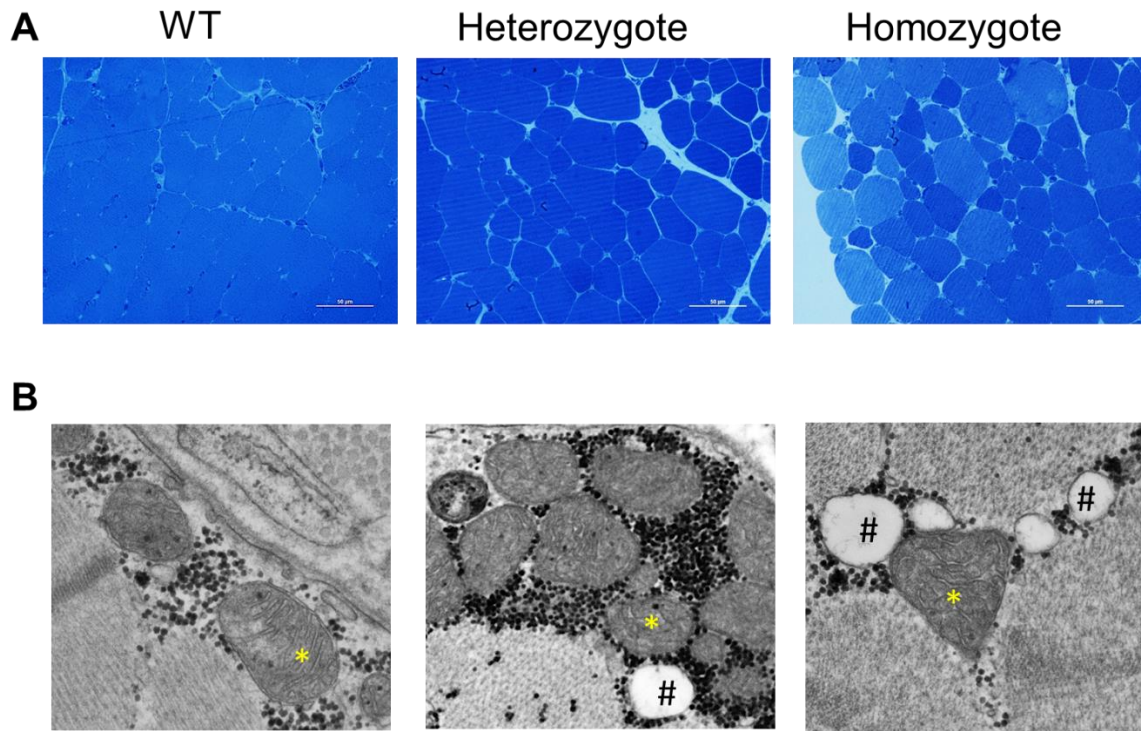


**Figure 31. Skeletal muscle histological phenotype in ALPL c.1077C>G targeted sheep.** (A) Representative light microscopic evaluation (40X magnification, size bar, 50 µm) of Richardson's stained 500nm sections of 2 month old gluteus muscle reveal variable sized muscle fibers in mutants compared to homogeneously sized WT fibers. (B) Representative electron micrographs (original magnification 44,000X) of HPP mutants compared to WT reveal abnormal mitochondria cristae ultrastructure (\*) and higher fat content (#).

## Discussion

An ideal animal model of a human disease should satisfy several criteria: i.) the model should closely approximate the condition under investigation; ii.) the model should allow longitudinal study and permit appropriate tests to be performed; and iii.) specific reagents should be available. To date, the use of murine models has been driven almost exclusively by the availability of mouse genetics and their minimal animal costs; the ability to manipulate the rodent genome, the short reproductive cycles, and the generation of a range of genetically

identical inbred strains of mice has forced investigators down the murine route [39]. These important advantages have led to the acceptance of often less than accurate murine models as sufficient for research into human disorders. However, unlike humans, rodents have smaller long bones with thin fragile cortices that lack Haversian remodeling, which is the fundamental process by which larger animals, including sheep and humans, model and remodel their skeletons throughout life [40-42]. Additionally, mice are monophyodont (one set of teeth), while sheep and humans are diphyodont (two sets of teeth), including primary and secondary sets [34, 43-45]. In order to more accurately model the associated musculoskeletal and dental phenotypes of HPP, we utilized domestic sheep as a new animal model.

Collectively, results of the sheep *ALPL* missense-mutation (c.1077C>G) model of HPP described in this chapter demonstrate an accurate recapitulation of many clinical manifestations observed in individuals with HPP, satisfying the most stringent criteria for an animal model for the study of human musculoskeletal disease and marking a major advance beyond existing and largely limited murine models.

The missense mutation in the sheep *ALPL* gene (1077C>G) was generated using CRISPR/Cas9, producing the first large animal model of HPP, with a primary TNSALP deficiency and the associated musculoskeletal and dental phenotype. Gene editing was efficient with a specific point mutation incorporation rate of 66.6%, demonstrating the utility of the sheep genome for precise editing. Children with the same 1077C>G mutation are reported to manifest rickets, skeletal pain, bone deformity, fracture, muscle weakness, seizures, and premature tooth loss [24, 46]. Interestingly, mutant sheep were also born with a variable clinical presentation, similar bone deformity, dental defects consistent with human HPP (**Figure 30**), and apparent structural muscle defects (**Figure 31**).

The novel structural and ultrastructural mitochondrial defects observed in muscle biopsies are the first to suggest a mechanism for HPP-related muscle weakness and may provide insights into the mechanism underlying the muscle weakness commonly observed in HPP patients. This ovine model also provides opportunities to follow HPP progression longitudinally, allowing repeated bone and muscle biopsies, timed administration of treatment(s), evaluation of primary and secondary tooth development and retention, and long-term assessment of periodontal health and interventions such as orthodontics and dental implants.

A sheep model for HPP represents a novel and critical first step in an ongoing effort to study the lifelong etiopathology of HPP. Throughout life, the extracellular accumulation of the primary TNSALP substrate, inorganic pyrophosphate (PP<sub>i</sub>), has been associated with tooth loss, rickets or osteomalacia, and myasthenia in HPP [2]. However, the relative importance of PP<sub>i</sub> over other known TNSALP substrates (pyridoxal 5'-phosphate and phosphoethanolamine) has not been directly determined and have been examined only cross-sectionally in groups of affected individuals [2]. The sheep HPP model provides the first real opportunity to enable repeated sampling of affected animals prospectively with repeated biopsy and molecular interrogation. This is particularly relevant since HPP-causing mutations in the *ALPL* gene cannot be studied in depth due to the limitations of rodent models [45].

The recently approved bone-targeted TNSALP enzyme replacement therapy, Asfotase Alfa, has demonstrated improvement to skeletal mineralization, including ribs, with improved respiratory function and survival in life-threatening perinatal and infantile HPP [1, 5, 47]. The impact of the intervention on the skeleton is profound and dramatic, yet little is known regarding the time-course of effects on muscle, teeth, and other tissues. Indeed, significant improvements in patient growth, strength, motor function, agility, and quality-of-life have been observed prior

to any changes in skeletal mineralization [46]. We hypothesize that the HPP sheep described here provide a unique opportunity to address fundamental HPP questions regarding muscle, bone, and tooth development. There is still much to learn regarding HPP pathophysiology, including muscle weakness [11] and our ongoing studies into the biology of myasthenia and premature tooth loss in HPP sheep will provide novel insight into new treatment approaches likely to improve patient care.

### Future Directions

Similar to DS and other genetic disorders, the clinical presentation of HPP is very complex and highly variable. Furthermore, the pathophysiology of some of the clinical phenotypes of HPP, such as the muscle weakness or premature tooth loss, is not well understood. Thus, the development of the HPP sheep model described in this chapter provide an opportunity to better understand the mechanisms underlying these pathologies. Changes in the BMU, either molecular or cellular, that disrupt the complex processes of skeletal development and homeostasis profoundly impact the musculoskeletal system. Therefore, understanding the possible alterations in the molecular signals in HPP could prove to be beneficial. Proteomics and gene expression profiling of whole bone marrow and muscle could be performed and provide insight into the possible mechanisms responsible for HPP phenotypes.

### **References**

1. Whyte MP. Hypophosphatasia - aetiology, nosology, pathogenesis, diagnosis and treatment. *Nat Rev Endocrinol*. 2016;12(4):233-46.
2. Whyte MP, Wenkert D, Zhang F. Hypophosphatasia: Natural history study of 101 affected children investigated at one research center. *Bone*. 2016;93:125-38.

3. Camacho PM, Mazhari AM, Wilczynski C, Kadanoff R, Mumm S, Whyte MP. Adult Hypophosphatasia Treated with Teriparatide: Report of 2 Patients and Review of the Literature. *Endocr Pract.* 2016;22(8):941-50.
4. Khandwala HM, Mumm S, Whyte MP. Low serum alkaline phosphatase activity and pathologic fracture: case report and brief review of hypophosphatasia diagnosed in adulthood. *Endocr Pract.* 2006;12(6):676-81.
5. Whyte MP. Heritable metabolic and dysplastic bone diseases. *Endocrinol Metab Clin North Am.* 1990;19(1):133-73.
6. Whyte MP, Essmyer K, Geimer M, Mumm S. Homozygosity for TNSALP mutation 1348c>T (Arg433Cys) causes infantile hypophosphatasia manifesting transient disease correction and variably lethal outcome in a kindred of black ancestry. *J Pediatr.* 2006;148(6):753-8.
7. Whyte MP. Hypophosphatasia: An overview For 2017. *Bone.* 2017;102:15-25.
8. Fedde KN, Blair L, Silverstein J, Coburn SP, Ryan LM, Weinstein RS, et al. Alkaline phosphatase knock-out mice recapitulate the metabolic and skeletal defects of infantile hypophosphatasia. *J Bone Miner Res.* 1999;14(12):2015-26.
9. Foster BL, Sheen CR, Hatch NE, Liu J, Cory E, Narisawa S, et al. Periodontal Defects in the A116T Knock-in Murine Model of Odontohypophosphatasia. *J Dent Res.* 2015;94(5):706-14.
10. McKee MD, Nakano Y, Masica DL, Gray JJ, Lemire I, Heft R, et al. Enzyme replacement therapy prevents dental defects in a model of hypophosphatasia. *J Dent Res.* 2011;90(4):470-6.
11. Millan JL, Whyte MP. Alkaline Phosphatase and Hypophosphatasia. *Calcif Tissue Int.* 2016;98(4):398-416.
12. Yadav MC, de Oliveira RC, Foster BL, Fong H, Cory E, Narisawa S, et al. Enzyme replacement prevents enamel defects in hypophosphatasia mice. *J Bone Miner Res.* 2012;27(8):1722-34.

13. Whyte MP, Greenberg CR, Salman NJ, Bober MB, McAlister WH, Wenkert D, et al. Enzyme-replacement therapy in life-threatening hypophosphatasia. *N Engl J Med*. 2012;366(10):904-13.
14. Delmas PD, Vergnaud P, Arlot ME, Pastoureau P, Meunier PJ, Nilsson MH. The anabolic effect of human PTH (1-34) on bone formation is blunted when bone resorption is inhibited by the bisphosphonate tiludronate--is activated resorption a prerequisite for the in vivo effect of PTH on formation in a remodeling system? *Bone*. 1995;16(6):603-10.
15. Chavassieux P, Pastoureau P, Boivin G, Chapuy MC, Delmas PD, Meunier PJ. Dose effects on ewe bone remodeling of short-term sodium fluoride administration--a histomorphometric and biochemical study. *Bone*. 1991;12(6):421-7.
16. Newman E, Turner AS, Wark JD. The potential of sheep for the study of osteopenia: current status and comparison with other animal models. *Bone*. 1995;16(4 Suppl):277S-84S.
17. Kreipke TC, Rivera NC, Garrison JG, Easley JT, Turner AS, Niebur GL. Alterations in trabecular bone microarchitecture in the ovine spine and distal femur following ovariectomy. *J Biomech*. 2014;47(8):1918-21.
18. Les CM, Spence CA, Vance JL, Christopherson GT, Patel B, Turner AS, et al. Determinants of ovine compact bone viscoelastic properties: effects of architecture, mineralization, and remodeling. *Bone*. 2004;35(3):729-38.
19. Les CM, Vance JL, Christopherson GT, Turner AS, Divine GW, Fyhrie DP. Long-term ovariectomy decreases ovine compact bone viscoelasticity. *J Orthop Res*. 2005;23(4):869-76.
20. Turner AS. The sheep as a model for osteoporosis in humans. *Vet J*. 2002;163(3):232-9.
21. Crispo M, Mulet AP, Tesson L, Barrera N, Cuadro F, dos Santos-Neto PC, et al. Efficient Generation of Myostatin Knock-Out Sheep Using CRISPR/Cas9 Technology and Microinjection into Zygotes. *PLoS One*. 2015;10(8):e0136690.

22. Hu R, Fan ZY, Wang BY, Deng SL, Zhang XS, Zhang JL, et al. RAPID COMMUNICATION: Generation of FGF5 knockout sheep via the CRISPR/Cas9 system. *J Anim Sci.* 2017;95(5):2019-24.
23. Niu Y, Zhao X, Zhou J, Li Y, Huang Y, Cai B, et al. Efficient generation of goats with defined point mutation (I397V) in GDF9 through CRISPR/Cas9. *Reprod Fertil Dev.* 2017.
24. Ukarapong S, Ganapathy SS, Haidet J, Berkovitz G. Childhood hypophosphatasia with homozygous mutation of ALPL. *Endocr Pract.* 2014;20(10):e198-201.
25. Ran FA, Hsu PD, Wright J, Agarwala V, Scott DA, Zhang F. Genome engineering using the CRISPR-Cas9 system. *Nat Protoc.* 2013;8(11):2281-308.
26. Huang MC, Cheong WC, Lim LS, Li MH. A simple, high sensitivity mutation screening using Ampligase mediated T7 endonuclease I and Surveyor nuclease with microfluidic capillary electrophoresis. *Electrophoresis.* 2012;33(5):788-96.
27. No E, Zhou Y, Loopstra CA. Sequences upstream and downstream of two xylem-specific pine genes influence their expression. *Plant Sci.* 2000;160(1):77-86.
28. Song J, Yang D, Xu J, Zhu T, Chen YE, Zhang J. RS-1 enhances CRISPR/Cas9- and TALEN-mediated knock-in efficiency. *Nat Commun.* 2016;7:10548.
29. Gonzalez F, Sulon J, Garbayo JM, Batista M, Cabrera F, Calero P, et al. Early pregnancy diagnosis in goats by determination of pregnancy-associated glycoprotein concentrations in plasma samples. *Theriogenology.* 1999;52(4):717-25.
30. Whyte MP, Rockman-Greenberg C, Ozono K, Riese R, Moseley S, Melian A, et al. Asfotase Alfa Treatment Improves Survival for Perinatal and Infantile Hypophosphatasia. *J Clin Endocrinol Metab.* 2016;101(1):334-42.
31. Whyte MP. Hypophosphatasia: Enzyme Replacement Therapy Brings New Opportunities and New Challenges. *J Bone Miner Res.* 32(4):667-75.
32. Bianchi ML. Hypophosphatasia: an overview of the disease and its treatment. *Osteoporos Int.* 2015;26(12):2743-57.

33. Rodrigues TL, Foster BL, Silverio KG, Martins L, Casati MZ, Sallum EA, et al. Hypophosphatasia-associated deficiencies in mineralization and gene expression in cultured dental pulp cells obtained from human teeth. *J Endod.*38(7):907-12.
34. Weinreb MM, Sharav Y. Tooth Development in Sheep. *Am J Vet Res.* 1964;25:891-908.
35. Martins L, Rodrigues TL, Ribeiro MM, Saito MT, Giorgetti AP, Casati MZ, et al. Novel ALPL genetic alteration associated with an odontohypophosphatasia phenotype. *Bone.*56(2):390-7.
36. Foster BL, Nociti FH, Jr., Somerman MJ. The rachitic tooth. *Endocr Rev.*35(1):1-34.
37. Millan JL, Whyte MP. Alkaline Phosphatase and Hypophosphatasia. *Calcif Tissue Int.*98(4):398-416.
38. Nakamura-Takahashi A, Miyake K, Watanabe A, Hirai Y, Iijima O, Miyake N, et al. Treatment of hypophosphatasia by muscle-directed expression of bone-targeted alkaline phosphatase via self-complementary AAV8 vector. *Mol Ther Methods Clin Dev.*3:15059.
39. Scheerlinck JP, Snibson KJ, Bowles VM, Sutton P. Biomedical applications of sheep models: from asthma to vaccines. *Trends Biotechnol.* 2008;26(5):259-66.
40. Delmas PD. Biochemical markers of bone turnover for the clinical assessment of metabolic bone disease. *Endocrinol Metab Clin North Am.* 1990;19(1):1-18.
41. Pastoureau P, Vergnaud P, Meunier PJ, Delmas PD. Osteopenia and bone-remodeling abnormalities in warfarin-treated lambs. *J Bone Miner Res.* 1993;8(12):1417-26.
42. Parfitt AM. The cellular basis of bone remodeling: the quantum concept reexamined in light of recent advances in the cell biology of bone. *Calcif Tissue Int.* 1984;36 Suppl 1:S37-45.
43. Wheeler DL, Lane JM, Seim HB, 3rd, Puttlitz CM, Itescu S, Turner AS. Allogeneic mesenchymal progenitor cells for posterolateral lumbar spine fusion in sheep. *Spine J.*14(3):435-44.



44. McKee MD, Hoac B, Addison WN, Barros NM, Millan JL, Chaussain C. Extracellular matrix mineralization in periodontal tissues: Noncollagenous matrix proteins, enzymes, and relationship to hypophosphatasia and X-linked hypophosphatemia. *Periodontol* 2000.63(1):102-22.
45. Foster BL, Ramnitz MS, Gafni RI, Burke AB, Boyce AM, Lee JS, et al. Rare Bone Diseases and Their Dental, Oral, and Craniofacial Manifestations. *J Dent Res*. 2014;93(7 suppl):7S-19S.
46. Whyte MP, Madson KL, Phillips D, Reeves AL, McAlister WH, Yakimoski A, et al. Asfotase alfa therapy for children with hypophosphatasia. *JCI Insight*. 2016;1(9):e85971.
47. Fedde KN, Michel MP, Whyte MP. Evidence against a role for alkaline phosphatase in the dephosphorylation of plasma membrane proteins: hypophosphatasia fibroblast study. *J Cell Biochem*. 1993;53(1):43-50.

## CHAPTER VI

### SUMMARY

Skeletal diseases derived from genetic abnormalities are complex and often times vary in their clinical manifestations. The majority of these conditions are defined as rare disease, affecting less than 200,000 individuals. Collectively, rare disease places a significant financial burden on society and health care ecosystems. Thus, a complete understanding of the disease pathophysiology is essential, but sorely lacking. However, *in vivo* models that accurately recapitulate these rare bone pathologies can serve as tools for evaluating therapeutic treatments while providing insight into normal bone physiology. Therefore, the goal of this work was to evaluate in murine models the low bone mass phenotype found in DS and develop an appropriate of human Hypophosphatasia that recapitulate the associated skeletal defects observed in this disorder.

In DS, the low bone mass phenotype is defined by low bone turnover due to decreased osteoclast and osteoblast activity. These changes in bone cell activity decrease the utility of anti-resorptive agents in people with DS. Thus, we examined the effects of a known bone anabolic agent – sclerostin antibody (SclAb). Male Ts65Dn and age-matched WT littermate mice (8 weeks old) were treated with 4 weekly *i.v.* injections of 100 mg/kg SclAb. Analysis by DXA, microCT, and *ex vivo* bone marrow cultures revealed that SclAb had a significant anabolic effect on both controls and Ts65Dn DS mice that was osteoblast mediated, without significant changes in osteoclast numbers. Additionally, comparative gene profiling by RNAseq of whole femurs from 7 month old male Ts65Dn mice and WT provided insight into the molecular mechanisms underlying this unusual and rare bone phenotype.

Moreover, we successfully generated the first large animal model of a rare human bone disease using CRISPR/Cas9 to introduce a single point mutation in the tissue nonspecific alkaline phosphatase (TNSALP) gene (ALPL) (1077C>G) in sheep. Compared to wild-type (WT) controls, HPP sheep have reduced serum alkaline phosphatase activity, decreased tail vertebral bone size, and metaphyseal flaring, consistent with mineralization deficits observed in human HPP. Oral radiographs and computed tomography revealed thin dentin and wide pulp chambers in incisors, and radiolucency of jaws in HPP vs. WT sheep. Skeletal muscle biopsies reveal aberrant fiber size and mitochondrial cristae structure in HPP vs. WT sheep. These genetically engineered sheep phenocopy HPP and provide a novel large animal platform for the longitudinal study of HPP progression, as well as other rare bone diseases.

## APPENDIX

### AWARDS AND HONORS

#### Awards and Honors

Spring 2018	College of Veterinary Medicine and Biomedical Science (CVMBS) at Texas A&M University “Outstanding Graduate Student Award” for 2017-2018
Spring 2018	First Place in Graduate Student Platform Presentation: CVMBS Graduate Student and Post-Doctoral Research Symposium
Spring 2018	CVMBS High Impact Achievement Award for Large Grant Recipient
2017	Invited speaker for the ASBMR Career Development Webinar Series: “Unpacking Mentorship: How to Find, Utilize, and Build Mentor Relationships in the Bone, Mineral, and Musculoskeletal Community”
2017	Graduate/Medical Student Podium Talk “Best Talk” Award at the 2017 Orthopaedic Research Society (ORS) Southwest Regional Symposium
2016 - 2017	TAMU/Texas Heart Institute Center for Cell and Organ Biotechnology Innovation Grant (add grant title) with a successful renewal application for additional funding
2016 - 2018	William Townsend Porter Pre-doctoral Fellowship - American Physiological Society, successfully renewed for additional funding (add title of your application)
2017	ASBMR 2017 39 <sup>th</sup> Annual Meeting Young Investigator Diversity Travel Grant for abstract “Genetically Engineering a Sheep Model of Hypophosphatasia”
2017	FASAB/Marc Mentored Poster/Platform Travel Award to attend the 2017 Experimental Biology Meeting in Chicago, IL
2016 - 2017	Graduate Student Association President - CVM
August 2016	ASBMR Young Investigator Travel Grant to attend the 38 <sup>th</sup> American Society for the Bone and Mineral Research (ASBMR) Conference in Atlanta, GA
July 2016	Research Abstract selected for a Plenary Poster Presentation at the ASBMR Meeting

\*plenary posters are the most highly ranked abstracts selected as posters and presented at ASBMR

- June 2016 CVM Graduate Student Advanced Development Training Award
- April 2016 ASBMR Young Investigator Travel Award to attend ECTS Ph.D. Training course (Oxford, UK)
- 2015 Director of Mentorship for Interdisciplinary Biomedical Sciences, UAMS
- 2013 - 2015 Initiative for Maximizing Student Development Program/Funding Award, UAMS
- 2013 - 2015 Graduate Student Association Representative, UAMS

### **Poster/Oral Presentations**

- Spring 2018 Experimental Biology Meeting, San Diego, CA
- Fall 2017 Graduate Research Recruitment Day Flash Talk Presenter. Texas A&M University
- Fall 2017 Genetic Engineering to produce a sheep model of Hypophosphatasia. Orthopaedic Research Southwest Regional Symposium in Houston, TX
- Fall 2017 Genetically engineering a sheep model of Hypophosphatasia, 39<sup>th</sup> ASBMR 2017 Annual Meeting in Denver, CO
- Spring 2017 Modeling Hypophosphatasia in *Ovis aries* (sheep) using CRISPR/Cas9: Development of phenotypically relevant large animal models for human bone disease. Experimental Biology Meeting in Chicago, IL
- Fall 2016 Similarities between IL-8 and RANKL Stimulation of Osteoclast Formation Suggests a Highly Conserved Signaling Cascade that Facilitates Bone Resorption in Breast Cancer, Attended and presented research at the 2016 American Society for Bone and Mineral Research (ASBMR) Conference in Atlanta, GA
- October 2016 Similarities between IL-8 and RANKL Stimulation of Osteoclast Formation Suggests a Highly Conserved Signaling Cascade that Facilitates Bone Resorption in Breast Cancer, Attended and presented research at the 2016 American Society for Bone and Mineral Research (ASBMR) Conference in Atlanta, GA

- Fall 2015 Improving Bone Mass in Down Syndrome; 37<sup>th</sup> ASBMR 2015, Seattle, WA
- Fall 2014 Becoming Aware of the Rare: A Better Understanding of Rare Bone Phenotypes  
in Down Syndrome and Hypophosphatasia Patients  
-Annual Biomedical Research Conference for Minority Students (ABRCMS), San  
Antonio, TX
- Fall 2014 Low Bone Mass in Down Syndrome Patients: A Rare Bone Disease  
36<sup>th</sup> Annual American Society for Bone and Mineral Research (ASBMR)  
Conference, Houston, TX